FACOLTÀ DI SCIENZE MATEMATICHE, FISICHE E NATURALI

DIPARTIMENTO DI SCIENZE DELLA TERRA E DEL MARE

DOTTORATO DI RICERCA IN GEOLOGIA – XXIII CICLO

Settore Scientifico Disciplinare GEO/04 Geografia Fisica e Geomorfologia

WATER EROSION PREDICTION BY STOCHASTIC AND EMPIRICAL MODELS IN THE MEDITERRANEAN: A CASE STUDY IN NORTHERN SICILY (ITALY)

Silvia Eleonora Angileri

Tutors:

Prof. Valerio Agnesi

Università degli Studi di Palermo

Prof. Volker Hochschild

Eberhard Karls Universität Tübingen

Coordinatore:

Prof. Enrico Di Stefano

CONTENTS

Acknowledgement

I would like to express my deep and sincere gratitude to my supervisors Prof. Dr. Valerio Agnesi and Prof. Dr. Volker Hochschild, who always supported me throughout my Ph. D. This thesis would not have been accomplished without the encouragement of the University of Palermo and the University of Tübingen who gave me the possibility to carry out my research.
Furthermore, I would like to heartily thank Dr. Christian Conoscenti, Dr. Michael Märker and Dr. Edorado Rotigliano, who guided me through the analytic and statistic modelling and for their always motivating advices.
Moreover, I want to enunciate my warmest thanks to Dr. Lucia Fallo for the provided opportunity to work in the sedimentology laboratory and for her unlimited courtesy I experienced.
Geraldine, thank you so much for your time and words, not only based on work.
A particular thanks to Mich for his linguistic advices.
Certainly I would like to thank my whole family for all their support and for never loosing trust in me and all my friends who always built me up and made me laugh.

Abstract

The present thesis aimed to explore the methodological advantages as well as limitations in applying different modelling approaches to predict water soil erosion in Mediterranean environments. The research was accomplished in the central northern part of Sicily (Italy), considering this region to be representative of Mediterranean environmental conditions. In this region soil degradation problems, due to water erosion are becoming more and more serious. Consequently, defining models being able to predict erosion susceptibility and to discriminate environmental factors causing erosion is important to protect soil resources.

The prediction of the spatial distribution of soil erosion processes was carried out by means of GIS tools and multivariate statistical analysis.
A stochastic gradient boosting model (TreeNet) was proposed to classify erosion and mass wasting processes and to define the functional relationship between spatial data sets of driving factors and response variables. The TreeNet method allowed identifying a susceptibility model that accurately fits the relationship between a set of several attributes and the activity of different erosion processes with a high resistance to over-training. Moreover, a better understanding of the prediction model was provided by the evaluation of the relative overall importance of the predictive variables in the tree construction. In order to estimate the overall prediction skill of the model, the ROC (Receiver Operating Characteristic) curves for each of the predicted process were constructed. Results illustrated an outstanding and excellent performance of the TreeNet method to predict bank and gully erosion, respectively. Sheet and rill erosion and mass wasting phenomena prediction attested to acceptable and poor performance of the model. The erosion susceptibility model was exploited to regionalize the information in areas characterized by the same geo-environmental conditions.

Among erosion processes, gully susceptibility was most intensely investigated due to their high contribution to soil loss in the Mediterranean. A GIS layer containing 260 ephemeral and permanent gullies was constructed by field surveys and interpretation of high detailed aerial images and a set of 27 environmental attributes was selected as explanatory variables. The statistical analysis was defined on the scale of grid cells and slope units. The functional relationships between gully occurrence and spatial variability of the controlling factors was explored by carrying out forward stepwise logistic regression

analysis that allowed to calculate the probability of mapping units hosting gullies. Results of validation showed acceptable to excellent accuracy of the predictive models, illustrating a more stable performance of susceptibility models defined on cell scale. Finally, further logistic regression analysis was carried out to generate a cell- and a slope-unit based gully erosion susceptibility map, both demonstrating an excellent fitting precision.

Furthermore, a procedure to evaluate the impact of anthropogenic activity on soil erosion dynamics by means of empirical methods was proposed. In cultivated catchments, man-induced elements influencing runoff processes are mainly linked to alteration of original terrain morphology and to the consequently spatial soil redistribution pattern.
In order to simulate the impact of anthropogenic elements on soil loss, data related to the characteristics of these rural elements and to their spatial distribution in the basin were collected and included in soil erosion modelling procedures. The interplay between the RUSLE (Revised Universal Soil Loss Equation) and the USPED (Unit Stream Power Erosion Deposition) models allowed to define the spatial distribution of man-induced impacts on soil erosion processes. In the study area farmer activities play an important role in modifying the natural flow-path, on both field and basin scale. Unpaved roads resulted the main cause of important transformation mechanisms in the agricultural landscape. These linear features influence the drainage patterns and consequently soil erosion dynamics.

The results of this study confirmed the reliability of the adopted methods that are objective, reproducible and able to be exploited to produce accurate erosion susceptibility maps: A useful instrument for land management and planning. In addition, the research demonstrated that spatial occurrence of erosion processes is strongly influenced by human pressure modifying the natural flow path of water, underlining the necessity to more specifically include this factor in erosion prediction modelling.

Zusammenfassung

Die vorliegende Dissertation zeigt sowohl die methodologischen Vorteile, als auch die Grenzen der Anwendung unterschiedlicher stochastischer und quantitativer Modelle zur Vorhersage von Bodenerosion im Mittelmeerraumauf. Mit der Wahl des Forschungsgebietes im nördlichen Teil von Sizilien (Italien), stellvertretend für die allgemeinen mediterranen Umweltbedingungen, wurde ein Raum bestimmt, der zunehmend von Degradations- und Desertifikationsprozessen betroffen ist. Diese sind zumeist auf extreme Bodenabspülungs- und Abtragungsvorgänge zurückzuführen. Folglich ist es unerlässlich, Vorhersagemodelle zur Bodenerosionsanfälligkeit zu erstellen, um die natürlichen Bodenressourcen zu schützen.

Unter Einbeziehung von GIS Methoden und multivariater Statistik konnte eine Voraussage der räumlichen Verteilung von Bodenabtragungsprozessen im Untersuchungsraum erstellt werden. Ein stochastischer Verlauf (TreeNet) beschreibt und klassifiziert Erosions- und Massenverluste und definiert gleichzeitig die Beziehungen zwischen den räumlichen Umweltfaktoren und den Erosionsformen als abhängiger Variable. Die Methode des stochastischen Entscheidungsbaumes erlaubt es, ein Vulnerabilitätsmodell zu erstellen, das die Beziehungen zwischen den Attributen und den Bodenabtragungsprozessen eindeutig charakterisiert. Um die Vorhersagegenauigkeit des Modells zu prüfen, wurden “ROC (Receiver Operating Characteristic) curves“ für jeden einzelnen Vorhersagefall erstellt. Die Modellergebnisse zeigen hervorragende Leistungseigenschaften für die Vorhersage von Seiten-/Ufererosion und ausgezeichnete Passgenauigkeit für Erosionsrinnen (Gullies). Die Vorhersage von flächenhaften Erosionsprozessen (Rillen-Interrillenerosion) hingegen erreichte bei der Modellierung nur ausreichende bzw. keine zufriedenstellenden Ergebnisse. Im Folgenden sind die Resultate der TreeNet Modellierung ausgewertet und auf Gebiete übertragen worden, die die gleichen physiogeographischen Bedingungen aufweisen (Regionalisierung).

Besonderes Augenmerk wurde auf den Bodenabtrag durch Gullies gelegt, die vor allem im Mittelmeerraum für den zunehmenden Grad an Degradation verantwortlich sind. Hierfür wurde ein GIS-Layer mit ca. 260 ephemeren und permanenten Erosionsrinnen erstellt, der aus hochauflösenden Luftbildern abgeleitet und im Gelände validiert wurde. Drüber hinaus wurde aus einem digitalen Höhenmodell ein Set von 27 Umweltattributen

gewonnen. Die statistische Auswertung wurde im Maßstab der Rasterzellengröße und spezifischen topographischen Hangeinheiten durchgeführt. Ein räumlicher Zusammenhang zwischen Gully-Auftreten und den vorherrschenden Umweltfaktoren wurde anhand von logistischer Regressionsanalyse erstellt. Zusätzlich wurden die Analysen in Hinblick auf spezifische topographische Hangbereiche ausgewertet. (terrain-units). Die Ergebnisse zeigten eine befriedigende bis ausgezeichnete Genauigkeit der Vorhersagemodelle, wobei die Vulnerabilitätsmodellierungen im Rasterzellenformat die beständigsten Ergebnisse zeigten. Um letztendlich eine Risiko- und Vorhersagekarte von Erosionsprozessen auf Basis von Raster- und Hangeinheiten zu erstellen, sind weitere logistische Regressionsanalysen durchgeführt worden, die allesamt eine herausragende Qualität aufweisen.

Um die Auswirkungen der anthropogenen Einflussfaktoren auf Bodenerosionsvorgänge abzuschätzen, sind Feldstudien in landwirtschaftlich genutzten Gebieten durchgeführt worden. Diese zeigen zumeist ein stark verändertes oberflächliches Abflussverhalten und unterliegen folglich einem neugeordneten Sedimentations- und Depositionsregime. Anhand der Erosionsmodelle RUSLE (Revised Universal Soil Loss Equation) und USPED (Unit Stream Power Erosion Deposition) wurde die räumliche Verteilung der anthropogenen Einflussfaktoren bestimmt und in die Bodenerosionsmodellierung mit einbezogen.
Landwirtschaftlich überprägte Flächen und unbefestigte Wege sind Kennzeichen des anthropogenen Landoberflächenwandels und beeinflussen das natürliche Abflussverhalten und somit auch die Bodenerosionsdynamik.

Die Forschungsergebnisse veranschaulichen nicht nur die Zuverlässigkeit der angewandten Methoden sondern vor allem die Möglichkeit der Regionalisierung und Ausweitung der statistischen Analyse auf geomorphologisch identische Flächen und somit das Erstellen von geeigneten Risiko- und Gefahrenkarten hinsichtlich Bodenerosionsvorgängen. Diese liefern heutzutage in der Planung und im Oberflächenmanagement einen wichtigen Beitrag zur Vorhersage von Auswirkungen des Landnutzungswandels. Die zunehmende räumliche Ausdehnung von Degradations- und Desertifikationvorgängen ist nicht zuletzt anthropogenen Ursprungs und unterstreicht die Notwendigkeit, Bodenerosionsprozesse in zukünftige Vorhersagemodellierungen mit einzubeziehen.

Chapter 1

INTRODUCTION

1.1 Significance of soil erosion in the Mediterranean

Erosion by water is a natural geologic process that has created vast zones of fertile soils on alluvial flood plains around the world. However, the accelerated soil loss by anthropogenic impact is considered a destructive process that also prevents the reformation of fertile soils. On a global scale, soil erosion triggered by water contributes severely to land degradation and desertification processes (Eswaran et al., 2001). Authors tried to define a numerical relation between morphogenetical and pedogenetical processes. Pimentel et al. (1976) consider an upper limit of acceptable soil loss of about 11-12 ton/ha/year, corresponding to a formation rate of 25 mm of soil in 30 years. Barrow (1994) estimated that the soil loss is currently 16–300 times faster than its development and consequently soil is essentially a non-renewable resource.

On continental scale, countries are differently affected in severity, depending on their spatial, economic, environmental and cultural context. UNEP[1] (1986) estimated that 2 billion hectares of land, that was once biologically productive, has been irreversibly degraded since 1000 AD. Brown (1984) evaluated a global erosion soil loss of 26 billion Mg/ha/yr, while Oldeman (1994) affirmed the area affected by severe water erosion is 1094 Mha, of which 751 Mha are severely affected. In Europe 11% of the used land is considered to be affected by severe water erosion problems (Oldeman, 1994). Among that, the Mediterranean countries are considered the most vulnerable ecosystem (Kosmas et al., 2000). Moreover the Mediterranean region is characterized by a history of agricultural activity of more than eight thousand years (Butzer, 2005). That, together with a significant increase in runoff and erosion caused by extreme precipitation events (Nearing, 2001), modified the geomorphological and hydrological dynamics on the hillslope-drainage network, leading to further mass movements and finally soil loss.

Direct consequences of soil erosion create strong environmental impacts and high economic costs by its effects both on local and regional scale. It can affect agricultural production and contribute to the contamination and quality of water resources (Pimentel et al., 1995). Moreover, soil erosion decreases the organic matter content, the fine grained soil particles content, the water holding capacity and the depth of the top soils (Ritchie, 2000). Indirectly, erosion can lead to or reactive superficial landslides (Conoscenti et al.,

[1] United Nation Environmental Program

2008b), by locally increasing the steepness of the slopes, damaging infrastructure and constituting a risk for population security.

In the last 40 years the scientific world community recognized the importance of protecting and restoring the soil resources on international scale. The Rio summit (UNCED, 1992), UN Framework Convention on Climate Change (UNFCCC, 1992), the Kyoto Protocol (UNFCC, 1997) and the UN Framework Convention to Combat Desertification (UNFCD, 1996) are some of the international conferences where soil erosion problems were taken into account. They have been considered one of the main causes of soil degradation, desertification process and consequently loss of biodiversity, threat to food security and increase in world poverty. On a global point of view soil erosion phenomenon is a considerable source of soil organic carbon emission to the atmosphere in form of CO^2 and CH^4, causing impact on global warming (Lal, 2004).

The present thesis research investigates the significance of erosion and sedimentation processes in the Mediterranean region[2]. Countries of the Mediterranean basin are characterized by a history of agricultural activity of more than eight millennia (Butzer, 2005) and a similar socio-cultural heritage.
During the last decades, the meteorological conditions showed a significant increase of erosive power of rainfall (Nearing, 2001). Consequently geomorphological and hydrological dynamics on the hillslope-drainage network system changed as well. In this context, analyzing and modeling the processes that contribute to an increase of soil degradation is important in order to reduce additional socio-economic and environmental effects.

Previous studies showed that rapid and uncontrolled land use changes (e.g. land abandoning, tillage mechanization, deforestation, soil sealing, etc.) are one of the main causes of soil loss increase in Mediterranean basins (e.g. Martìnez-Casasnovas and Sànchez-Bosch, 2002, Van Rompaeya et al., 2007, Märker et al., 2008).

[2] The term “Mediterranean region” in the present thesis regards to as the catchment limits of the area contributing to the Mediterranean Sea, excluding the other Mediterranean bioclimatic zones of the world (central coastal California, central coastal Chile, the southern tip of Cape Province, South Africa and the southern extremities of Western and South Australia).

Human activity influences soil erodibility and rain erosivity, contributing to destroy natural vegetation and modify the morphological setting by covering with artificial elements (roads, bridges, caves, etc). Moreover the human pressure contributes indirectly to global climatic change. The potential impact of climate change on erosion processes can be associated by shifts in mean annual rainfall amount, rainfall intensity and temporal distribution.

1.2 Erosion processes

Water, wind and gravity are the principal factors of erosion processes. Energy supply by these physical agents determines the detachment and transport of soil particles. Deposition is the third and last phase of erosion phenomenon, and occurs when energy apply by the erosive agents is not sufficient to transport soil particles. The distance of physical displacement may range from a few millimetres to thousands of kilometres, and the time lap from detachment to eventual deposition may range from some seconds to thousands of years (Lal, 2001).

The erosion process starts when raindrops strike the surface of the soil and break down clods and aggregates (Ellison, 1947). This is commonly referred to as rainsplash or raindrop splash erosion (Thorne, 1990). Raindrops cause disaggregation and splashing of soil particles and at the same time surface compaction, reducing the soil infiltration capacity (Pagliai, 1988). In addition, raindrops falling on wet soil form a crater; that is accompanied by a blast which bounces water and soil back into the air forming a circle around the crater. The impact of rain is linked to the kinetic energy of precipitation and its spatial and temporal distribution during a storm event.

Runoff processes occur when water produces a shear stress on the soil surface that can detach and transport the sediment rate. Runoff generates a thin sheet across the soil surface called sheet flow. Two basic processes are involved in sheet flow genesis: first, soil particles are detached from the body of the soil, and second the particles are transported away from their original location. At the beginning of a rain storm event falling raindrops are able to detach much larger amounts of soil particles than runoff processes. If the rainfall continues, the flowing water entrains and transports detached particles along the slope (Hudson, 1995).

Several factors control overlandflow phenomenon, including: Morphological conditions, soil texture and structure, initial moisture content, flow depth and rate, presence of cracking and swelling on soils, vegetation density and organic matter content. Former researches demonstrated the existing of three different mechanisms by which storm overlandflow may be generated: Horton overland flow, Subsurface flow and Saturation overland flow (Dunne, 1983). The latter is developed during a rain event when the soil becomes saturated by the perennial groundwater table, rising to the surface, or by lateral or vertical percolation above an impeding horizon (Dunne and Black, 1970). The soil saturation transports groundwater slowly through the topsoil emerging and flowing over the ground surface (Dunne, 1983). Subsurface flow occurs when part of the infiltrated effective rainfall circulates more or less horizontally in the superior soil layer and appears at the surface through drain channels. The presence of a relatively impermeable shallow layer favours this flow. The subsurface flow in unsaturated regimes can be the base flow in the area with large slopes and dominant in humid regions with vegetal covering and well-drained soils (Dunne, 1983).

In arid and semiarid landscapes, where vegetation density and therefore infiltration rates are low, and in disturbed area of humid landscapes (e.g. cultivated fields, paved areas, rural roads) storm runoff is principally generated for Hortonian overland flow (Dunne, 1983). This term was introduced by Robert E. Horton (1933), who first developed a theory of the relationship between infiltration and runoff and their consequences for land and water management. The Hortonian overland flow occurs when rainfall rate exceeds the infiltration capacity of soil and water starts to flow in the direction of the steepest unimpeded slope. The occurrence of this kind of overlandflow depends mainly on the surface characteristics that control infiltration, morphology, vegetation and soil type (Dunne, 1983).

When overland flow converges from various regions of the upland area, it becomes more concentrated. Depth and velocity of sheet flows reach critical values that do not allow the laminar flow to be maintained; consequently turbulent water flow is generated. Overlandflow becomes sufficiently erosive forming shallow channels, referred to as “rills”; small drains on the slope surface that are sediment source area and sediment transportation route (Lei et al., 1998). In the area between two rills runoff occurs, and is

also referred to as ‘inter-rill erosion’. In the inter-rill area erosion processes are dominated by precipitation, whereas in rill channels erosion is mostly defined by runoff.

Runoff water accumulation and flowing in narrow channels can, over short a period, remove soils from narrow areas at considerable depth. In this particular situation gully erosion occurs (Morgan and Nearing, 2011). Gullies represent an important source in dry land environments, contributing on average 50-80% on sediment production (Bull and Kirkby, 2002). In gully erosion, the action of raindrop impact is not considered an important process in terms of sediment particle detachment (Poesen et al., 2003). Runoff process is not the only geomorphological process affecting gully genesis and development (Fig. 1.1).

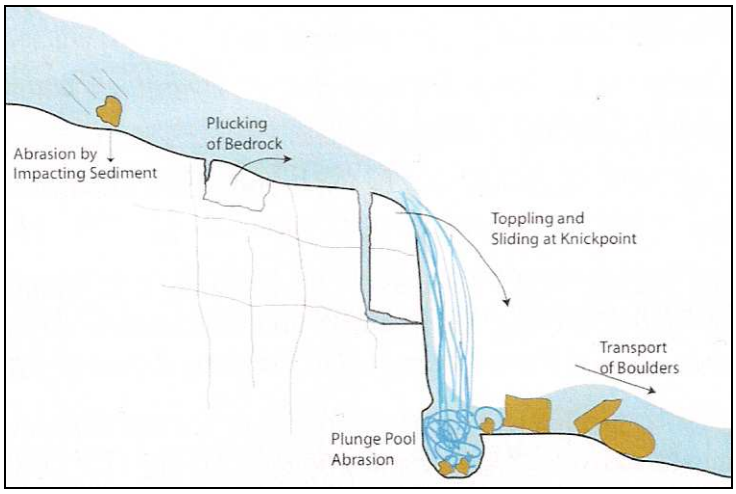

Figure 1.1. Erosion and transport processes at the gully headwall. Source: Lamb (2008).

Often, it is possible to recognize mass wasting processes on the gully-head area and gully walls (principally slumping and block failure), when slope stability is reduced by undercutting or loss of soil cohesion. Cracks in gully walls are also cause of side-wall instability. The macro-porosity that characterizes the cracked soils maintains the preferred path of overlandflow-waters expanding fissures, isolating cracks and triggering the sidewall falls. In general the collapsed material tends to modify the cross section of the

gully, transforming a rectangular gully cross-section shape into trapezoidal form (Sidorchuk, 1999), and contributing to the retreat of the gully head position.

Moreover, two subsurface process, seepage and piping, can be involved in gullies development. The origin and progression of gullies has often been related to piping or tunnel erosion where high hydraulic gradients occur in dispersive materials. Piping may have an important role in the beginning and development of bank gullies and gullies forming on badlands areas in the Mediterranean area (Poesen et al., 2003, Buccolini et al., 2010). Seepage is groundwater that emerges from rocks or sediments. It determines instability of gully head walls, leading to mechanical and chemical erosion and consequently to wall collapse (Lamb, 2008).

1.3 Factors controlling soil erosion

The interplay of climate, lithology, vegetation, morphological conditions and human pressure defines the location and extent of the different types of erosion processes. These factors can influence two important environmental properties: Erosivity and erodibility. Their balance characterizes erosion process entity. Erosivity is referred to the capacity of rain and runoff to provoke erosion (rain erosivity), while erodibility is defined as the inherent resistance of soil to erosion processes (soil erodibility). Both proprieties are influenced by the presence of vegetation. The canopy and the litter intercept raindrops reducing the raindrop impact and overlandflow, influencing physical properties, such as water storage capacity, bulk density, porosity and roughness. Moreover, the organic carbon increases the formation of soil aggregates and so decreases soil erodibility.

In Mediterranean landscapes, different studies tried to qualify and quantify the role of vegetation cover in runoff processes. Lopez-Bermudez et al. (1998) demonstrated in experimental plots, how runoff and sediment loss rates depend on the efficient control of vegetation cover, even in abandoned fields where a good capacity to recover its pedological and vegetation characteristics after disturbances was recognized (Fig. 1.2).

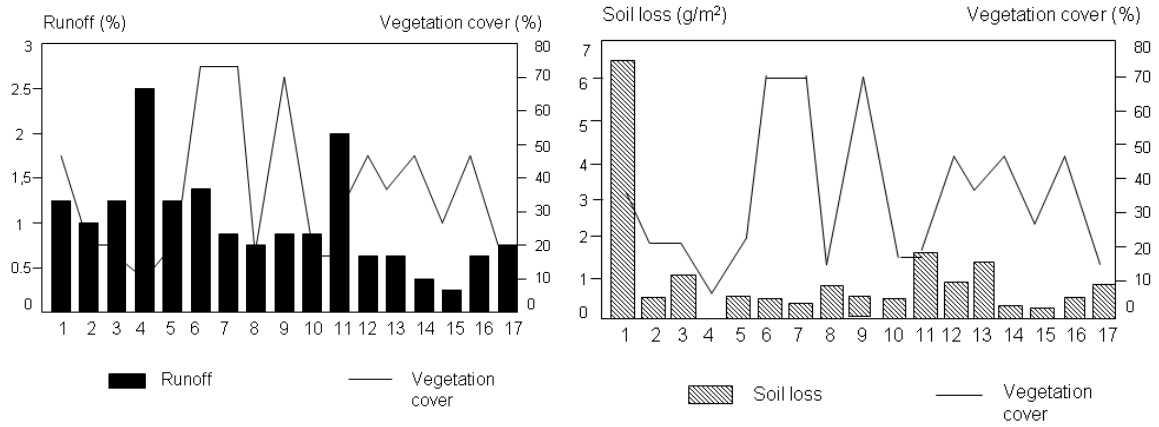

Figure 1.2. Relationship between runoff–vegetation cover and soil loss–vegetation cover. Source: Modified from Lopez-Bermudez et al. (1998).

Recent investigations (e.g. Martìnez-Casasnovas and Sànchez-Bosch, 2002, Van Rompaeya et al., 2007, Märker et al., 2008) showed that rapid and uncontrolled land use changes (e.g. land abandoning, tillage mechanization, deforestation, soil sealing, etc.) are one of the main causes of soil loss increase in Mediterranean basins. Human activity influences soil erodibility and rain erosivity, contributing to destroy natural vegetation and modify the morphological setting by covering with artificial elements (roads, bridges, caves, etc.).

Furthermore, the human pressure contributes indirectly to global climatic change. The potential impact of climate change on erosion processes can be associated by shifts in mean annual rainfall amount, rainfall intensity and temporal distribution. Different scenarios have been worked out for the Mediterranean environment; the most accepted assumes that temperature and precipitation trends will lead to conditions similar to those dominating arid and semiarid landscapes (Lavee, 1998). Figure 1.3 shows the water redistribution processes and spatial patterns under different climatic conditions from arid to semiarid and humid zones.

Principal factors influencing the rain erosivity are intensity and precipitation amount. In the Mediterranean, the frequent occurrence of convective events and the presence of long dry periods followed by heavy bursts of erosive rainfall are causes of high soil vulnerability

potential (Wainwright and Thornes John, 2003). The erosivity of superficial runoff is a function of rain intensity, water flow velocity, vegetation cover and morphological characteristics of the surface. Roughness, slope and depth of the flow are some of the features that can be considered to analyze the extent of runoff processes.

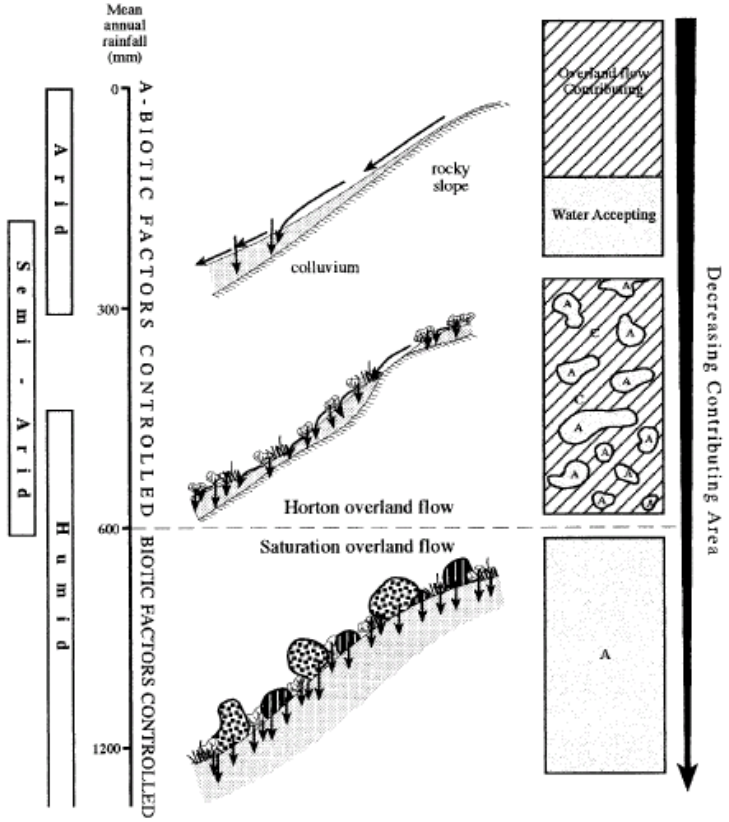

Figure 1.3. Rainfall redistribution under different climatic conditions (A: Water accepting area; C: Overland flow contributing area). Source: Lavee et al. (1998).

Erodibility is principally related to soil moisture and structure, texture, mineralogical and chemical composition of substrates. These characteristics influence temporal and spatial variability as well as shape and type of the runoff process (Hochschild, 1999). Soil with medium to fine texture, low organic matter content and weak structure is characterized by a high erosivity (Bajracharya and Lan, 1998). In semiarid and arid environments of the Mediterranean region, soils are characterized by low organic content and significant

amount of rock fragments, parameters considered decreasing erodibility (Poesen 1992, Valentin, 1994).

1.4 Morphology and classification of erosion landforms

A landform is defined as a physical feature of the earth's surface having a characteristic recognizable shape produced by natural causes (Bates and Jackson, 1995). Erosion landforms can be described by analyzing their general structure and shape and defining its dimensions (morphometry); these parameters are some of the possible keys to deduce the dominant geomorphic process responsible for the nature, origin and development of the landforms. Mediterranean landscape is characterized by features that are related to erosion in its various forms. In the majority of regions, water erosion and mass movements are the dominant processes because of the high relief energy that dominates wide parts of the region.

Regarding to water erosion landforms classification, a first big distinction can be done in relation to the spatial distribution and shape of the erosion features along the slope, consequently leading to two kinds of erosion processes: Diffuse and linear.
Rainsplash and sheet flow are disturbance-driven processes that have been termed diffusive because of the resulting sediment flux is thought to be primarily slope-dependent (Roering et al., 1999). Sheet erosion removes a thin layer of fertile soil, easily recognized in landscape by its typical light-coloured soil patches on hillsides. Often, when sheet flow is the dominant erosion process in the slope, the soil organic matter is loose and soil aggregates are destroyed, resulting in reduction of vegetation and soil cover on the surface. Sheet erosion in Mediterranean areas is often associated with pasture activities; Animals crossing and standing cause soil compaction and grass vegetation cover destruction.

Runoff remains diffuse until it is able to transport the detached particles, but unable to initiate incision. Rills and gullies (Fig. 1.4) are runoff products, that develop in concentrated flow zones, located not only in natural drainage lines, but also along (or in) linear landscape elements, such as drill lines, dead furrows, parcel borders and access roads (Poesen, 1993).

Both rills and gullies are characterized by linear shape (rills often parallel at the top of the hill and convergent at the bottom) and a clear distinction between these two landforms is not yet provided. Different Authors tried to develop an objective criterion to distinguish these two landforms. Hauge (1977) proposed to use a critical cross-sectional area of 929 cm^2. Other criteria include a minimum width of 0.3 m and a minimum depth of about 0.6 m (Brice, 1966), or a minimum depth of 0.5 m (Imeson and Kwaad, 1980). Nevertheless, it must be acknowledged that the transition from rill to ephemeral gully represents a continuum and any classification of this hydraulic erosion form into separated classes can be objective (Morgan and Nearing, 2010).

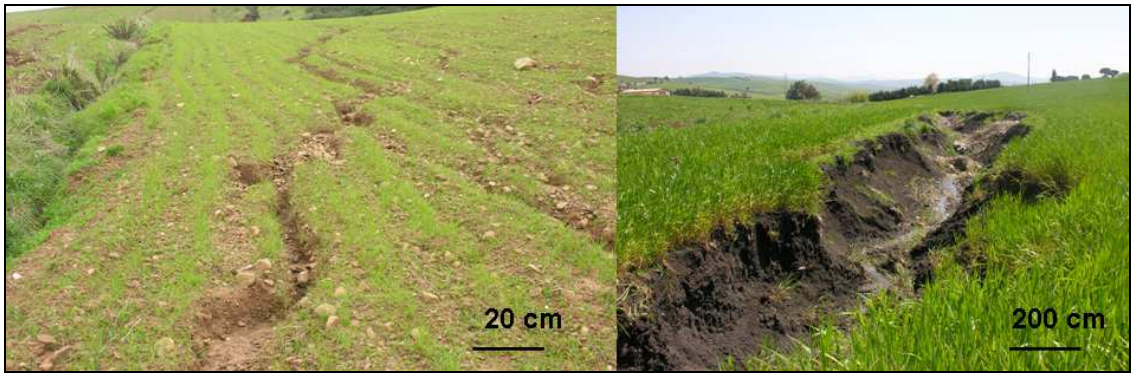

Figure 1.4. Rill (left) and gully (right) erosion processes in crop fields (Sicily, Madonie Mountains, 15.04.2010).

When rills and gullies are able to transport a great amount of sediment it's possible to recognize a depositional area, occurring when the overland flow meets a lower slope. The deposited sediment is often characterized by the presence of fine material that may cause surface sealing and consequently reduces water infiltration and ventilation. As consequences anaerobic conditions underneath the sealed surface and the oxygen content decreases, reducing roots development. Sodium or sodic clays may also be deposited by the floods. The sodium interferes with most crop plant growth and can cause soil dispersion.

Regarding gullies, different criteria can be adopted to classify and describe them. Observing their morphological characteristics, gullies can be described by:

- plan form (linear, bulbous, dendritic, trellis, parallel and compound gullies, axial gullies with a single headcut, digitate and frontal gullies);
- position in the landscape (valley-floor, valley-side, valley-head gullies, or bank and hillslope gullies, continuous and discontinuous gullies);
- shape of gully cross-section (V and U-shaped gullies).

Foster (1986) introduced the term ephemeral gully erosion to include concentrated flow erosion, larger than rill erosion but less than classical gully erosion. They are considered small channels that can be easily filled by normal tillage, even if they tend to reform again in the same location (Soil Science Society of America, 2001). Poesen (1993) suggested classifying ephemeral gullies using the width/depth ratio. Deep, narrow and wide gullies are respectively characterized by with/depth ratio minor, equal and bigger than 1, corresponding to an increase of potential total soil loss and crop damage.
Moreover, a common distinction, based on temporal variability and/or consequences with field tillage operations, can be operated between permanent and ephemeral gullies. The Soil Science Society of America defined as permanent gullies channels too deep to be easily ameliorated with ordinary farm tillage equipment. Their cross section typically ranges from 0.5 to as much as 25–30 m depth (Poesen et al., 2003).

In gullies, longitudinal and transversal profile shapes (gully length, depth and width of the cross section) are important parameters that have been the object of several monitoring activities and measurements of soil loss rate. Moreover the headcut position of a gully, characterized by an abrupt change in elevation, can be considered the principal source of sediments and its slope migration is one of the main parameters investigated in soil erosion processes.

In clay substrates it is often possible to observe the presence of typical plunge pools (Fig. 1.1). This morphological element can contribute to the headwall instability and gradual retreat. Plunge pool development is essentially controlled by water flow erosivity (water fall height and unit flow discharge) and soil erodibility characteristics (Louise et al., 2002). Study results established different quantitative equations, based on topographic and

environmental factors (e.g. slope, drainage basin area, land use), to predict gully starting position in the slope and gully retreat rate during the time (Poesen et al., 1993).
Before being deposited eroded soil is transported over a certain distance depending on landform characteristics, roughness and magnitude of runoff events. Not all of the detached and transported soil enters the river network. Continuous gullies form parts of the river network (zero-order river or bank gully). Unlike discontinuous they are connected with the rest of the drainage system and considered an important source of sediments. Eroded and evacuated sediments from continuous gullies rapidly take part of the stream sediment yield.

Recent studies suggest that most of the sediment transported by streams is deposited in sinks during and after rainstorms. The mass flow originated from landslides and landslide–gully complexes located in headwater catchment, directly connected with the river network (Hicks et al., 2000). Regarding continuous gullies, literature offers limited criteria to distinguish between gullies and 1st order river channels. Montgomery and Foufoula-Georgiou (1993) established an interval of upslope contributing area, from 10^4 m^2 to $10^6 m^2$, as transitional area for hydrological hillslope and channel processes beginning

Concerning environmental conditions, if intense sheet and gully erosion occurs accompanied by several mass wasting and piping processes, typical badlands landscape can be generated. Badlands (or *Calanchi*) indicate an extremely dissected landscape, characterized by steep and barren slopes (Phillips, 1998; Moretti and Rodolfi, 2000). Those landforms preferentially develop in regions, as the Mediterranean, characterized by both strong climatic oscillations, with changes in humid and arid conditions, and considerable anthropogenic pressure (pastures, periodic fires, etc.,) (Fairbridge, 1968).

1.5 The Sicilian Inland as experimental area

Sicily is one the largest islands in the Mediterranean (25,707 km^2), situated between 36° and 38° N and between 12° and 15° E. Due to its bar ycentre position in the middle of the Mediterranean Sea, Sicily can be considered an ideal laboratory to analyze the relationship between driving factors and erosion processes.
This statement is due to three main environmental characteristics:

- the high variability of climatic condition;
- the rapid land use change;
- highly erodible soils.

Rainfall data of Sicily shows a growing complexity from annual to monthly scale up to single extreme events. Meteorological data analysis (period 1954-2005) marked a significant spatial and temporally (within decades) variability in the pluviometric regime (Drago et al., 2000). D'Asaro et al., (2007), by analysing rainfall intensity trends in Sicily (datasets from 1916 to 1999), concluded that no significant drift can be recognised on regional scale, while both, negative and positive trends have been noticed locally. However, observing anomalies on daily precipitation rate, during the period 1952–2008, Sicily registers the highest positive rate anomaly (0.4 mm/day) respect to the entire Mediterranean area (Grauso et al., 2011).

The actual land use in Sicily is predominantly typified by agricultural surface (about 63% of the whole area); main crops are grain, vine, olive, citrus, pure and mixed fruit trees and various traditional agro-forestry systems of cultivation. A study, conducted by Falcucci et al. (2007), about the changing land-use/land-cover pattern in Italy over the last 40 years, pointed out the general and intense changes that occurred from 1960 to 1990 in the Sicilian Region (Fig.1.5).

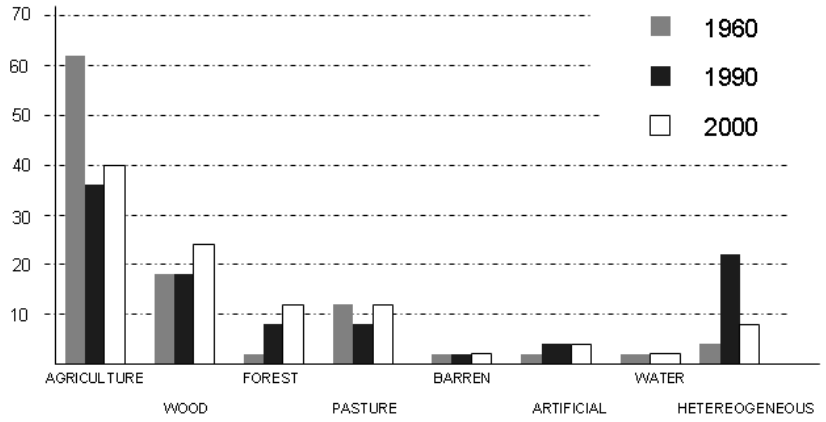

Figure 1.5. Land cover changes in Sicily for the period 1960–2000. AGRICULTURE indicates ''Agricultural areas'', WOOD ''Wood cultivations''; FOREST ''Forests''; PASTURE ''Pastures and grasslands''; BARREN ''Barren areas''; ARTIFICIAL ''Artificial areas'', HETEROGENEOUS ''Heterogeneous agricultural areas'', WATER "Water bodies". Source: Modified from Falcucci et al. (2007).

The outcropping lithologies are mainly built by clayey and marly-clayey substrates, limestone and clastic materials. About 62% of the Sicilian surface is characterized by hills, while 24% can be ascribed to mountains and only 14% to plains. Substrates are mainly represented by less-developed soils, Regosols and Lithosols, characterized by high erodibility, subjected to a continuous organic matter deployment and to a destruction of soil aggregates (Fierotti,1988).

As a consequence of described natural and anthropogenic factors influencing soil erosion processes the fertile top-soil is deteriorating, causing the impoverishment and land abandoning of the region, whose socio-economic conditions are critically based on agricultural activities.

Chapter 2

OBJECTIVES

2.1 Main goals

The aim of the research described in this thesis is to explore the possibility to predict soil erosion by applying statistical and empirical methods, and to develop a simple procedure to evaluate the impacts of anthropogenic factors on soil loss.
The specific objectives of this study are:

I. to analyze the functional relationship between dependent and independent variables for accurate qualitative erosion and mass wasting susceptibility mapping;
II. to achieve the spatial variability of gully erosion susceptibility by using two different types of mapping units: grid cells and slope units;
III. to define a methodology to evaluate the impact of man-induced elements on soil erosion processes in agricultural catchments.

2.2 Research framework

The central aspect of the present research is to explore the methodological advantages as well as limitations in applying different modelling approaches to predict soil erosion by water in the Mediterranean, using the Sicilian region as experimental area.

In Sicily the increase of soil erosion and degradation problems during the last decades, as testified by the soil resource impoverishment and by the high frequency of superficial landslide occurrence, led to the investigations of erosion triggers and the possible feedback prediction. Several works related to soil erosion and mass wasting problems were developed in this region; they are mainly focused on the solution of empirically and physically based models (De Jong et al., 1999, Amore et al., 2004, Conoscenti, 2006, Bagarello et al., 2011, Di Stefano and Ferro, 2011) and probabilistic-phenomenological methods (Capra and Scicolone, 2002, Conoscenti et al., 2008a, Conoscenti et al., 2008b, Rotigliano et al., 2011, Conoscenti et al., 2011, Agnesi et al., 2011).
By considering the scarcity of experimental data and the limited works conduced in the Sicilian region, the present thesis aims to contribute to add a gusset to the state of the art of knowledge.

At watershed or regional scale empirically and physically based models are hardly applicable, because of the high resolution required for the input data and of the high cost and time consuming procedures used for morphometric measures; as a consequence, a statistical approach is usually preferred when susceptibility for large areas is investigated.

A common measure of the probability of occurrence of soil erosion processes in a specific area can be evaluated using the susceptibility concept; the measure of this propriety consist on the ordinal categories of probabilities for relative frequency or density of specific erosion processes in homogeneous terrain entities. Methods exploited to define susceptibility conditions to hydrogeological hazards are based on the principle that new landforms are more likely to occur under the same environmental conditions that, in the past, led to their formation (Guzzetti et al., 1999). These conditions can be identified on the basis of statistical relationships between the spatial occurrence of landforms and the variability of a set of physical attributes; the environmental parameters, which are supposed to express the controlling factors of the erosion process, are taken as explanatory variables to predict the behavior of the dependent variable.

Several statistical modeling techniques have been applied to represent the propensity of an area to soil erosion processes and to investigate the relative importance of specific environmental variables: Multivariate analysis (e.g. Conoscenti et al., 2008a); Logistic regression (Meyer and Martinez-Casasnovas, 1999, Ohlmacher and Davis, 2003, Ayalew and Yamagishi, 2005; Mueller et al., 200, Nefeslioglu et al., 2008, Nandi and Shakoor, 2009, Akgün and Türk, 2010, Bai et al., 2010, Yalcin et al., 2011, Lucà et al., 2011), Decision Tree models (e.g. Kuhnert et al., 2007, Märker et al., 2011); Multivariate Adaptive Regression Splines (Gutiérrez et al., 2009a); Bayesian models (e.g. Neuhäuser and Terhorst, 2007, Rouet et al., 2009); Artificial intelligence tools (Artificial Neural Network and Fuzzy Logic, e.g. Mitra et al., 1998, Tayfur et al., 2003) and CART analysis (Geissen et al., 2007, Bou Kheir et al., 2007, Gutiérrez et al., 2009b). Many of the mentioned statistical approaches focused on evaluating landslide or erosion susceptibility and only few analyzed different geomorphological processes in the same breath.

Moreover, between erosion processes gullies, that in the Mediterranean significantly contribute in soil loss problems (10% up to 94% of the total erosion, Poesen et al., 2003), received not enough interest from scientists. Gully erosion studies have been principally

focusing on topographic threshold values for initiation, distribution and location of gullies by adopting physical (Montgomery and Dietrich, 1992, Desmet et al., 1999; Samani et al., 2009) or statistical approaches (Kakembo et al., 2009). Alternatively, estimation of soil loss produced by gully erosion is achieved by means of experimental approaches based on morphometric analysis of gullies derived by field and remote data (Vandaele and Poesen, 1995; Martinez-Casanovas, 2003; Casali et al., 2006; Della Seta et al., 2007; Della Seta et al., 2009; Buccolini and Coco, 2010; Cappadonia et al., 2011). A probabilistic function, defined on a multivariate basis, by computing the density of erosion landforms in homogeneous spatial domains, was used by Conoscenti et al. (2008a) to generate susceptibility maps for areal and linear water erosion processes. Similar techniques, but implemented by means of bivariate analysis were exploited for gully erosion susceptibility zonation on watershed scale by Conoscenti et al. (2011), Conforti et al. (2011) and Lucà et al. (2011).

Considering empirical and physical-based deterministic approach several models have been explored under different environmental and socio-economic conditions: The USLE (Universal Soil Loss Equation, Wischmeier and Smith, 1959), the CREAMS (Chemicals, Runoff and Erosion from Agricultural Management Systems; Knisel 1980), the EGEM (Ephemeral Gully Erosion Model; Capra et al. 2005; Merkel et al. 1988; Woodward 1999), the WEPP (Water Erosion Prediction Project, Flanagan and Nearing, 1995), etc. These models are founded on the solution of fundamental physical or empirical equations describing stream flow and sediment transport. The main problem in applying physical methods is that the solution of them involves a large and complex amount of input parameters, often requiring a previous calibration being many of existing empirical models be developed in different environmental conditions (Beck et al., 1995).

Moreover, despite the increase of models able to simulate hydrological components influencing water erosion on catchment scale, few attentions has been shown regarding to the anthropogenic impacts on soil erosion processes. Studies generally investigated the land management factor focusing on generating alternative scenarios to predict land use change impacts and soil loss and design correct policies of land-planning (e.g. Märker et. al. 2008 a, Robichaud et al., 2007, Pacini at al., 2003).

In particular, rural infrastructure such as roads, tillage furrows, field boundaries, ditches and irrigation channels are often linear features part of the permanent drainage network. These elements are known to modify the natural overland flow path and influence runoff process dynamic. Rural infrastructures can contribute to the basin runoff and sediment yield by several mechanisms: (1) Modification of surface roughness and infiltration characteristics due to compaction mechanism (Dijck, 2000); (2) Cut-bank intercepting the subsurface flow by rerouting via the faster overland flow towards a more rapid run off (Costa and Bacellar, 2007); (3) Ditches and culverts capture both, surface runoff and subsurface flow runoff channelling more directly to stream networks (Ludwig et al., 1996; Souchere et al., 1996, Cerdan et al., 2001;); (4) Roads construction can also increase landslide events on road cut-slopes and hillslopes by altering the flow-paths as well as the shear stress and pore water pressures (Costa et al., 2007).

The prediction of man-induced change effects in erosion/deposition dynamics in rural systems was scarcely investigated (Ziegler and Giambelluca, 1997, Jones et al., 2000, Wemple et al., 2001, Motha et al., 2004, Borselli at al., 2008, Märker at al., 2008 b), consequently the relationship between the spatial distribution of linear landscape elements and surface runoff in cultivated catchments is not sufficiently understood.

Chapter 3

METHODS

3.1 Applied methods

To achieve the aims of the present thesis different methodological approaches were employed. The first two goals were reached by using two statistical models as investigator to generate erosion susceptibility maps: the TreeNet and the Logistic regression analysis. Both methods define quantitative relationships between a set of environmental parameters and the occurrence of erosion landforms. Finally the USPED and the RUSLE models were chosen between empirical methods to predict the impact of man-induced elements on soil loss phenomenon.

3.1.1 The TreeNet model

Among existing methods the TreeNet (Salford Systems implementation, cf. Friedman, 1999) was selected to classify different typologies of erosion and mass wasting features in terrain units characterized by homogeneous erosion dynamics (ERUs, Märker et al., 1999). The TreeNet model employs a learning algorithm to identify a model that best fits the relationship between an attribute set (named predictor or independent variables) and a class label of input data (named response or dependent variables). The employed method is a stochastic gradient boosting model (Elith et al., 2008).

The trees construction process splits the observations into subsets, according to whether or not they are less than a particular value of one of the predictor variables: Subsets characterized by similar values for the response variable are formed. The predicted value of the response variable for each node of the tree is the mean of its value for the subset of observations at that node. A variety of impurity or diversity measures exist to chose the best predictor. Particularly, the TreeNet model computes several hundred to thousands of small classification trees, each one contributing to construct a portion of the model. During this training process, each tree improves on its predecessors through boosting. Gradient boosting constructs additive regression models by sequentially fitting a simple parameterized function to current residuals by least squares at each interaction (Friedman, 1999). The model build up procedure incorporates randomness to improve the execution speed and model robustness.

The advantages of using the TreeNet model are related to different strengths: Being not sensitive to data errors in the input variables; automatic variable subset selection; handling data without pre-processing; resistance to outliers; automatic handling of missing

values; robustness to fragmentary, partially inaccurate data; high speed and resistance to over-training (Friedman, 2002).

3.1.2 The logistic regression analysis

The evaluation of gully erosion susceptibility by adopting two different types of mapping units was achieved by the application of a multivariate approach, based on the logistic regression analysis (cf. Hosmer and Lemeshow, 2000). This statistical technique can work with a variety of types of independent variables, such as categorical, binary, ordinal or continuous; moreover, it is free of data distribution constraints (Nandi and Shakoor, 2009; Bai et al., 2010; Yalcin et al., 2011) and robust also when input data is auto-correlated (Davis and Ohlmacher, 2002; Mathew et al., 2009), as often happens when dealing with environmental attributes.

Logistic regression evaluates the probability (P) of an event occurring, by estimating the probability that a case will be classified into one of two mutually exclusive categories as opposed to the other category of the dependent dichotomous variable (Menard, 1995; Ohlmacher and Davis, 2003).

In this study the event occurring is represented by the presence of gully erosion landforms within a mapping unit and the logistic regression is exploited to predict a binary variable that could be equal to 1 (presence of gully) or 0 (absence of gullies). Since 0 and 1 are only arbitrary codes and have not intrinsic meaning, the response variable Y is transformed into a *logit* function of Y, that is expressed as the natural log of the *odds* of the event occurrence or not:

$$logit(Y) = \ln\{P(Y=1)/[1- P(Y=1)]\} \quad (1)$$

where $P(Y=1)$ is the probability that the statement in parentheses is true.

Logistic regression analysis allows for identifying the relationships between the dependent variable (Y) and the independent variables (X), by means of the equation:

$$logit(Y) = \alpha + \beta_1 X_1 + \beta_2 X_2 + \ldots. + \beta_n X_n \quad (2)$$

where α is in intercept of the model, n is the number of independent variables, β_i (i = 1, 2, 3, …., n) is the slope coefficient of the model and X_i (i = 1, 2, 3, …., n) is the independent variable.
By converting the *logit*(Y) back to the probability P that (Y=1), the logistic model can be expressed as:

$$P(Y=1) = e^{logit(Y)} / [1 + e^{logit(Y)}] \quad (3)$$

The equation (3) ensures that, for any given case, the probability $P(Y=1)$ will not be less than 0 or greater than 1, with $logit(Y) = \pm \infty$.

The algorithm of logistic regression applies the *maximum likelihood* technique to maximize the value of the *log-likelihood* (LL) function, the latter indicating how likely it is to obtain the observed values of Y, given the values of the independent variables and coefficients (Menard, 1995). The function LL, multiplied by -2, allows for calculating a statistic, called *negative log-likelihood* (-2LL), which has approximately a χ^2 distribution. The *negative log-likelihood* of a regression model could be used to evaluate its fitting with the observed data: smaller -2LL values indicate a better fitting of the model to the data (Hosmer and Lemeshow, 2000). The difference between the values of -2LL computed for the logistic regression model with only the intercept (D_0) and for the full model (D_M) is usually indicated as *model chi-square* and can be used in χ^2 test of significance of the regression coefficients (Ohlmacher and Davis, 2003; Akgün and Türk, 2010); if the difference (D_0-D_M) is statistically significant ($p \leq 0.05$), the null hypothesis can be rejected, indicating that a better prediction of $P(Y=1)$ is obtained with the contribution of the independent variables (Menard, 1995).

In this study, logistic regression analyses were performed by means of the open source software TANAGRA (Rakotomalala, 2005), adopting a forward stepwise strategy to select the explanatory variables.

3.1.3 RUSLE and USPED models

A new procedure to evaluate the impact of man-induced element in erosion processes is proposed as third objective of the present investigation. The Revised Universal Soil Loss

Equation (RUSLE, Renard et al., 1997) and the Unit Stream Power Erosion/Deposition (USPED, Mitasova et al., 1996) were employed to reach this goal.
They are based on established mathematical equations representing erosion parameters, and were chosen to simulate soil erosion process by the scenario analysis. Both models are empirical methods, based on a different assumption. The RUSLE model estimates soil loss caused by raindrop impact and overland flow (interrill erosion), plus rill erosion. It does not estimate gully or stream-channel erosion; the assumption is that particles detachment is controlled by the sediment content of the flow, when the sediment load reaches the carrying capacity of the flow, detachment can no longer occur (Wischmeier and Smith, 1978). On the contrary the USPED is a model which predicts that spatial distribution of erosion and deposition rated for transport limited case of erosion process (Mitasova et al., 1996). In the RUSLE approach, erosion is calculated only along straight flow lines, without full consideration of the influence of flow convergence and divergence (Warren, 2005). Moreover while the RUSLE only predict erosion, the USPED model can assess both erosion and deposition patterns. A limit of the USPED model, respect to the RUSLE, is that it does not allow to evaluate actual sediment dynamics and time variations of pattern, just the relative strength or intensity of the phenomena.

The RUSLE model is based on five components: R (Rainfall erosivity factor), K (Soil erodibility factor), LS (Topographic factor), C (Cover management factor), and P (Support practice factor). Multiplying these predictor factors the average annual soil loss per unit area (A, t/ha year) is calculate as described in the following:

$$A = R \times K \times LS \times C \times P \tag{4}$$

Soil erosion processes are strictly related to the erosive power of precipitation, expressed by the concept of rainfall erosivity factor (R factor), one of the environmental components of the Universal Soil Loss Equation (USLE, Wischmeier and Smith, 1965), and its revised form (RUSLE, Renard et al., 1997). The R factor is the sum of the individual storm intensity (EI-value) within a year, averaged over a long time scale, to accommodate apparent cyclic rainfall patterns (Renard and Freimund, 1994).
Soil erodibility expresses inherent soil resistance to erosional processes (Bryan, 2000). It can be modelled using the Erodibility index (K factor), inferred from soil loss measured at

standard erosion plots, characterized by a length of 22 m and 9 % slope (Wischmeier and Smith, 1978). K values can be expressed by an empirical equation containing data related to organic matter (OM), soil texture (M), classes of aggregate structure (s) and soil permeability (p).

The LS factor describes the combined effect of slope, length and steepness and can be considered as a measurement of the sediment transport capacity by runoff. Slope length is defined as the horizontal distance from the origin of the overland flow to the point where either the slope gradient decreases enough that deposition begins or runoff becomes concentrated in a defined channel (Wischmeier and Smith 1978).

Regarding C factor, Wischmeier and Smith (1978) proposed a calculation method on the base of crop development stage, soil biomass content, residual effects of previous tillage operations and on climate; these characteristics of vegetation and agriculture practices were transformed into continuous numerical variables and related to soil loss volumes by developing quantitative relationships from a large amount of data acquired on a number of experimental plots. C values range from 0 to 1 (no-dimensional), reflecting the potential of vegetation cover to protect soil from rainfall and runoff erosion. Values tending to 0 reduce soil loss amount, offering a good protection to soil, in contrast high values reflect the protecting power of vegetation.

The P factor represents the ratio between soil loss with a specific support practice and the corresponding loss with upslope and downslope tillage (Guobin et al., 2006). These practices take the role to contrast erosion by modifying the flow pattern, grade, or direction of surface runoff and by reducing the amount and rate of runoff (e.g. terracing).

The USPED is a model that predicts the spatial distribution of erosion and deposition in the case of stationary flow, with rainfall uniformly distributed. The assumption of the model is that the detachment and deposition soil rates (D_r) are proportional to the difference between the sediment transport capacity (T) and the sediment flow rate per unit width (q_s) (Foster and Meyer, 1972), as described:

$$D_r = \sigma(r)\left[T(r) - \left|q_s(r)\right|\right] \tag{5}$$

where $\sigma(r)$ is the first order reaction term dependent on soil and cover proprieties.

For the transport capacity limited case, we assume that the sediment flow rate, $q_s(r)$, is approximated to the sediment transport capacity *T*(r) (Moore and Burch, 1986).

$$\left|q_s(r)\right| = T(r) = K_t(r)\left|q(r)\right|^m \sin b(r)^n \quad (6)$$

where *q*(*r*) is the water flow rate ($m^3\ m^{-1}\ s^{-1}$), *b*(*r*) is the slope (express in degree), K_t is transportability coefficient dependent on soil and cover; *m* and *n* are constant coefficients, which value is related to the predominant erosion process occurring in the study area that depend on the type of flow and soil properties. For situations where rill erosion dominates, these parameters are usually set to *m* = 1.6 and *n* = 1.3; where sheet erosion prevails, they are set to *m* = *n* = 1.0 (Moore and Wilson, 1992; Foster, 1994).

In condition of steady state (rain intensity uniformly distributed), water flow *q*(*r*) can be expressed as a function of upslope contributing area *A*(*r*) as following:

$$q(r) = A(r) \cdot i \quad (7)$$

where *i* is the rain intensity.
Consequently the relation (6) is reduced to:

$$\left|q_s(r)\right| = T(r) = K_t(r) \cdot \left(A(r) \cdot i\right)^m \cdot \sin b(r)^n \quad (8)$$

Different variants of the USPED model exist (Moore & Burch, 1986; Mitasova et al., 1996) and in the present thesis the version proposed by Mitasova (1996) was used.

Net erosion or deposition within a grid cell, *ED(r)*, is calculated as the divergence of sediment flow (change in sediment transport capacity) in the direction of flow (Warren, 2005). The equation that describes net erosion/deposition in each grid cell (*r*) is:

$$ED(r) = div\left[q_s(r)\right] = K_t\{\left[grad(h)\right] \cdot s \cdot \sin(b) - h\left[k_p + k_t\right] \quad (9)$$

where *s* is an unit vector on the steepest slope direction, *h* is the overlandflow water depth, k_p and k_t are the profile and the transversal terrain curvature.

Due to the gap of experimental data, the USPED model combines the USLE/RUSLE parameters to estimate the transportability coefficient K_t as described:

$$K_t = R \times K \times C \times P \quad (10)$$

The solution of equation 9 will predict erosion in areas experiencing an increase in sediment transport capacity and consequently deposition in areas showing a decrease.

3.2 Models performance evaluation

A quantitative evaluation of the model performance was done to determine the suitability of the model for geomorphological applications and to identify those aspects of the methodology that need improvements.

The ability of the applied models to correctly predict erosion processes was evaluated by constructing confusion matrix obtained by crossing the number of true positive (TP), false positive (FP), false negative (FN) and true negative (TN) cases predicted by the model (Table 3.1). TP is the number of units for which the class assigned was correctly predicted; FP is the number of cells for which the right classification was not found but the model assigned presence; FN is the number of units for which the class was observed but the model predicted absence; finally, TN represents the number of counts for which absence was correctly classified by the model.

The confusion matrix allowed assessing different statistical indices that quantitatively describe the accuracy of the model (Table 3.1). The combination of different indices can help the user to understand not only how good the performance of the model is, but also to discriminate the possible origin of misclassification.

Predicted	Observed Presence class X	Absence class X
Presence class X	TP	FP
Absence class X	FN	TN

Measure	Formula
Overall Accuracy (Ac)	(TP + TN) / N
Sensitivity (Sn)	TP / (TP + FN)
Specificity (Sp)	TN / (FP + TN)
False Positive Rate (FPR)	FP / (FP + TN)
False Negative Rate (FNR)	FN / (TP + FN)

Table 3.1 Scheme of the confusion matrix used to evaluate the predictive accuracy of the model (left). TP = true positive cases; FP = false positive cases; TN = true negative cases; FN = false negative cases (left). Statistical indices measure the model accuracy (right).

The models' predictive performance was also assessed by constructing the Receiver Operating Characteristic (ROC) curves (Goodenough et al., 1974; Lasko et al., 2005) and by computing the values of the Area Under the ROC Curve (AUC; Hanley and McNeil, 1982). A ROC curve plots true positive rate TP (sensitivity) against false positive rate FP (1-specificity), for all possible cut-off values; sensitivity is computed as the fraction of cells hosting erosion process that were correctly classified as susceptible, while specificity is derived from the fraction of cells free of analyzed process that were correctly classified as not-susceptible.

The closer the ROC curve to the upper left corner (AUC = 1), the higher the predictive performance of the model; a perfect discrimination between positive and negative cases produces an AUC value equal to 1, while a value close to 0.5 indicates inaccuracy in the model (Fawcett, 2006, Reineking and Schröder, 2006, Nandi and Shakoor, 2009, Akgün and Türk, 2011). In relation to the computed AUC value, Hosmer and Lemeshow (2000) classified a predictive performance as acceptable (AUC > 0.7), excellent (AUC > 0.8) or outstanding (AUC > 0.9).

Chapter 4

STUDY AREA

4.1 Introduction

To achieve the objectives of the thesis the San Giorgio river basin, a small catchment (9.5 km^2 surface) situated in the Madonie Mountains (Sicily, Italy) was chosen as training and test area for model building. The obtained results were exported in a larger sector surrounding the experimental area (67 km^2 surface). In this section, a brief description of the Madonie Mountain group is given and the general setting of the research area is presented.

4.2 The Madonie Mountains

The complex mountain system of Madonie is one of the main massifs in Sicily, covering a large territory (around 40.000 km^2) in the Central-Northern part of the inland (Fig. 4.1). These mountains, localized in the administrative province of Palermo, stretch a 48 km wide area of the Sicilian interior sector.

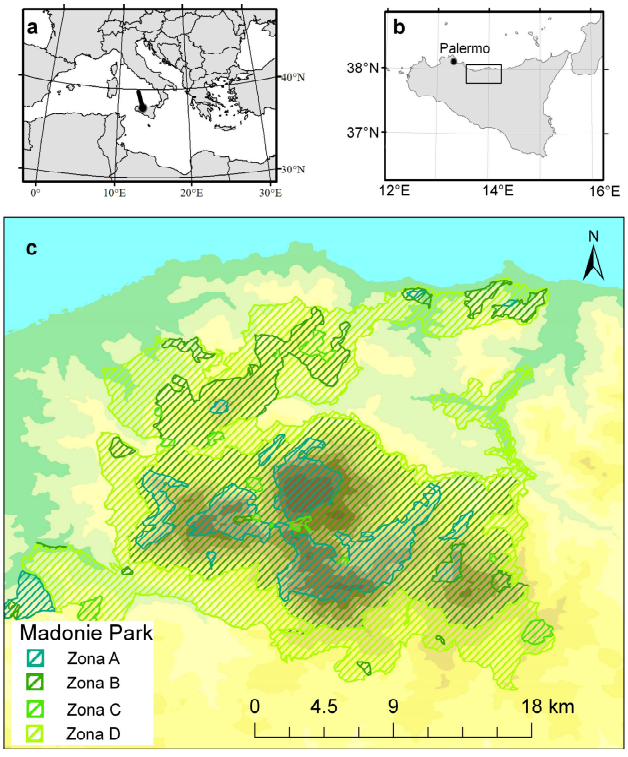

Figure 4.1. Madonie Mountains localization in the Mediterranean (a) and in Sicily (b). The natural park delimitation zones (d), A, B, C and D reflect the level of restriction and protection of the area.

The Madonie Mountains cover a territory that contains fundamental sources for the reconstruction of the natural history of the central Mediterranean (Catalano et al., 1996). Its geographical position, geological and structural arrangement and ongoing morphodynamic processes store quite a few natural archives and proxies to be conducted in paleoclimate and morphologic research (Agnesi, 2004). Furthermore, the variety of geomorphological and climatic features leads to the identification of different ecosystems that allow gaining and preserving a high biodiversity level (Raimondo et al., 2004).

In order to protect and preserve the natural and cultural heritage of the Madonie Mountains, the Sicilian Region conferred them the status of a 'Natural Park' in 1989. Subsequently, the region joined the European Geopark Network in 2001. The administrative boundaries of the Madonie Park define a certain part of the Madonie chain, bordered by small farming towns and villages. Since the establishment of the Natural Park and an increase in eco-sustainable tourism allowed the conservation and the valorisation of the traditional farming activities, soil quality and productivity has risen consequently. In contrast, close-by regions surrounding the Madonie Park have experienced vast land use and degradation trends due to the expansion and intensification of cultivated acreages and the lack of restrictions and regulations. Furthermore, massive use of destructive tillage techniques and the consequent decrease of natural vegetation cover have led to a rise in diffusive wildfire. These factors enhance the erosion processes and consequently the soil degradation of the entire territory. Understanding, predicting, and developing methods to control erosion processes are the first steps to contribute to soil protection improvement.

The geomorphological setting of the Madonie territory is extremely diversified and includes many of the morphological features that typically characterize the Sicilian landscape (Agnesi et al., 2000). The massif is built by carbonatic and arenaceous-clayey rocks, reaching up to 1979 m a.s.l. (Pizzo Carbonara) in the central interior, marking the second highest peak in entire Sicily. The great diffusion of calcareous rocks shows characteristic aspects of Karst formation, that has widely shaped the high Madonie landscape (Agnesi, 2006). Several dolines, dry valleys, poljes and caves indicate the presence of karst processes all over the region. The hilly areas surrounding the high relieves of the Madonie is mainly covered by siliciclastic and marly-substrates, where the

main features are deep and superficial landslides movements, mostly active, and linear erosion gullies involving and mobilizing great volume of soil.

4.3 Study area location and description

The study area is located in the western part of the Madonie Mountains and encloses the headwaters of the Fiume Imera Settentrionale and the Fiume Imera Meridionale, two of the main important fluvial systems of Sicily (Fig. 4.2a).

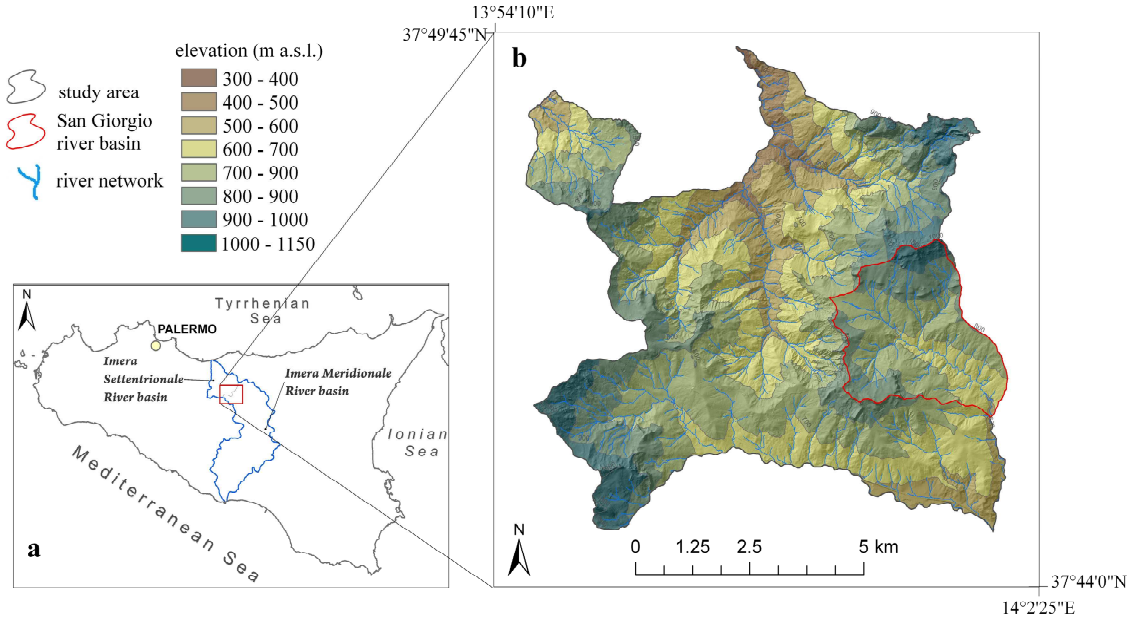

Figure 4.2. Study area: location (a), topography and hydrography (b).

The waterway of the Imera Settentrionale and the Imera Meridionale rivers constitutes a clear line of historical and cultural demarcation in the Sicilian landscape. The Fiume Imera Meridionale is the longest Sicilian River (144 km) that flows into the Straight of Sicily situated along the southern coast. The Imera Settentrionale river basin covers a surface of around 342 km^2, with a flow path length of 35 km and a discharge into the Tyrrhenian Sea.

The climate of this part of Sicily represents an example of the Mediterranean climate type, being characterized by wet and mild winter and hot and dry summer stages. Precipitation is mainly concentrated in a few rainy days over the winter stage, while summer period is characterized by dry to arid conditions and periods of drought. Mean monthly precipitation shows minimum values in August (10 mm) and maximum values in December (130 mm), with a mean annual average precipitation of 660 mm (values based on the period 1956-2000). Long-term mean annual temperature is 15.7℃, ranging from a maximum of 21℃ to a minimum of 10℃.

By means of aerial photographs (02.09.2007, resolution 0.25 m) land use of the study area was mapped. Remote sensing mapping operation was backed by means of field checks; the latter allowed testing the reliability of the images interpretation and enhancing the detail of the results. A number of 12 land use typologies were recognized and a map showing the spatial distribution of the different categories was constructed (Fig. 4.3).

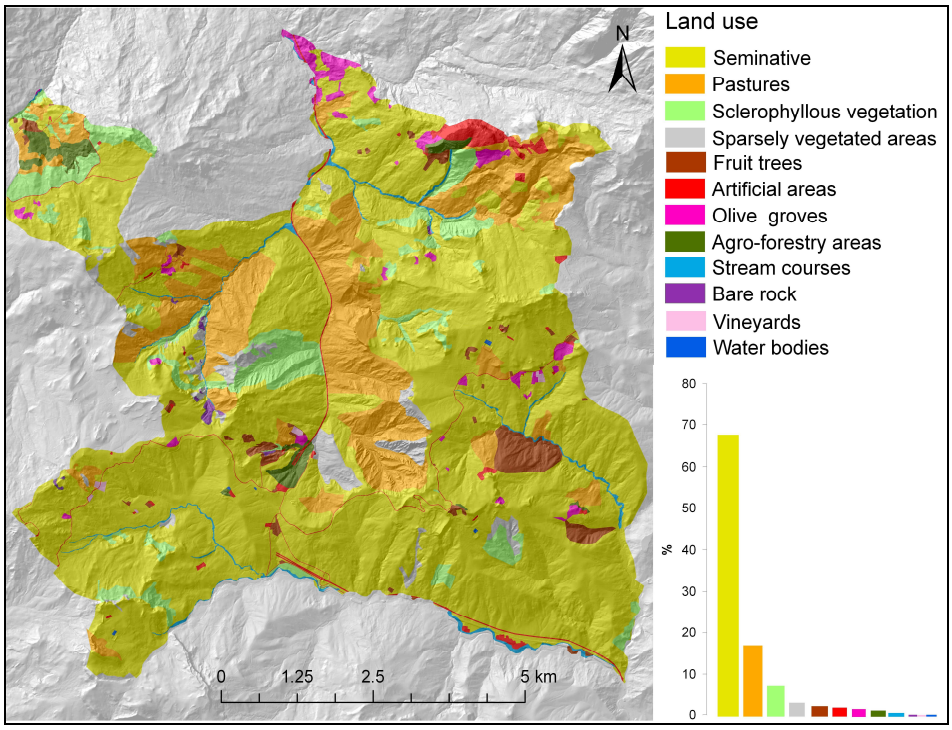

Figure 4.3. Land use map of the study area. The percentage of surface for each land use category is indicated.

The landscape is mainly characterized by agriculture surface, including seminatives (67.4% surface) and pastures (15.9% surface). The presence of sclerophyllous vegetation (6.5%) is normally linked to land abandoning and the following reconversion of these limited portions of landscape into natural vegetation cover. Sparsely vegetated area and bare rocks occupy areas where the runoff process has removed the top soil layer or where the bedrock crops out. Permanent crops category is represented by olive groves, vineyard and fruit trees plantations (3.6% surface).

Soils principally are *Typic* and *Lythic Xerorthenses*, part of the *Xerartens* group. They are generally poorly developed with a thin depth and are characterized by fine-medium texture. In the eastern part of the study area, soils are described as *Lithic Xerorthents,* referred to as poor developed soils, containing rocks fragments of considerable size. Following the International Soil Classification System, soils are denominated *Eutric* (CMeu), *Vertic* (CMvr) and *Chromic Cambisols* (CMcr) (ISSS Working Group RB, 1998).

Geological data and maps of the study area (Catalano et al., 1978, Abate et al., 1982, Abate et al., 1988, Abate et al., 1992) point out that, soils developed in substrates mainly characterized by clayey sediment outcrops, ranging from Upper Cretaceous to Lower Messinian. In particular, three principal sedimentary terrains are distinguishable. They are referred to as: *Argille Varicolori* sequences (also named *Argille Variegate* and *Argille Scagliose,* Upper Cretaceous–Oligocene), *Numidian Flysch* Formation (Late Oligocene–Early Miocene) and late-orogenic units *Terravecchia* Formation (Upper Tortonian–Lower Messinian), built by fluvial-delta deposits (clays, sandstones and conglomerates).

From a geomorphological point of view the area is shaped by an accelerating erosion process, consequences of an interaction between climatic conditions and litho-structural characteristics of outcropping terrains (Agnesi et al., 2007). Altitude values range from 370 m to 1150 m a.s.l. The landscape is characterized by moderate slope gradients, with a mean steepness of 10°, ranging from 0° to 51°, in terrupted by few steep convex slopes and narrow ridges.

During the early winter period in the study area tillage operations expose the bare soil to the impact of rainsplash and runoff processes, exacerbating rainfall erosivity. As consequences in this period, erosion by water starts detaching and transporting the fertile

top-soil, generating gullies and rills when the overlandflow is channelized. Shallow rotational slides, mud flows and complex landslides also occur, characterized by different intensity and frequency but in general causing permanent damage to farming production and representing a risk for the population. In addition, a certain part of the study area shows the presence of typical "*Calanchi*" (Moretti and Rodolfi, 2000) landforms, as result of the interplay between highly erodible clay soils and local geo-structural conditions (Agnesi et al., 2007).

Chapter 5

DATA COLLECTION

5.1 Rainfall erosivity

The climatic conditions influencing water erosion phenomenon were widely investigated over a 30 year-research. Obtained records allowed constructing and calibrating different rainfall erosivity equations, employed for hydrological simulation processes both at single rainfall events and long time scale.

The first authors, who provided an equation quantifying the rainfall erosivity factor (R factor), were Wischmeier and Smith (1959). They defined the R factor as a function of the Erosivity Index (EI_{30}), or index of aggressiveness of the rain, as following:

$$R = \frac{1}{N}\sum_{1}^{N} EI_{30} \tag{11}$$

where E is the total storm kinetic energy (MJ ha^{-1}), I_{30} indicates the intensity of the maximum 30 minutes rainfall intensity (mm h^{-1}) and N the number of observed years. The single storm Erosivity Index, EI_{30}, has to be calculated by using storm rainfall amount and intensity for all erosive events occurring in a year. At least 20–22 years of rainfall data are needed to deduce the mean rainfall factor (Wischmeier and Smith, 1978).

Several alternative erosivity indexes were pointed out to be more highly correlated to soil loss for particular scale or locations (Fournier, 1960, Hudson, 1971, Grimm et al., 2003, etc.). Moreover, frequent unavailability of detailed rain data in the Mediterranean and Sicilian region, led to develop simplified methods for the estimation of the R factor (Table 5.1). In 1983, D'Asaro and Santoro, based on the data recorded by 42 Sicilian rainguage stations, defined a relation (Table 5.1, Eq. 12) between the R factor and the rainfall intensity of 1 and 24 hours duration in a 2 year-return time. The lack of required data for the entire Region, led to a second simplified equation (Table 5.1, Eq. 13) to model rainfall erosivity in Sicily. Later, in agreement with the hypothesis of Fournier (1960) and Arnoldous (1980), who affirmed that rain erosivity does not only depend on the absolute amount of rainfall, but on its frequency and intensity, Ferro et al. (1991) developed a new relationship (Table 5.1, Eq. 4) for the Sicilian territory. In order to estimate the impact of a single storm event, Bagarello and D'Asaro (1994) derive a relationship (Table 5.1, Eq. 15), where the Erosivity Index is linked to the daily precipitation amount and the maximum 60 minutes rain intensity.

Model	Parameters	Authors	
$R = -102 + 2.91 \cdot I_{1,2} + 30.93 \cdot I_{24,2}$	$I_{1,2}$ and $I_{24,2}$ is rainfall intensity of 1 and 24 hours duration and a return period of 2 years	D'Asaro and Santoro, 1983	(12)
$R = 0.21 \cdot z^{-0.1} \cdot \left(\frac{P}{R_{days}} \right)^2$	z elevation (m); R_{days} the mean annual number of rainy days	D'Asaro and Santoro, 1983	(13)
$R = 0.524 \cdot \left[\sum_{i=1}^{12} \frac{p^2{}_{i,j}}{P_j} \right]^{1.59}$	$p_{i,j}$ is the total precipitation (mm) of the generic month i of the year j; P_j, is the total precipitation (mm) of the year j	Ferro et al., 1991	(14)
$EI_{30} = k \cdot d \cdot \left(h_{\max} \right)^{1.95}$	d is the daily rain depth (mm); h_{max} is the maximum 60 minutes rain intensity (mm h^{-1}); k is a coefficient set to 0.15	Bagarello and D'Asaro, 1994	(15)
$EI_{30-annual} = 0.124 \cdot \left[P^{0.9} + \left(d^{0.85} \cdot h \right) \right]^{1.294}$	d is the annual maximum daily rainfall (mm); h is the annual maximum hourly rainfall (mm)	Grauso et al., 2010	(16)

Table 5.1 Simplified erosivity models applied in the Sicilian territory. R is the average annual rainfall erosivity (MJ mm ha^{-1} h^{-1} $year^{-1}$), EI_{30} indicated the single storm Erosivity Index, $EI_{30\text{-}annual}$, is the annual erosion index (MJ mm ha^{-1} h^{-1}) and P is the mean annual precipitation value (mm).

Recently Grauso et al. (2010) developed a model (Table 5.1, Eq. 16) to assess the annual Erosivity Index ($EI_{30\text{-annual}}$) in the Sicilian region. Authors rearranged and calibrated the model developed by Diodato (2004) for the entire Mediterranean area. The variables contained in the model are related to annual precipitation data and to the maximum annual daily and hourly rainfall values.

In this thesis the $EI_{30\text{-annual}}$ values were computed by using the Grauso et al. (2010) model (Table 5.1, Eq. 16), containing rainfall data sets on different timescales. The advantage given by applying this model is that the variables involved are easily variable whereas the computation of the EI_{30} is time consuming and requires a continuous long record of rainfall intensities that is not available for the study area.

5.1.1 Data collection and models estimation

In this thesis, the model developed by Grauso et al. (2010) (Table 5.1, Eq. 16) was used to asses the annual Erosivity Index ($EI_{30\text{-}annual}$) and the R-factor by averaging the annual values for the number of observed years (Eq. 1). Equations (6) and (1) were applied to rainfall data sets from 11 rainguage stations, located next to the study area (maximum distance 20 km) (Fig. 5.1).

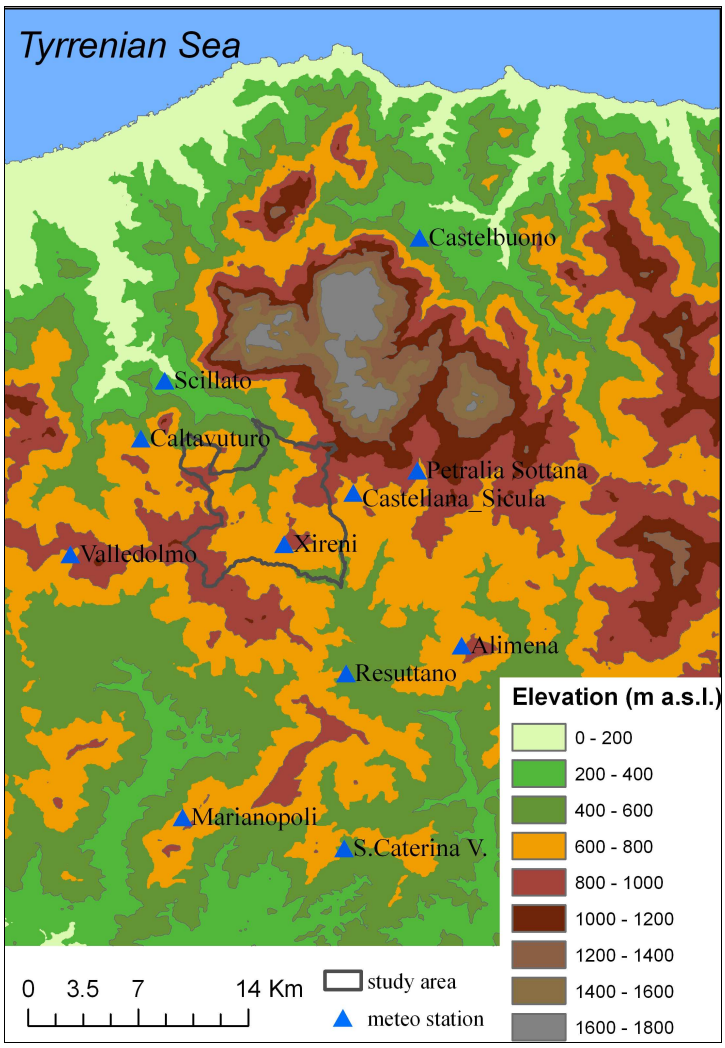

Figure 5.1. Rainguage stations location and elevation data.

In Table 5.2 the precipitation characteristics and the R values, computed for each rainguage stations over the observation period (1980-2006), are reported. Highest R-

values (over 1300 MJ mm/ha h year) were estimated in Petralia, S. Caterina V. and Castelbuono rainguage stations, while the lowest value is situated in the Marianopoli one. Figure 5.2 shows the relation between precipitation and erosivity values. These two parameters maintain a certain correspondence in the main locations. S. Caterina V. station diverges from this trend, showing low value of precipitation but high erosivity, reflecting the presence of heavy storm rainfall events.

Raingauge station	Elevation (m a.s.l.)	Observation period (years)	Mean annual rainfall (mm)	Rain days	R factor (MJ mm/ha h year)
Alimena	775	26	551	66	1200
Caltavuturo	635	24	599	67	851
Castelbuono	380	27	807	76	1336
Castellana Sicula	481	10	665	79	1222
Marianopoli	720	27	370	49	690
Petralia Sottana	935	27	789	85	1410
Resuttano	642	24	539	65	970
S. Caterina V.	606	26	508	62	1390
Scillato	376	27	678	75	1200
Valledolmo	750	23	611	79	886
Xireni	779	18	668	75	1176

Table 5.2 Rainguage stations elevation, period of observation and mean annual precipitation data. R factor evaluated during the period 1980-2006.

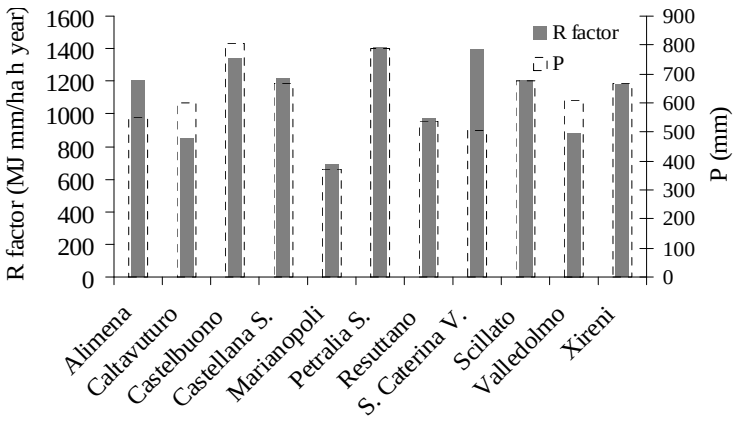

Figure 5.2. Erosivity factor (R factor) and annual precipitation (P) values evaluated during the period 1980-2006.

To represent the temporal distribution of the Erosivity Index during the 25 years considered, a graph was constructed describing the plotted average value of the estimated $EI_{30\text{-annual}}$ for the entire area (Fig. 5.3).

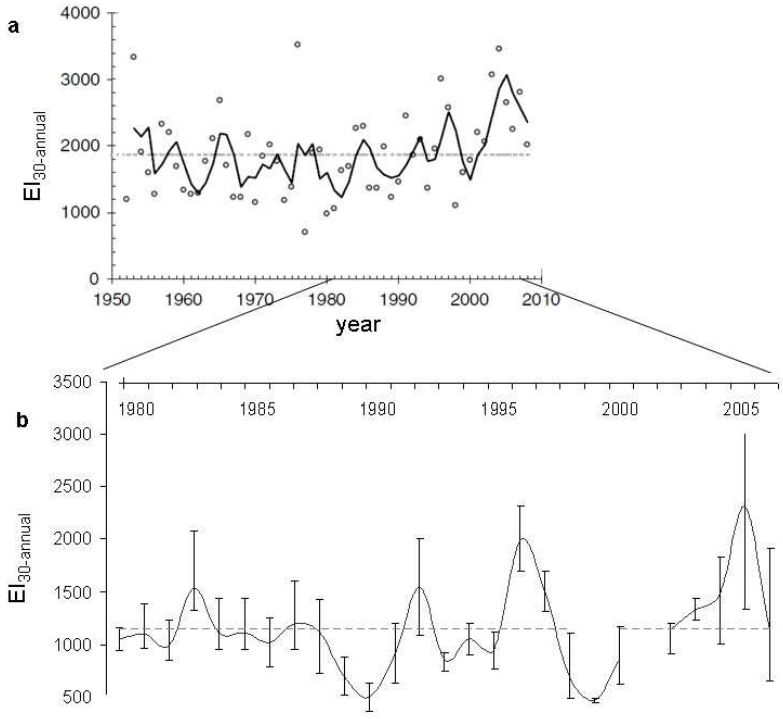

Figure 5.3. Annual Erosivity Index ($EI_{30\text{-annual}}$, MJ mm/ha h) temporal distribution in the Sicilian Region (a) (Grauso et al., 2010) and in the study area (b). At regional scale (a) the annual time evolution of the rainfall erosivity (dots), during the period 1950-2008, is averaged upon 104 stations of the Sicily region; the long-term erosivity mean value (horizontal line) and 3-year average moving window (bold curve) are drawn. In the study area (b) the Erosivity Index values, averaged upon the 11 stations, are described (curve line) during the period 1980–2006. The $EI_{30\text{-annual}}$ interval range (maximum and minimum) and the mean values (dashed line) are described.

As it can be seen in Figure 5.3 (b), in the study area the mean annual Erosivity Index shows a large variability throughout the years (with a gap in 2002 and 2003, where no sufficient data is available) and an increasing change ramping from 1990 to 2005. The figure also points out the variation range between the maximum and minimum values.

During the last 25 years, this gap increases resulting in a larger variability of erosivity within the analyzed rainguage stations. This trend is similar to that obtained by Grauso et al., (2010) for the Sicilian region (Fig. 5.3 a); Both, on regional scale (Fig. 5.3 a) and local scale (Fig. 5.3 b) the erosivity annual values increase during the period 2000-2005, with a peak in 2005 when the Erosivity Index reaches a value of 2315 MJ mm/ha h in the study area.

5.1.2 Rainfall erosivity map

In climatology a common practice is to interpolate data using both stochastic and deterministic methods. To express the spatial variability of the erosivity factor in the study area the Spline method was selected. Figure 5.4 shows the spatial distribution of mean R-values, computed for the period 1980-2006. In the study area R-values range from 915 to 1300 MJ mm/ha h year, resulting in more aggressive rainfall erosivity in the north east sector of the study area.

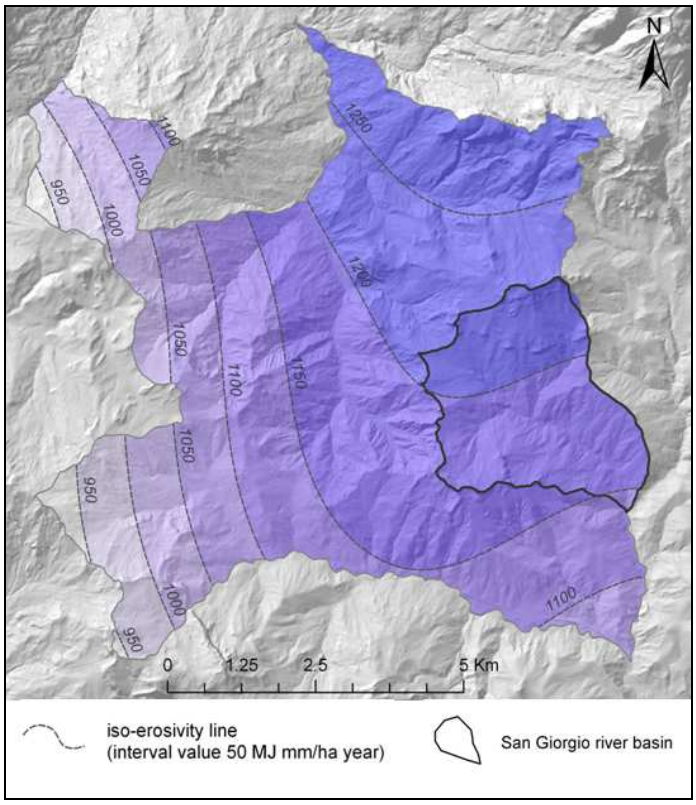

Figure 5.4. Study area Erosivity factor (R factor, MJ mm/ha h year).

5.2 Soil erodibility

The erodibility factor (K factor, t m^2 h ha^{-1} hJ^{-1} cm^{-1}) was developed to quantify soil erodibility conditions. The first mathematical relationship to evaluate K-values was introduced by Wischmeier and Smith (1978).

They described the K factor as following:

$$K = \frac{\left[2.1\times10^{4}(12-OM)M^{1.14}+3.25(s-2)+2.5(p-3)\right]}{100}\times 0.1317 \qquad (17)$$

where organic matter (OM), soil texture (M), classes of aggregate structure (s) and soil permeability (p) are the required data.

Studies demonstrated that the calculation of the K factor using the described equation (Eq. 17) is reliable only for low aggregate and medium texture soils. Consequently, in order to overcome this drawback, Renard et al., (1997) developed a new relationship, that indicates grain size distribution in soil as the only parameter required to estimate soil erodibility. Following this hypothesis the K-value (t ha h/ha MJ mm) can be computed as:

$$K = 0.0034 + 0.0405\cdot e^{\left[-\frac{1}{2}\left(\frac{\log D_g + 1.659}{0.7101}\right)^2\right]} \qquad (18)$$

where D_g is the mean geometric of diameters in soil particles size (mm), expressed by:

$$D_g = e^{\left(0.01\sum_{i=1}^{n} f_i \ln m_i\right)} \qquad (19)$$

where n is the number of size classes in which the distribution curve has been divided, f_i is the weight percentage of particles falling in the i-size class and m_i, the arithmetic mean of the diameters corresponding to the limits of i-class.

The simplification imported by Renard et al. (1997) (Eq. 18) is justified by considering the fact that the grain-size distribution influences the porosity, the aggregate formation, the organic matter content and permeability of the soil; Parameters included in the

Wischmeier and Smith equation (Eq. 17). Moreover, the use of the Renard equation (Eq.18) is recommended on small river basin scales, where the dynamics of erosion and/or deposition processes are strongly affected by soil texture and where detailed data sets are available (Bryan, 2000).

Soil erodibility conditions in the San Giorgio river basin were investigated in order to describe the intrinsic characteristic of topsoil to contrast the rainfall and runoff erosive action. The necessity to explore erodibility characteristics comes from the lack of previously related works in the study area. By analysing several soil samples and applying the Renard et al. (1997) relation (Eq. 18), a map showing the spatial distribution of erodibility was constructed.

5.2.1 Data collection

Data related to texture characteristics of soils in the study area are necessary to assess the K factor. Consequently, the first step was to explore previous works conduced grouping the same Sicilian sector, where grains size distribution in soil is investigated.

Montana et al. (2011), in a work related to the textural and mineralogical composition of clay substrates in the western part of Sicily, pointed out the strong relation between grain size of soil particles and outcropping lithology where soil development takes place. Results show how the *Argille Varicolori* samples, collected in Castellana Sicula (eastern sector of the study area), belong to silty-clay and silt-clay-loam textural classes. The *Numidian Flysch* Formation shows a silty-clay texture.The *Terravecchia* Formation, falling in silty-clay-loam, silty-clay and clay-loam textural classes.
Cappadonia et al. (2011) sampled and analysed soils in the upper Imera Settentrionale river basin, relating the mineralogical and textural composition of topsoil to erosion process activities. Results show how on hillslope and on catchment scale, grain size distribution is mainly related to litology outcropping, topographic conditions, land use and intensity of runoff processes.

The second step was to obtain texture information about soils in the San Giorgio river basin. A sampling design strategy was elaborated and a number of 72 soil samples were taken and analysed.

5.2.2 Soil sampling methodology

The aim of developing a sampling strategy is to maximise the efficiency of the sampling scheme while ensuring that the variability within the sampling area is adequately characterised. To obtain that, the San Giorgio river basin was segmented into discrete entities (soil units), combining land use, lithology and landform layers (Fig. 5.5a).

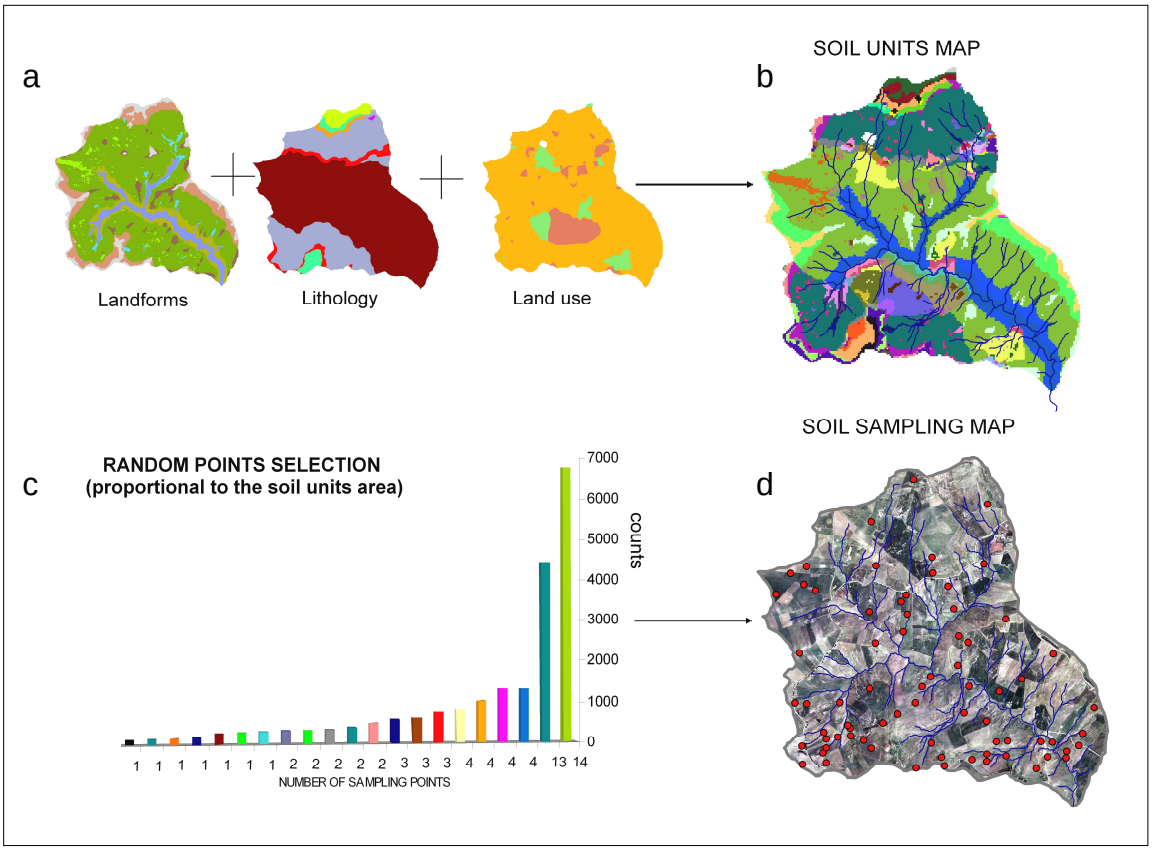

Figure 5.5. Soil sampling strategy. Four steps are described: Overlay of landforms, lithology and land use layers (a); segmentation in discrete soil units (b); quantification of the number of samples per soil unit (c), random selection of sampling points (d).

The three selected layers were considered to be influencing the soil grain size distribution on catchment scale. The landform map expresses the influence of runoff, eroding and transporting sediments along the slopes and the possible translocation and redistribution of soil particles. Land use affects soil texture principally depending on vegetation type and tillage operations. Lithology outcropping influence on texture characteristics was described in the previous section. While for outcropping lithologies (Table 5.3) and land

use (Table 5.4), information was simply extracted from previous data, to obtain a map showing landforms, a tested methodology, described by Jenness (2006), was followed. Landform layer was created combining the grids of Topographic Position Index (TPI) and Slope.

Outcropping lithology	surface (m^2)
Clays and marls (Argille Varicolori)	7179996
Clays and silts (Terravecchia Fm.)	1245690
Coralline Biolitites	483903
Sandstone (Terravecchia Fm.)	403974
Conglomerates (Terravecchia Fm.)	132532

Table 5.3 Outcropping lithologies in the San Giorgio River basin.

Land cover	surface (m^2)
Seminatives	7952097
Permanent crops	864019
Pastures	656074

Table 5.4 Land cover categories in the San Giorgio River basin (simplified version of the land use map).

The intersection generates a Slope-Position grid, classified into different landform categories. To create the TPI grid for each cell of the digital elevation model (resampled to cell size 5x5m), the difference between the elevation of a cell and the mean elevation of all the grid cells included in a moving circular window was estimated. Two different TPIs were constructed, setting a searching radius at 200 m and 500 m. After that, combining these two TPI grids (TPI_{200} and TPI_{500}) with the Slope grid, a 10 class-landform classification regime was derived and a map constructed. The landscape of the San Giorgio river basin is represented by 8 landform categories (Table 5.5).

The overlay of the three described layers, land use, outcropping lithology and landforms, subdivided the San Giorgio river basin into 59 units (named soil units, Fig. 5.5b). The units that cover a surface smaller than one hectare were not considered representative of

significant soil texture diversity and so their border dissolved to the closest patch. The final map contains 25 different soil units.

Landform	Surface (m^2)
Open slopes	5774400
Upper slopes, mesas	957200
U-shaped valleys	727200
Canyons, deeply incised streams	667600
Mountain tops, high ridges	611200
Midslope ridges, small hills in plains	363200
Plains	238800
Midslope drainages, shallow valleys	139200

Table 5.5 Landform categories in the San Giorgio river basin.

The next step was to set a total number of 72 samples, whose spatial location was identified by randomly selecting a defined number of points for each unit (Fig. 5.5d). The number of samples per soil unit, taken randomly, is proportional to the total surface described by each defined unit (Fig. 5.5c). Soil samples were collected exporting the 20cm topsoil.

5.2.3 Soil analysis and texture data

The relative proportion of different grain sizes of mineral particles defines the texture in soils. The particle-size distribution was evaluated by separating the relative proportion of sand, silt and clay, in each of the 72 collected soil samples, using the USDA[1] particle sizes classification. Samples were pre-treated in laboratory; they were dispersed in aqueous solution and soil aggregates were degraded by chemical (hydrogen peroxide) and mechanical (shearing action) instruments. The use of a chemical reagent was necessary being sampled soils characterized by high level of organic matter. Subsequently grains fraction bigger than 2 mm was separated using pore-size filters. Remaining sediment was analysed by the use of Laser Particle Size Analyzer (*Fritsch*

[1] United States Department of Agriculture

Particle Sizer AUTOSIEB/A20). Soil particle-size analysis allowed evaluating the texture of sampled soils and the USDA-texture triangle was used to define the soil textural classes (Fig. 5.6).

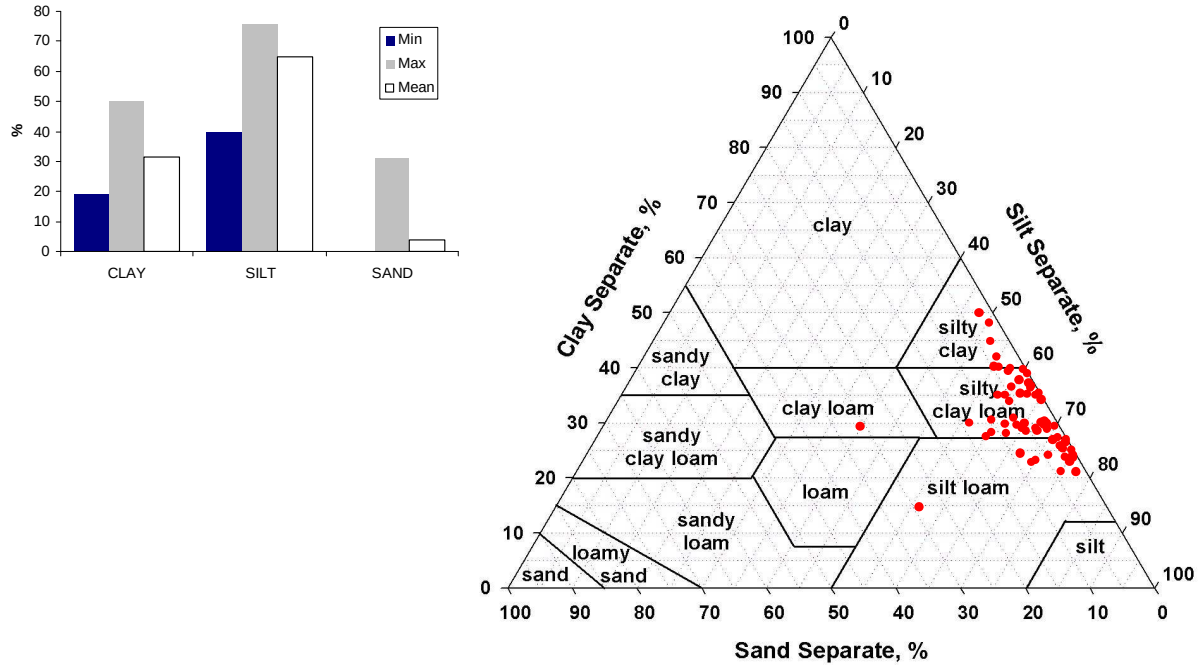

Figure 5.6. Proportions of sand, silt and clay, in each of 72 collected soil samples (left) and USDA textural triangle used to represent the grain size distribution of the 72 soil samples (red points) (right).

Results (Fig. 5.6) showed how soils in the study area mainly belong in silty-clay-loam, silt-loam and silty-clay textural classes, according to previously works (Montana et al., 2011, Cappadonia et al., 2011). Only few samples deviate from the described textural classes distribution; they show highest content of sand (30%). By checking the location of this outliner samples, they belong to the sandstone level of the Terravecchia Formation, which obviously influences the sand content.

5.2.4 Soil erodibility map

Soil texture results were utilized to compute the erodibility values (K-values) for each by the use of the Renald et al. (1997) relation (Eq. 11). K-values range from 0.032 to 0.062 t ha h/ha MJ mm (SI units) (Std. Deviation and mean value of 0.0036 and 0.048, respectively). Analysed soils can be considered high erodible on the basis that K-values normally range from 0.013 to 0.059 SI units (Renarld et al., 1997). Results are justified by the high silt and clay content in the study area soils.

In the San Giorgio river basin a map of the Erodibility factor was generated (Fig. 5.7), by interpolating the punctual information using the Spline method. A spatial gradient associated with the topography and the outcropping lithology can be observed in Figure 5.7; highest K-values are located in the upper slopes of the catchment while lower values resulted in the river outlet and in plain zones.

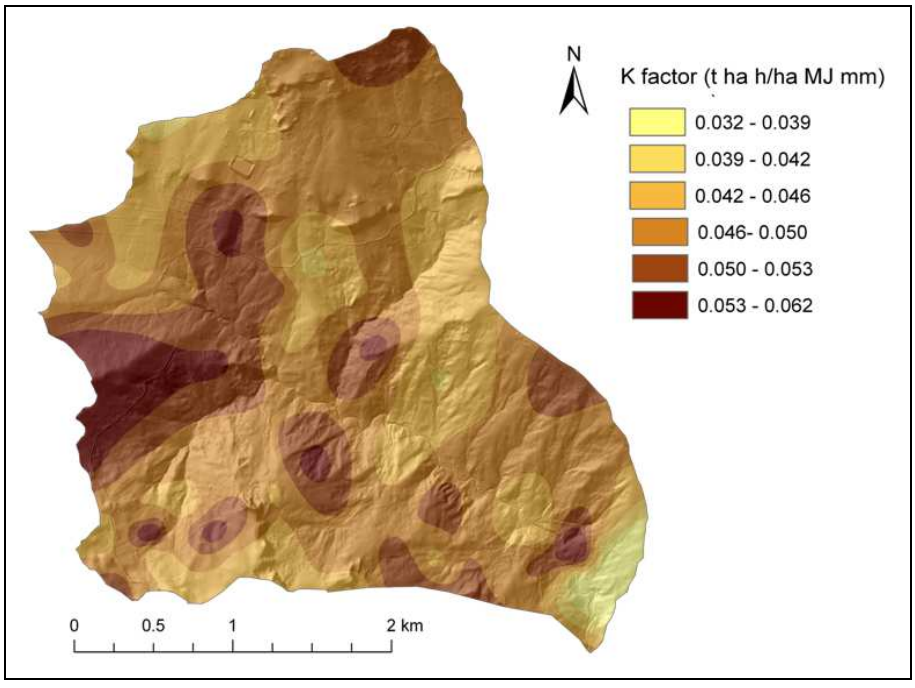

Figure 5.7. Erodibility factor (K factor, t ha h/ha MJ mm) in the San Giorgio River basin.

5.3 Terrain attributes

A digital elevation model (DEM) consists of a spatially registered set of elevation points that collectively describe a topographic surface. Studies demonstrated the direct dependence of topographic and hydrologic attributes on resolution and accuracy of the applied DEM (Jenson and Domingue, 1988; Claessens et al., 2005) and hence soil erosion models application results are indirectly linked to terrain model characteristics (Zhang and Montgomery, 1994, Zhang et al., 2009). Both, the grid scale and the original density of independent elevation points influence DEM resolution and the nature of artefacts incorporated in a DEM (Montgomery, 2003). Using a large scale DEM imposes basic limitations for simulating erosion processes; a fine-scale grid may include elements like roads, culverts and field boundaries that can modify the local topography and are useful for hydrological simulation and erosion processes modelling (Zevenbergen, 1987).

In the present thesis a high resolution DEM was employed: A LiDAR DEM (2m grid size), produced for the entire Sicilian Region. The DEM was resampled to 5m grid size to reduce the number of analyzed cells and simplify the data processing. The elevation datasets were pre-processed with the Planchon and Darbox fill algorithm (Planchon and Darbox, 2001). This operation corrects and partially eliminates construction errors (Olaya and Conrad, 2008). Several topographic indices and two kinds of mapping units were selected to build up the erosion susceptibility models.

5.3.1 Topographic indices

To model the erosive power of runoff, in terms of potential discharge volume, flow velocity and transport capacity, different topographic indices were employed. The SAGA GIS (System for Automated Geoscientific Analyses) (Conrad, 2007) and the ArcView 2.3 (ESRI) software were used to derive primary and secondary attributes from the DEM.
A number of 14 topographic indices were used to predict soil erosion and mass wasting processes by means of the TreeNet method (Table 5.6 A). Primary attributes included: Elevation, Slope, Aspect, Analytical hillshading, Plan and Profile curvature, Curvature classification, Convergence index, Altitude above channel network, Catchment area. All these parameters describe hillslope morphometry and stream channel. Secondary attributes were also computed: Stream Power Index, Lenght-Slope factor (LS-factor), Topographic Wetness Index.

Topographic indices	Method	A	B	C
Altitude above channel network	Olaya & Conrad, 2008	x		
Analytical hillshading	Olaya & Conrad, 2008	x		
Aspect	Zevenberg & Thorn, 1987	x		x
Catchment area	Olaya & Conrad, 2008	x		x
Convergence Index	Köthe & Lehmeier, 1993	x		
Curvature	Zevenberg & Thorn, 1987	x		
Curvature classification	Dikau, 1989	x		
Elevation	-	x	x	
LS factor	Moore and Wilson (1992)	x	x	x
Overland flow distances to channel network	Olaya and Conrad, 2008		x	
Plan curvature	Zevenberg and Thorn, 1987	x	x	x
Profile curvature	Zevenberg and Thorn, 1987	x	x	x
Slope	Zevenberg and Thorn, 1987	x	x	x
Stream Power Index	Beven and Kirby, 1993	x	x	
Topographic Position Index	Jenness, 2006		x	
Wetness index	Beven and Kirby, 1993	x	x	

Table 5.6 Topographic indices utilized for the three applied methodologies: the mass wasting and erosion prediction by means of the TreeNet method (A); the gully susceptibilities model construction using the logistic regression analysis (B); and the RUSLE/USPED models used to predict the impact of anthropogenic changes in erosion processes (C).

In the gully erosion susceptibility model construction 9 topographic attributes were used (Table 5.6 B). Between these variables the topographic position index (TPI) was considered, representing the erosion/accumulation capacity of the terrain. It is expressed by the quantitative relation between the elevation of a cell and its surrounding cells; the topographic position index was computed for each cell by using the algorithm of Jenness (2006) and selecting a buffer of 100 m to identify the neighbouring cells.

The potential effects of the river network system on gully erosion was investigated for grid cell units by calculating the flow distance to the river network; the latter attribute was computed by using the module of SAGA GIS (Olaya, 2004) “Overland flow distances to channel network” and selecting the algorithm “multiple flow direction”.

Finally the topographic factor used for the prediction of soil loss changes due to man-induced elements was expressed by the LS- factor (RUSLE topographic factor) and by combining the profile and the tangential curvature, upslope contributing area, slope and aspect grids (USPED topographic components) (Table 5.6 C). These topographic factors were derived from the 2 m grid size DEM, to underlie the impact of micro-morphological components on erosion/deposition processes. In this thesis, the LS factor has been

calculated using the approach of Moore and Wilson (1992) and Desmet and Govers (1996), as described in the following relation:

$$LS(r) = (m+1)\left(A_r / a_0\right)^m \left(senb_r / b_0\right)^n \quad (20)$$

where A_r is the upslope contributing area (m) and b_0 is the steepest slope angle (radians), a_0 and b_0 are constant equal respectively to 21.1 and 0.09. Coefficients m and n are constant, with values related to the predominant erosion process occurring in the study area. These parameters are set to m = 1.6 and n = 1.3 (Moore and Wilson, 1992; Foster, 1994).

5.3.2 Mapping units

The selection of suitable mapping units is a necessary step in modeling the spatial occurrence of geomorphological processes and related landforms. Regular square cells represent the most popular method for partitioning the territory in modeling susceptibility to landslide and water erosion phenomena. According to CLUs partitioning criteria, the San Giorgio River basin was subdivided in 376,099 grid cells characterized by 5m side size, simply identified by rasterizing the basin (Fig. 5.8).

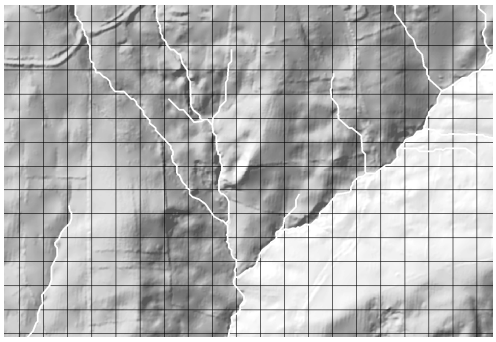

Figure 5.8. Detail of the San Giorgio River basin subdivision in grid cell units (CLUs) 5m grid size.

Susceptibility analysis is also performed by adopting hydro-morphometric terrain units. In the present thesis, in addition to grid cell units (CLUs), a spatial partitioning of the study area by identifying terrain units of various size and shape, was performed.

The basin was subdivided in spatial domains which boundaries coincide with fluvial streams and water divides (Fig. 5.9 a); these terrain units, known as slope units (SLUs; e.g. Van Den Eeckhaut et al., 2009, Rotigliano et al., 2011), are defined on the basis of morphodynamic and hydrological criteria. 353 SLUs, having an average extension of 3.66ha, were semi-automatically derived by processing a Digital Elevation Model (DEM), with a ground resolution of 5 m (Fig. 5.9 b). Spatial analysis tools of ArcView GIS 3.2 (ESRI, 1999) and ArcGIS 8.1 (ESRI, 2001) and other scripts freely available on the web (Basin, Amber, Point and Polyline Tools) were exploited to achieve this goal.

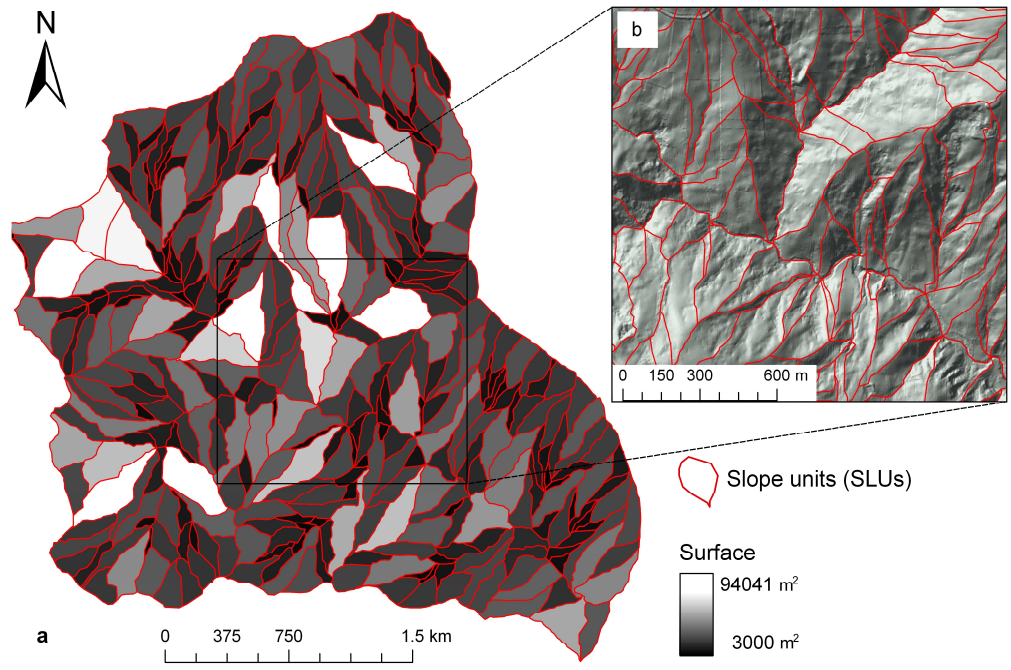

Figure 5.9. San Giorgio River basin slope units (SLUs) (red boundaries).The surface extension is represented by a grey-color scale. A detail of the SLUs is shown (b).

5.4 Erosion landforms inventory

The preparation of the inventory of the past landforms is a key step of all those susceptibility mapping techniques based on stochastic modeling and in this thesis was used to build up the prediction models and to validate their accuracy.

In the San Giorgio river basin, used as training and test area, four classes, containing specific triggering and controlling factors, are represented: mass wasting (shallow landsliding), bank erosion, gully erosion and sheet-interrill erosion.
The presence of these types of erosion processes was identified by means of: i) aerial photographs interpretation (two time-series data: 02.09.2007 and 10.03.2000) and landforms classification (Hochschild, 2003); ii) detailed field-work to check the mapped landforms and to characterize their morphometry by using a Global Positioning System (GPS) (Casali et al., 2006); iii) remote sensing and Geographic Information Systems (GIS) data integration (Campbell, 2002).

Evidences of sheet and rill erosion were difficult to identify from aerial photographs and their ephemeral nature does not always allow their field verification. Rill and sheet erosion were grouped as spatial, superficial erosion landforms and mapped as polygons. They produce a diffuse top soil loss and can be recognised by the presence of sparsely vegetated area and changes in soil colour (Fig. 5.10).

Figure 5.10. Sheet and rill erosion features detecting in aerial photos (10. 03.2000) (a) and checked *in situ* (14.05.2010) (b).

In the study area, a problem in collecting rill erosion features was the presence of cattle paths in disarrangement with rill landforms. Actually, the presence of cattle paths can trigger rills formation, but the relation is not absolute and in many cases does not represent a preferential water flow path. To correctly map sheet and rill erosion it is strictly necessary to combine remote sensing mapping with field checks.

260 linear erosion landforms classifiable as ephemeral and permanent gullies were mapped. To better recognise gullies, contour lines were derived from the DEM and overlaid on the aerial photographs (Fig. 5.11). In the San Giorgio river basin gullies can be classified as bank and hillslope gullies, characterised by V-shaped cross-sections.

Figure 5.11. Gullies detection by aerial images interpretation (10.03.2000) supported by the visualization of contour lines (2 m distance).

Morphometric measurements of gullies allowed better definition of processes generating these features. The maximum measured gully cross section depth data was about 2.5 m, while the gullies-length ranges from a few to 550 meters. Larger gullies signify depositional areas and are mostly characterized by medium-fine material (Fig. 5.12). Plunge-pools characterize the longitudinal morphology of permanent gullies while the gully head-cut retreat is often accompanied by lateral wall collapse.

Figure 5.12. Accumulation area for sediments eroded and transported by gully erosion in the San Giorgio basin (12.05.2011).

The mapped mass wasting processes are mainly represented by debris flow and earth slides. These shallow landslides types involve the upper part of the soil or substrate and deliver a high amount of sediments into the river network (Fig. 5.13 and Fig. 5.14). It was possible to identify 446 landslides, by means of aerial and satellite images.

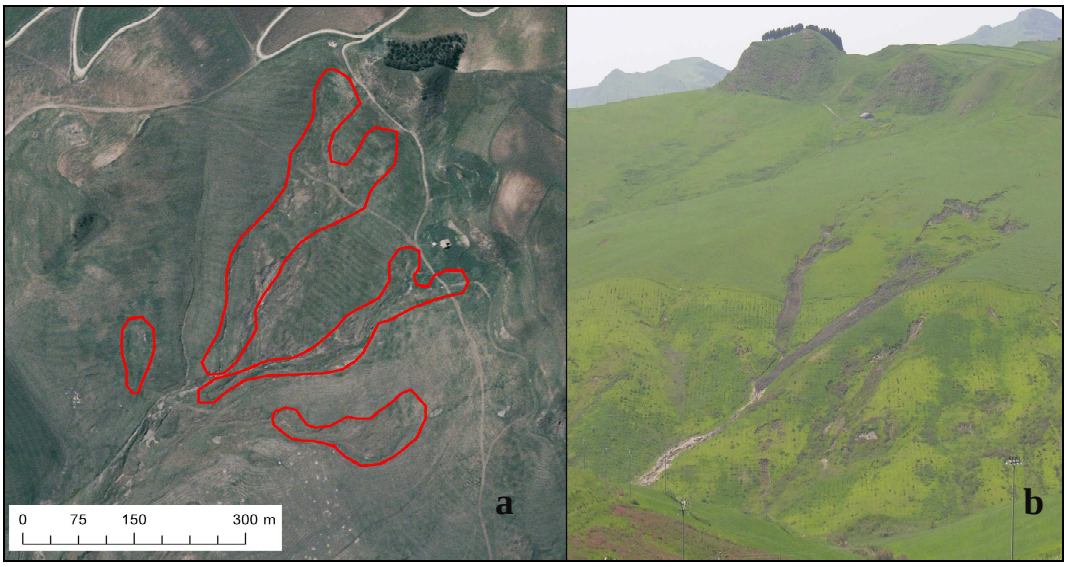

Figure 5.13. Debris flow process, acting in the western sector of the San Giorgio river basin, mapped from aerial photographs (02.09.2007) (a) and checked in field (10.04.2011) (b).

Figure 5.14. Landslides located in the upper part of the San Giorgio River basin (10.04.2011).

River bank erosion is the direct removal of banks and beds by flowing water. Typically, it occurs during periods of high stream flow action. Field work was carried out in July 2010 to map the thalweg by the use of a DGPS (Differential GPS, 2 cm resolution). Field data (Fig. 5.15 a) were integrated to the river network datasets, automatically extracted by the DEM (Fig. 5.15 b).

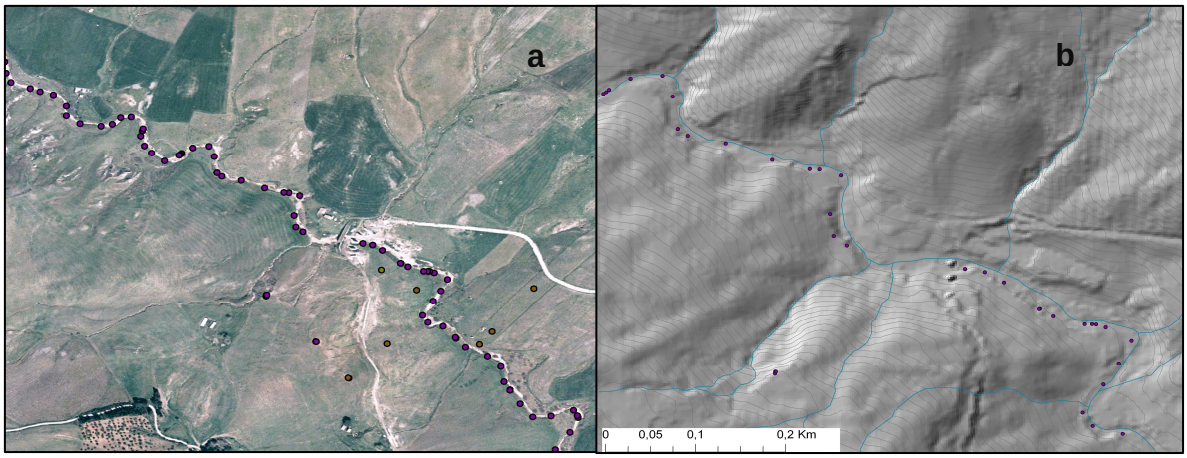

Figure 5.15. The GPS points, collected in July 2010, used to map the thalweg of the river San Giorgio (a). Collected points overlapped to the river network, extracted by the DEM (b).

The fluvial system was used as a base instrument to map and recognize bank-erosion *in situ*. Moreover, in order to allow a better characterization of bank-erosion processes (principally verified by wall collapse and breakdown), the mapping operation was carried out by comparing the two time-series data of aerial photographs (2000 and 2007) (Fig.

5.16). Results allowed the accurate mapping of stream-bank erosion process taking place in the San Giorgio catchment. Bank erosion process is diffuse in the widespread area of the San Giorgio river network, as a consequence of the high erodibility of the clayey soils (Fig. 5.17).

Figure 5.16. Bank erosion feature detection in two time-series data of aerial photographs: 2007 (02.09.2007) (a) and 2000 (10.03.2000) (b).

Figure 5.17. Bank erosion causing river walls collapse (12.05.2011).

The collected data (Table 5.7) is shown in a map illustrating the spatial distribution of mass wasting and erosion processes in the San Giorgio river basin (Fig. 5.18).

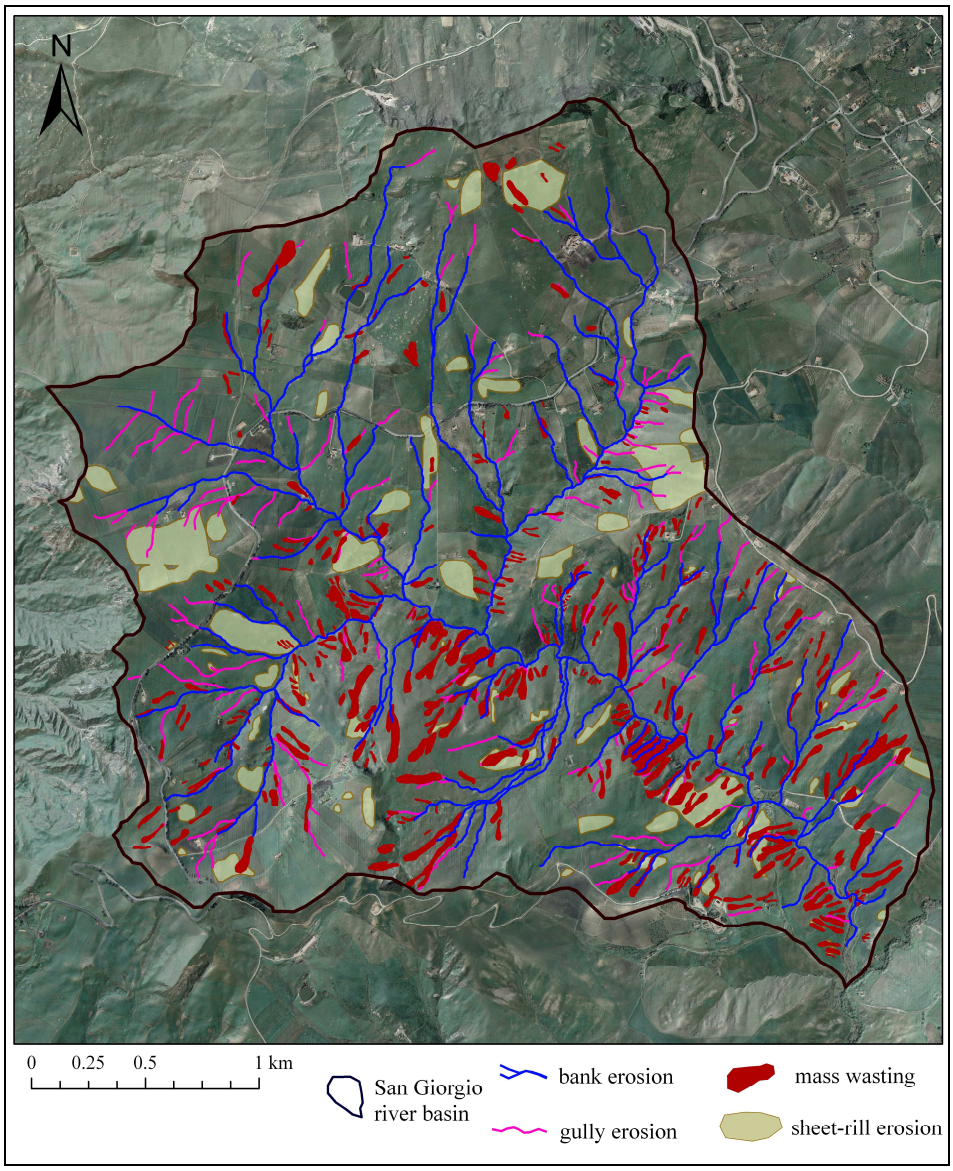

Figure 5.18. Erosion and mass wasting landforms in the San Giorgio River basin.

Landform	
Rill-interrill erosion	0.63 km^2
Gullies	260
Landslides	446
Bank erosion	0.3 km^2

Table 5.7 Number of erosion and mass wasting detected features (gullies and landslides) or affected surface (sheet, rill and bank erosion).

Chapter 6

PREDICTION OF MASS WASTING AND EROSION PROCESSES SUSCEPTIBILITIES USING THE TREENET MODEL

6.1 Modeling approach

In this application, among existing methods, the one proposed by Märker et al. (1999) was chosen to model erosion and mass wasting processes, and to reach the first objective of the thesis. The applied approach subdivided the studied area in Erosion Response Units (ERU; Märker et al., 2011). ERUs are distributed three-dimensional terrain units, which have homogeneous erosion process dynamics controlled by their physiographic properties and the management of their natural and human environment (Märker et al., 1999).
The TreeNet method (Salford Systems implementation, cf. Friedman, 1999) was proposed to classify ERUs and to analyze the functional relationship between the spatial distribution of erosion landforms and driving/predictor factors.

The San Giorgio River basin was selected to implement the erosion and mass wasting susceptibility model and to export results in the entire study area.
Layers (raster and vector) representing the spatial distribution of several predictor variables and describing different erosion and mass wasting processes were combined to delineate spatially homogeneous erosion process entities, ERUs (Märker, 2002; Flügel et al., 2003; Sidorchuk et al., 2003) (Fig. 6.1). An aggregated data matrix, where each row corresponds to an individual case while columnar data shows the dependent and independent variables, was constructed and used as input for the TreeNet model.

The San Giorgio River basin was selected to implement the erosion and mass wasting susceptibility model and to export results in the entire study area.
The procedure consists of the following steps: i) random selection of 50% of San Giorgio basin dataset (N= 191761); ii) random partition of the selected subset into a train (60% of N; N_{train} = 116508) and a test fraction (40% of N; N_{test} = 75253); iii) running and validating the TreeNet model for the N_{train} sets; iv) application of the model to the entire study area, in order to get information of the spatial distribution of the ERUs.

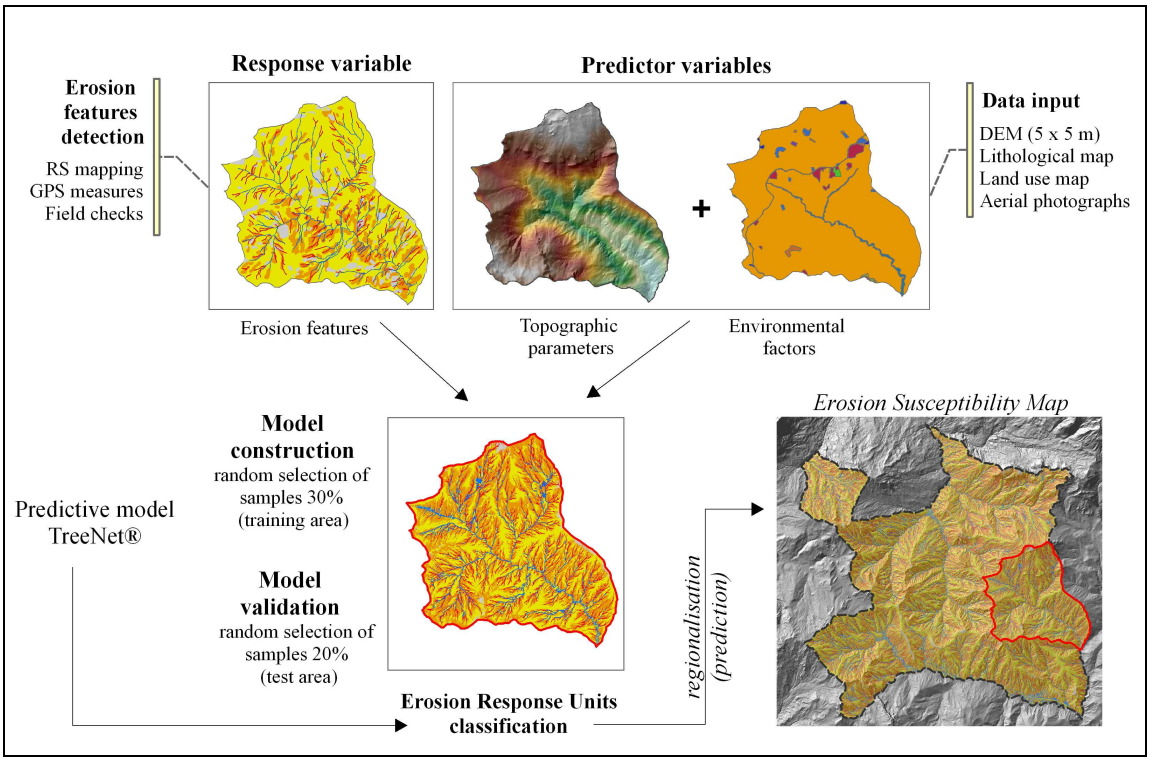

Figure 6.1. Flow-chart illustrating the procedure used to construct the erosion susceptibility map.

6.2 Model components

To analyze the functional relationship between spatial data sets of driving factors and response variables, data related to the model components needed to be collected. In particular, data regards dependent and independent variables. The water erosion driven features were assumed as the dependent response variables in the model application, since erosion landforms are the evidence of the action of soil erosion processes.

Different topographic and environmental raster layers were prepared to represent the spatial distribution of those factors which were supposed to control soil erosion and mass wasting processes. To model the spatial occurrence of geomorphological processes and related landforms the grid cell units (CLUs, 5m side size) partition criteria was used.

6.2.1 Response variable

Four geomorphologic conditions were defined to group the mapped units into five different classes, expressing the type of erosion process. Each one having specific triggering and controlling factors: i) mass wasting (shallow landsliding); ii) bank erosion; iii) gully erosion; iv) sheet and rill erosion. “No-erosion” class was attributed to those areas not hosting any evidence of active or inactive erosion processes. Table 6.1 shows the number of cases and relative frequency of each soil erosion class.

Response variable	N	%
gully erosion	10830	2.9
bank erosion	15676	4.1
sheet-rill erosion	25572	6.7
mass wasting	26905	7.1
no erosion	300789	79.2

Table 6.1 Response variables. N represents the number of cases for each type of response.

6.2.2 Predictors parameters

To model and predict the soil erosion process 17 independent parameters, reflecting topographic and environmental driving factors, were used.

Outcropping lithology (Table 6.2) and land use (Table 6.3) data were used as predictor variable expressing soil erodibility and cover management role in soil erosion and mass wasting processes development.

14 are the terrain attributes chosen to quantify the role played by topography in redistributing water in the land surface and in modifying the amount of annual solar radiation received by soils (Table 6.4).

Outcropping lithology
Clay substrates (*Terravecchia*; *Argille Varicolori*)
Coralline biolitites; Conglomerates; Marly limestones; Biocalcarenites
Evaporitic deposits; Trubi chalks

Table 6.2 Predictor variables: Outcropping lithologies (grouped).

Land use
Seminatives
Fruit trees
Pastures
Olive groves
Stream courses
Artificial areas
Sclerophyllous vegetation
Vineyards
Agro-forestry areas
Artificial lakes

Table 6.3 Predictor variables: Land use categories.

Topographic indices	Interval	Std. dev.
Altitude above channel network	0 / 43 m	14
Analytical hillshading	5.7 / 103	22.9
Aspect	0 / 360°	103
Catchment area	25 / 1196320 m^2	584
Convergence Index	-23.4 / 23.5	11.7
Curvature	-0.079 / 0.079	0.040
Curvature classification	0 / 8	-
Elevation	482 / 961 m	120
LS factor	0 / 73.21	26.74
Plan curvature	-0.040 / 0.040	0.02
Profile curvature	-0.053 / 0.053	0.027
Slope	0°/ 51.2°	5.37
Stream Power Index	0.025 / 10489223	49913
Wetness index	4.3 / 11.5	1.8

Table 6.4 Predictor variables: Topographic indices, interval value and standard deviation.

6.3 Results

6.3.1 Model performance evaluation

The evaluation of the classification performance was based on the count of the numbers of ERUs correctly and incorrectly predicted by the TreeNet model, both in test and training datasets. These counts were tabulated in a confusion matrix (Table 6.5), to represent the distribution of predicted and observed ERUs within each class.

		Observed class (%)					
		gully erosion	mass wasting	sheet rill erosion	river erosion	no erosion	FP cases
Predicted class (%)	gully erosion	**59.6 (61.3)**	17.7 (16.9)	7 (4)	26 (19.3)	10.5 (9.6)	8301 (11849)
	mass wasting	17.1 (19.7)	**53.5 (60.5)**	23.8 (24.5)	7.7 (10.3)	34.8 (43.1)	22737 (41478)
	sheet-rill erosion	3.1 (2.5)	12.9 (10.4)	**42.2 (64.5)**	0.5 (1.3)	16 (18.3)	10319 (17879)
	bank erosion	13.7 (13)	5 (4.9)	1.7 (2.3)	**64.5 (67.8)**	3.5 (4.2)	2700 (5038)
	no erosion	6.5 (3.4)	10.9 (7.3)	25.2 (4.6)	1.3 (1.4)	**35.2 (24.8)**	2006 (1355)
	observed cases	2153 (3787)	4812 (12113)	5160 (5918)	3128 (4579)	60000 (90111)	
	FN cases	870 (1460)	2237 (4790)	2980 (2099)	1111 (1475)	38865 (67768)	

Table 6.5 Confusion matrix for test and training (in brackets) data sets. Bold fonts represent the accuracy value (%) for each erosion class.

In the confusion matrix (Table 6.5) the diagonal elements represent the proportion of positive cases correctly predicted for each class (corresponding to the sensitivity of the model). The no-erosion class reaches a low efficiency, with value of 35.2% and 24.8% for test and training data, respectively. The results are in accordance to a previous work conducted in the Chianti area (Italy), using the TreeNet and RandomForest models (Märker et al., 2011). The no-erosion cases in fact, are the one showing the poorest results in the model performance evaluation. The highest percentages of true positive

cases, both for training and test data, correspond to gully (61.3% and 59.6%, respectively) and bank erosion (67.8% and 64.5%, respectively) response classes. Mass wasting and sheet-rill erosion classes have low sensitivity for the test data, corresponding to 53.5% and 42.2% respectively, while more accurate performances were obtained for the training set (60.5% and 64.5%).

Off-diagonal elements represent the percentage of ERUs that have been misclassified: Moving along a row or a column false negative (FN) and false positive (FP) cases can be observed. Table 6.5 shows that within the test dataset 34.8% (43.1% for the training data) of the ERUs predicted as mass wasting belongs to the no-erosion class. This misclassification can be justified considering that false negative counts also represent areas that have not yet developed the predicted phenomenon but prone to experiencing it in the future (Begueria, 2006). On the other hand 25.2% of the test ERUs classified as no-erosion belongs to sheet-rill erosion class (FN); this may be due to the ephemeral nature of this type of erosion, which can cause ambiguity in the detection and mapping phases (particularly considering the seasonal variability of its nature).

Furthermore, to measure the performance of the model, six statistical indices were derived (Table 6.6).

	gully erosion		mass wasting		sheet-rill erosion		bank erosion		no erosion		average value	
Ac	(0.89)	0.88	(0.60)	0.67	(0.83)	0.82	(0.94)	0.95	(0.41)	0.46	**(0.73)**	**0.76**
Sn	(0.61)	0.60	(0.60)	0.54	(0.65)	0.42	(0.68)	0.64	(0.25)	0.35	**(0.56)**	**0.51**
Sp	(0.89)	0.89	(0.60)	0.68	(0.84)	0.85	(0.95)	0.96	(0.95)	0.87	**(0.85)**	**0.85**
FPR	(0.11)	0.11	(0.40)	0.32	(0.16)	0.15	(0.05)	0.04	(0.05)	0.13	**(0.15)**	**0.15**
FNR	(0.98)	0.98	(0.90)	0.95	(0.96)	0.96	(0.97)	0.97	(0.53)	0.39	**(0.87)**	**0.85**
AUC	(0.86)	0.84	(0.66)	0.66	(0.85)	0.69	(0.92)	0.92	(0.55)	0.50	**(0.77)**	**0.72**

Table 6.6 Overall Accuracy (Ac), Sensitivity (Sn), Specificity (Sp), False Positive Rate (FPR), False Negative Rate (FNR) and Area Under the ROC Curve (AUC), for training (in bracket) and test data.

All the statistical indices reflect a high performance of the model for gully erosion, mass wasting, sheet-rill erosion and bank erosion classes. For these erosion classes in fact,

overall accuracy, sensitivity and specificity values show that the model is able to discriminate between different erosion processes and to correctly detect negative cases.
A different trend is clearly observed for the no-erosion category. For this class the model outcome for test data shows accuracy, sensitivity and specificity equal to 0.46, 0.35 and 0.87 respectively. This conflicting results highlight that the model is able to discriminate the ERUs for the four analyzed erosion classes, but has not the same ability to recognize environmental and topographic of conditions that characterize the not eroded ERUs.
In general, the TreeNet model underestimates the ERU counts belonging to no-erosion class and overestimate the others classes. These observations are confirmed by high false negative ratio (FNR) and low false positive ratio (FPR) values.

In order to estimate the overall prediction skill of the model the Receiver Operating Characteristics (ROC) curves (Fig. 6.2) were used. The AUC for test data set (blue) illustrates an outstanding performance of the TreeNet model for bank erosion prediction (0.92) and an excellent one for gully erosion (0.84). Sheet-rill erosion AUC values attest for acceptable performance of the model for test data set (0.7) while for training (pink) the result is excellent (0.85).
As expected, the lowest prediction is associated to the no-erosion class (AUC of 0.55 for training and 0.5 for test) and to mass wasting (AUC of 0.66 for training and test), with AUC values reflecting a poor performance of the model (Hosmer and Lemeshow, 2000). The average value of the AUC for all the erosion process (Fig. 8.2) indicates an acceptable performance of the model both for training and test data (0.77 and 0.72 respectively).

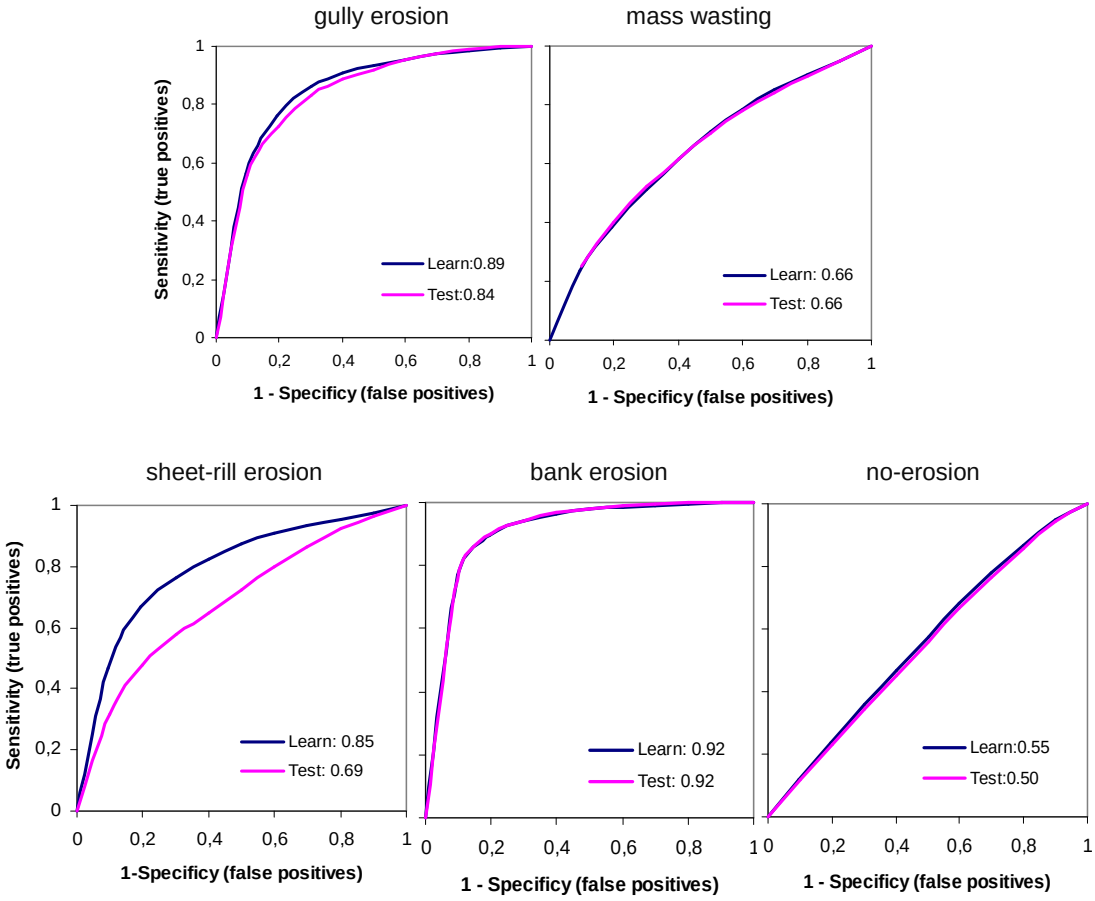

Figure 6.2. ROC curves for each erosion class for learning (blue) and test (pink) data set.

6.3.2 Influence of independent parameters on soil erosion and mass wasting processes

The purpose of using the decision tree is both to achieve a concise and perspicuous representation of the relationship between dependent and independent variables, and to exploit the importance (influence) of the predictor variables considered in the model.

For a single parameter a measure of its influence can be obtained by counting the number of times the it is selected for splitting, weighted by the squared improvement of the model as a result of each split and averaged over all trees (Friedman et al., 2002).

Figure 6.3 shows the overall variable importance of single predictors, where the relative influence of each variable is scaled so that the sum adds to 100, with higher numbers indicating stronger influence on the response. It is clearly highlighted that different process are governed by different combinations of variables. This fact helps to discriminate the membership of each ERUs to a determinate erosion class.

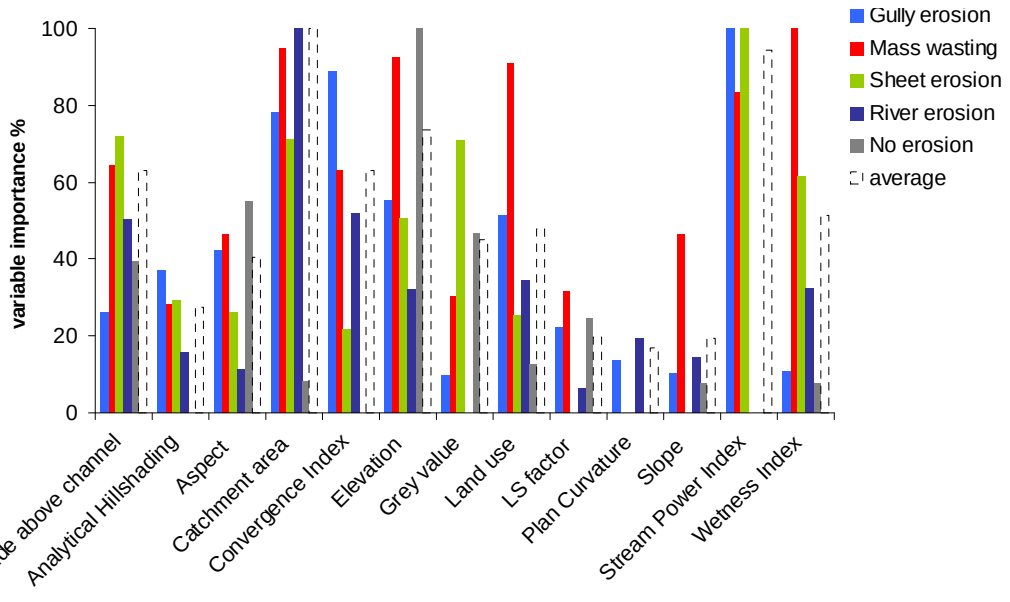

Figure 6.3. Variable importance (%) for predictive variables.

According to a work conducted in the Chianti area (Märker et at., 2011) and using the TreeNet model to predict erosion processes, erosion susceptibility is mainly linked to topographic factors. Stream power index, catchment area, elevation, altitude above the channel network and convergence index have an important role in the model prediction. These variables indicate a strong influence of surface runoff characteristics, triggered by the sub-basin dimension and channel network morphology.

Curvature, profile curvature and curvature classification have any influence in the ERUs classification. The low topographic control of the these predictor variables in the erosion prediction could be explained by the fact that these factors are directly associated with convergence index and plan curvature, which are already part of the model and are

sufficient to explain the spatial distribution of the target variables. Lithology´s influence in the ERUs classification can be neglected, since 94.4% of the study area is characterized by clay substrates (*Argille Varicolori* and *Formazione Terravecchia*). Thus, the variable can be considered as homogeneous for large parts of the study area.

Moreover having information about the variable importance, a better understanding of the environmental conditions responsible for a specific process can be made. Bank erosion is mainly influenced by the catchment area, since it is one of the parameters describing the amount of water available for a certain area and thus, triggering directly channel runoff that may erode the river banks.

The results obtained for gully erosion driving factors are of interest too. Convergence index, stream power index and catchment area are the most important parameters; these results are fully in accordance with previously studies regarding erosion prediction in Sicily. Capra and Scicolone (2002) demonstrate the strong influence of convergence index, stream power index and catchment area in gullies developing. A geostatistical approach applied in northern Sicily yield similar results, showing that linear erosion process susceptibility is mainly controlled by LS-factor, stream power index and topographic transverse profile (Conoscenti et al., 2008a).
Grey-value as predictor showed a very high importance (70.7%) for sheet-rill erosion susceptibility mapping. This process causes loss of minerals and organic matter in the topsoil, resulting in a different coloration in respect the no eroded one.

6.3.3 Soil erosion susceptibility map

The results, obtain by the TreeNet model, were exploited to regionalize the information in areas characterized by similar geo-environmental conditions. Consequently, all the driving factors considered in the ERUs classification were collected for the entire area. The dominant parameter combinations, represented by the tree structure, are now used to attribute specific erosion processes to areas characterized by a certain parameter combinations.

The scoring process of the entire data set of the entire study area allowed producing a map illustrating the spatially distributed erosion potential for each process (Fig. 6.4).

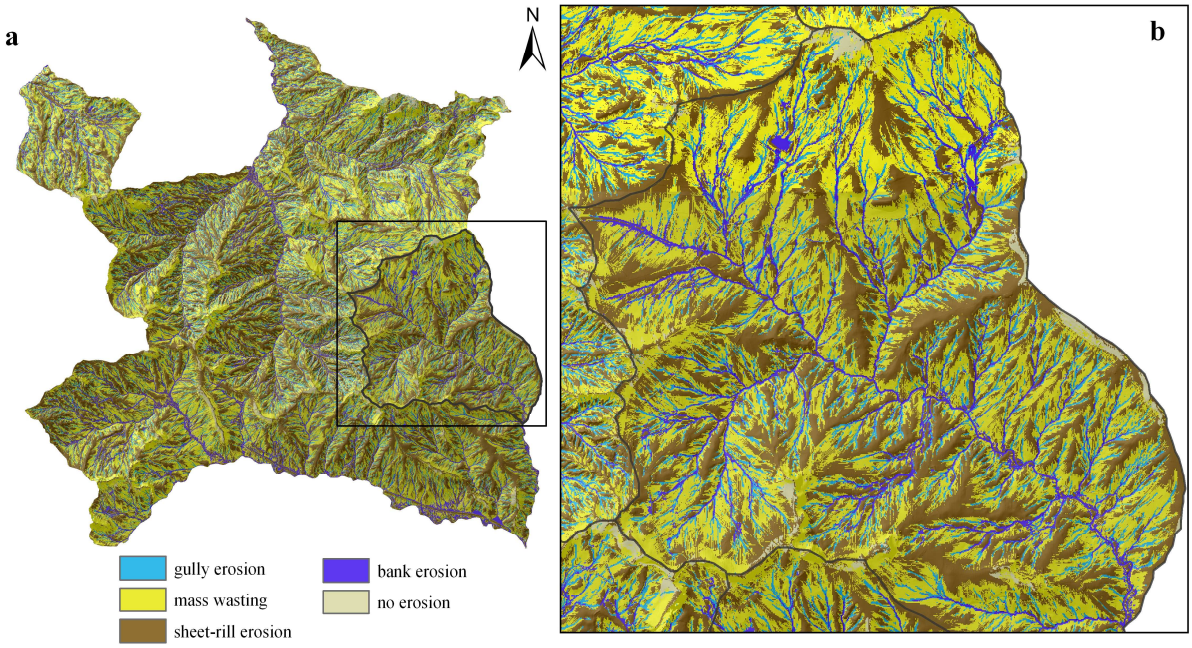

Figure 6.4. Soil erosion susceptibility map of the entire study area (a); detail view in the model build up area, the San Giorgio River basin (b).

Chapter 7

GULLY EROSION SUSCEPTIBILITY ASSESSMENT BY MEANS OF GIS-BASED LOGISTIC REGRESSION ANALYSIS

7.1 Modeling approach

In order to achieve the spatial variability of gully erosion susceptibility the logistic regression analysis was carried out to obtain probability values of gully occurrence on two different types of mapping units: grid cells (CLUs) and slope units (SLUs). The San Giorgio River basin was used to train and test the susceptibility models. The logistic regression analysis was performed by means of the open source software TANAGRA (Rakotomalala, 2005), adopting a forward stepwise strategy to select the explanatory variables.

The first stage was the production in ArcGIS of a data matrix, where each row corresponds to an individual case (i.e. a single grid cell or slope unit), while columnar data show the values of the explanatory and response variables. Since in multivariate statistical analysis it is desired that predictor variables share the same scale (Nefeslioglu et al., 2008) and have the same range as the dependent variable (Ripley, 1996), the selected environmental parameters were scaled between 0 and 1.

Despite the relatively large number (260) of ephemeral and permanent gullies that were recognized in the studied area, only 2.38% of the cell units hosts a gully; as a consequence, the 8,949 grid cells mapped as “positive” provide a quite low ratio of *gully presence* (1) / *gully absence* (0), when compared to the total number (376,099) of cells covering the area. Since a balanced subdivision of positive and negative cases (i.e. ratio equal to 1) in the training dataset used to prepare a multivariate statistical model is generally recommended (Süzen and Doyuran, 2004; Nefeslioglu et al., 2008; Van Den Eeckhaut et al., 2009; Bai et al., 2010; Frattini et al., 2010), logistic regression analyses were performed by selecting groups of training cells, balanced in terms of positive and negative cases. An equal distribution of presence and absence of gullies was also used as criterion for picking up training subsets of slope units, even if, in this case, the presence/absence ratio from the entire basin is not so far from 1 (158/195).

Since the acceptance of a predictive model requires the evaluation of its robustness to small changes of the input data (i.e. data sensitivity), gully erosion susceptibility models were prepared on 3 different samples of terrain units for both the types of spatial domains considered (cell and slope units).

The learning subsets of cell units were collected according to the following two steps: i) selection of three first samples ([A], [B], [C]) of 17,898 cells, each given by all the positive

cases in addition to the same number of negative cases (8,949 cells). The latter was randomly collected, maintaining a minimum distance of 25 m between each other and from positive pixels, in order to reduce the effects of spatial auto-correlation; ii) random selection of 14,318 cells (80% of the first sample), equally distributed between positive and negative cases. The cells not selected in the second step (3,580 for each of the first samples) were used to test the accuracy of the models.

The adopted strategy provided three training samples ($[A_{cal}]$, $[B_{cal}]$, $[C_{cal}]$) and three test samples ($[A_{val}]$, $[B_{val}]$, $[C_{val}]$). By applying a stratified random selection strategy, imposing 50% of positive cases within the subset, the 353 slope units were split into three calibration ($[D_{cal}]$, $[E_{cal}]$, $[F_{cal}]$) and three validation datasets ($[D_{val}]$, $[E_{val}]$, $[F_{val}]$), made up of 176 and 177 SLUs, respectively; since slope units can be considered as individual cases, morphodinamically independent (Rotigliano et al., 2011), the three training samples were collected without any spatial constraint. Finally, further logistic regression analysis were carried out to generate, for the entire study area, two gully erosion susceptibility maps, defined a grid cell and slope unit scale.

Validation procedures were finally adopted to evaluate the quality (i.e. reliability, robustness, degree of fitting and prediction skill) of susceptibility models. The accuracy of logistic regression in modeling susceptibility of the study area to gully erosion phenomena was evaluated by drawing, for each model, the Receiver Operating Characteristic (ROC) curves and by computing the values of the Area Under the ROC Curve. ROC curves were drawn both for the validation (test) and calibration (training) datasets, in order to evaluate predictive performances of the models and to further investigate their fit to the training observations; moreover, the difference between apparent accuracy (on training data) and validated accuracy (on test data) indicates the amount of overfitting (Märker et al., 2011).

7.2 Dependent and independent variables

7.2.1 Gully landforms

The gully landforms inventory, containing 260 linear erosion landforms classifiable as ephemeral or permanent gullies, was used to build up the model. The spatial distribution of gullies was coded as presence or absence of landforms in a mapping unit, and this

binary information was picked up as the dependent response variable for the statistical analysis.

7.2.2 Controlling factors

The grid cells and the slope units covering the study area were assigned with the values of a set of environmental parameters, in addition to the binary response (i.e. presence or absence of a gully) of the dependent variable. The explanatory variables were selected in order to reproduce the erodibility of outcropping materials, the erosivity of overland flow, the influence on erosion processes of topographic position and the effects of the river and road networks.

The dataset of the predictor variables consists of 24 attributes defined both for cell and slope units, 1 computed only for grid cells and other 2 calculated only for slope units (Table 7.1). For the cell units, the values of the attributes were derived directly from the raster layers that were generated for each of the factors; for the slope units, the environmental parameters were calculated by applying zonal statistics to the cells falling inside each terrain domain (Fig. 7.1).

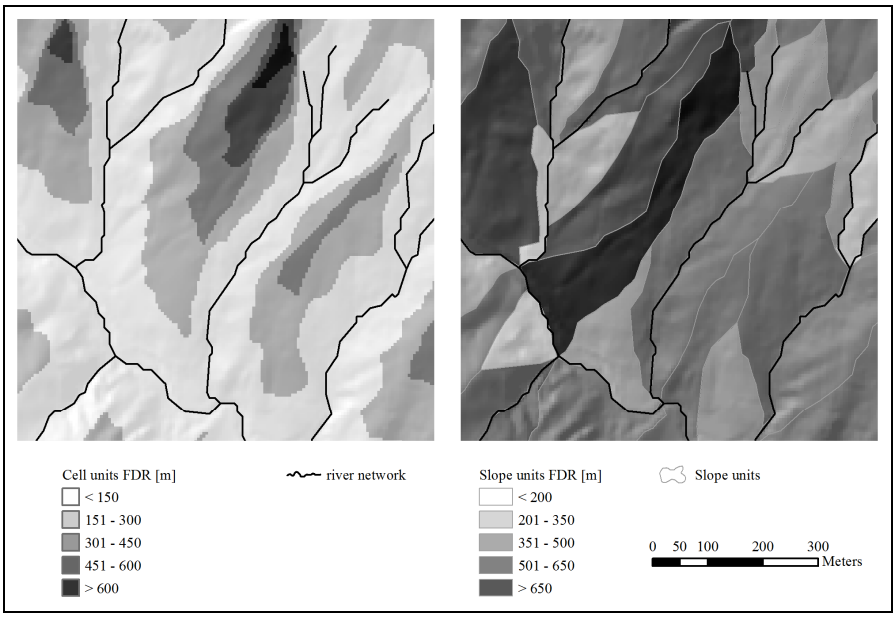

Figure 7.1. GIS layer of Flow Distance to River network (FDR), defined on the scale of cell units (left) and slope units (right).

Indipendent variables			Cell Units (CLU)	Slope Units (SLU)
Categorical variables			*Attribute values*	*Attribute values*
Bedrock lithology	clay	LTL_clay	binary response [0,1]	class relative frequency
	conglomerate	LTL_cong	binary response [0,1]	class relative frequency
	gypsum	LTL_gyps	binary response [0,1]	class relative frequency
	sandstone	LTL_sand	binary response [0,1]	class relative frequency
Land use	arable lands	USE_arab	binary response [0,1]	class relative frequency
	permanent crops	USE_crop	binary response [0,1]	class relative frequency
	pastures	USE_past	binary response [0,1]	class relative frequency
Slope aspect	North	ASP_N	binary response [0,1]	class relative frequency
	North-East	ASP_NE	binary response [0,1]	class relative frequency
	East	ASP_E	binary response [0,1]	class relative frequency
	South-East	ASP_SE	binary response [0,1]	class relative frequency
	South	ASP_S	binary response [0,1]	class relative frequency
	South-West	ASP_SW	binary response [0,1]	class relative frequency
	West	ASP_W	binary response [0,1]	class relative frequency
	North-West	ASP_NW	binary response [0,1]	class relative frequency
Continuos variables			*Attribute values*	*Attribute values*
Elevation		ELE	cell value	SLU mean value
Elevation range		ELR	/	range within the SLU
Slope angle		STP	cell value	SLU mean value
Plan curvature		PLC	cell value	SLU mean value
Profile curvature		PRC	cell value	SLU mean value
Stream Power Index		SPI	cell value	SLU mean value
Topographic Wetness Index		TWI	cell value	SLU mean value
Length-Slope Factor		LSF	cell value	SLU mean value
Topographic Position Index		TPI	cell value	SLU mean value
Distance From Roads		DFR	cell value	/
Road Network Length		RNL	/	total road lengths in the SLU
Flow Distance to River network		FDR	cell value	SLU maximum value

Table 7.1 Independent explanatory variables and method adopted for their calculation.

The effects of terrain erodibility conditions on distribution of erosion phenomena were explored by analyzing the spatial pattern of bedrock lithology, land use and slope aspect; while the first two attributes are widely recognized as having a direct control on water erosion, slope aspect could have a potential indirect effect, given its relation with

vegetation distribution and geo-structural conditions. The compass direction of slope values was reclassified in 8 categorical intervals.
For the statistical analysis, an explanatory variable was derived from each of the classes of lithology, land use and aspect; for cell units, these variables were defined by binary values (i.e. 1 for cells where the class occurs, 0 for cells where it doesn't), while the relative frequency of each class computed within the SLU was assigned to the slope units.

The erosive power of runoff, in terms of potential discharge volume, flow velocity and transport capacity, was modeled by means of 8 topographic attributes (see chapter 5). The potential effects on gully erosion distribution of road were investigated for grid cell units, by calculating the distance from the closest road segment. The total length of roads, calculated within each slope unit, was also considered as explanatory variables for presence or absence of gullies.

7.3 Results

By performing logistic regression analysis on the learning datasets, three gully erosion susceptibility models were obtained for each of the mapping unit types. The models fitting to the observed data was evaluated by computing, in addition to the statistic -2LL, the values of Cox and Snell and Nagelkerke R^2; the smaller the *negative log-likelihood* the better the fit of the model, while the pseudo-R^2 statistics grow with the "goodness of fit". The logistic regression component of the software TANAGRA provides also the results of the *model chi-square* test, which allows for assessing the global significance of the regression coefficients; the significance was evaluated also individually for each independent variable incorporated in the model by means of the Wald test.

7.3.1 Cell units models

The fit of the regression models with data observed from the training subsets of cells ($[A_{cal}]$, $[B_{cal}]$, $[C_{cal}]$) is quantitatively evaluated by the -2LL and pseudo-R^2 statistics, while model chi-square test shows the global significance of the regression coefficients.
The values of these parameters indicate a statistical significant fit of all the CLUs models with their training area (Table 7.2); moreover, since results are quite similar for the three

subsets of grid cells, the modeling approach demonstrated to be quite robust when changes of the learning dataset occur.

Samples	-2LL		Model Chi² test (LR)			R²-like	
	Intercept	Model	Chi-2	d.f.	P(>Chi-2)	Cox and Snell's R²	Nagelkerke's R²
[A_{cal}]	19849.0	14657.0	5192.0	15	0.0000	0.3041	0.4055
[B_{cal}]	19849.0	14683.3	5165.7	15	0.0000	0.3029	0.4038
[C_{cal}]	19849.0	14842.8	5006.1	15	0.0000	0.2951	0.3934

Table 7.2 Results of -2LL, Model Chi^2 test and R^2-like statistics computed for the regression models calibrated on the learning samples of grid cells.

Data reported in Table 7.3 show the statistical significance of the individual predictors that entered the three regression models. The forward stepwise process, which was applied by setting a minimum probability of 0.01 for variable selection at each step, picked 15 attributes in all the three learning environments.

Among the 25 analyzed physical attributes, 18 entered at least one of the regression models, 3 were incorporated in two models and 12 were selected for the three models; the latter 12 consist of all the continuous topographic attributes, with the exception of elevation, in addition to clay, south and north-east slope aspect. The Wald test addresses plan curvature and stream power index as the most significant independent variables for the three samples, followed by clay and profile curvature that are always above 100; sign and magnitude of β coefficients indicate concave (negative curvature) portions of slopes, characterized by high erosive power of runoff (high SPI values) and by the outcropping of clays, as the sectors more frequently affected by gully erosion processes.

The discrimination ability of the logistic regression models is resumed by the classification matrix of Table 7.4 where, both for training and test areas, observed positive and negative cells, predicted true/false positive and negative cases are reported together with the results of percent correct (Frattini et al., 2010; Märker et al., 2011).

Indipendent variables		Sample [A]			Sample [B]			Sample [C]		
		β coeff.	Wald test	Signif.	β coeff.	Wald test	Signif.	β coeff.	Wald test	Signif.
clay	LTL_clay	1.3141	147.70	0.0000	1.2897	145.42	0.0000	1.1846	129.37	0.0000
conglomerate	LTL_cong	/	/	/	/	/	/	/	/	/
gypsum	LTL_gyps	/	/	/	/	/	/	/	/	/
sandstone	LTL_sand	/	/	/	/	/	/	/	/	/
arable lands	USE_arab	/	/	/	0.2368	15.70	0.0001	/	/	/
permanent crops	USE_crop	-0.3084	16.99	0.0000	/	/	/	-0.4213	31.26	0.0000
pastures	USE_past	/	/	/	/	/	/	/	/	/
aspect N	ASP_N	/	/	/	0.3186	18.80	0.0000	0.2897	15.46	0.0001
aspect NE	ASP_NE	0.4938	77.64	0.0000	0.7038	149.10	0.0000	0.6866	141.93	0.0000
aspect E	ASP_E	/	/	/	0.3317	25.24	0.0000	0.2071	10.04	0.0015
aspect SE	ASP_SE	-0.2513	14.42	0.0001	/	/	/	/	/	/
aspect S	ASP_S	-0.5180	83.19	0.0000	-0.2911	25.28	0.0000	-0.4054	49.64	0.0000
aspect SW	ASP_SW	/	/	/	/	/	/	/	/	/
aspect W	ASP_W	-0.2997	10.59	0.0011	/	/	/	/	/	/
aspect NW	ASP_NW	/	/	/	/	/	/	/	/	/
elevation	ELE	/	/	/	/	/	/	/	/	/
slope angle	STP	-5.9556	94.51	0.0000	-5.4354	78.49	0.0000	-5.8642	94.17	0.0000
plan curvature	PLC	-10.6405	864.07	0.0000	-10.6499	846.98	0.0000	-10.3383	824.29	0.0000
profile curvature	PRC	-8.0140	130.57	0.0000	-8.4493	141.04	0.0000	-8.0181	129.76	0.0000
stream power index	SPI	10.8110	792.11	0.0000	10.2455	652.13	0.0000	10.7386	698.14	0.0000
top. wetness Index	TWI	-9.6810	111.05	0.0000	-8.8070	91.87	0.0000	-10.1823	126.99	0.0000
LS Factor	LSF	-33.4370	110.47	0.0000	-28.6700	65.92	0.0000	-31.5047	76.75	0.0000
top. position index	TPI	-1.8449	97.32	0.0000	-1.7730	89.61	0.0000	-1.8125	94.04	0.0000
dist. from roads	DFR	0.6482	34.11	0.0000	0.5599	26.06	0.0000	0.7023	41.24	0.0000
flow dist. to river	FDR	-0.5737	14.64	0.0001	-0.6769	20.27	0.0000	-0.5181	11.99	0.0005

Table 7.3 β coefficients, Walt test values and their significance computed for the individual predictors that entered the three regression models trained on grid cells.

Sample		Observed cases		Predicted cases					
				Percent correct		Positive		Negative	
[A]	Positive	(7159)	1790	(73.4)	72.4	(5254)	1296	(1905)	494
	Negative	(7159)	1790	(77.7)	78.2	(1596)	391	(5563)	1399
	Sum	(14318)	3580	(75.5)	75.3	(6850)	1687	(7468)	1893
[B]	Positive	(7159)	1790	(73.2)	72.5	(5240)	1297	(1919)	493
	Negative	(7159)	1790	(77.8)	76.6	(1590)	418	(5569)	1372
	Sum	(14318)	3580	(75.5)	74.6	(6830)	1715	(7488)	1865
[C]	Positive	(7159)	1790	(72.6)	74.7	(5201)	1338	(1958)	452
	Negative	(7159)	1790	(77.9)	76.6	(1585)	419	(5574)	1371
	Sum	(14318)	3580	(75.3)	75.7	(6786)	1757	(7532)	1823

Table 7.4 Observed positive and negative grid cells, predicted true/false positive and negative cases and percent correct for both calibration (in brackets) and validation datasets.

For the three samples quite similar accuracy arise, for both calibration and validation subsets of cells. Models show a slightly higher predictive ability for cells not affected by gullies, compared to cells where gullies occur. Predictive performance of the models was assessed also by means of a cut-off independent technique, based on drawing ROC curves and computing AUC values (Fig. 7.2).

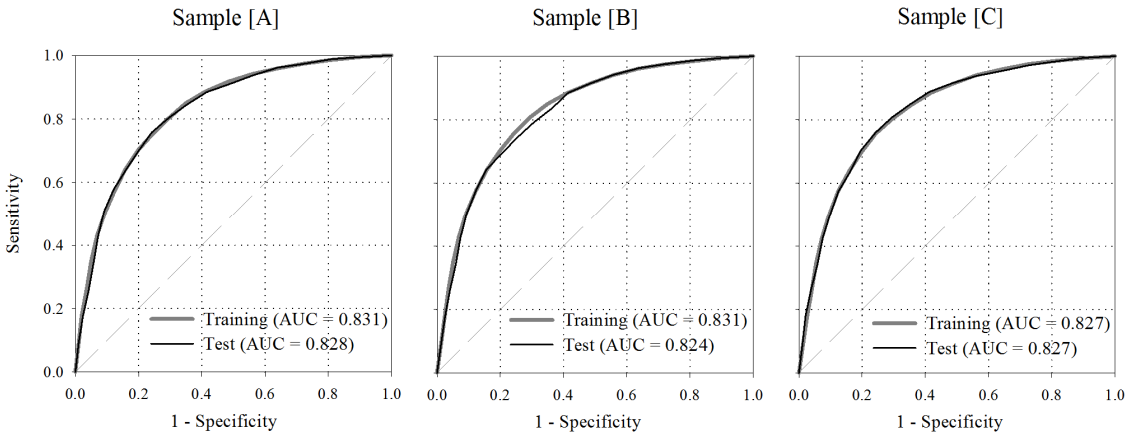

Figure 7.2. ROC curves and AUC values of the CLU-based regression models.

The latter indicate excellent (cf. Hosmer and Lemeshow; 2000) results for all the models both in the training and test subsets of cells; ROC curves are quite similar and, consequently, very small differences of AUC-values are observed.
Since both the classification matrix and AUC values indicate minor alterations of models predictive power between training and test areas, it can be concluded that the modeling procedure carried out at grid cell scale has not suffered from overfitting; moreover, models demonstrated robustness to changes of the learning samples.

7.3.2 Slope units models

Regression analysis carried out on the learning samples of the slope units ([D_{cal}], [E_{cal}], [F_{cal}]) provided three different susceptibility models. The computed values of the parameters -2LL, pseudo-R^2 and chi-square (Table 7.5) indicate that the models fit with the spatial occurrence of gullies in the training subsets with a statistical significance higher than 99%.

Nevertheless, in contrast with what observed for cell units, the goodness of fit of the susceptibility models seems less stable when changes of the SLUs learning samples are adopted. This is also confirmed looking at the individual predictors that entered the three regression models (Table 7.6): the forward stepwise strategy, which was applied setting a minimum probability of 0.05 for the selection of the variables, picked up 2, 5 and 4 predictors, of which only two (FDR and ELE) entered at least two models. The maximum flow distance to river, computed within the SLUs, demonstrated to be the best and most significant predictor of the gullies occurrence in the training areas, as it is the only attribute included in all the models, in addition to reaching the highest value of the Wald test in the learning samples [D] and [F]. The classification matrix computed for the SLU regression models (Table 7.7) indicates more enhanced differences of discrimination ability respect to what seen for CLU models. Values of percent correct are quite diverse for the three units samples and between learning and validation subsets of SLUs; moreover, in contrast with the regression models trained on cells, SLU models demonstrate better accuracy in predicting positive cases.

Samples	-2LL		Model Chi² test (LR)			R²-like	
	Intercept	Model	Chi-2	d.f.	P(>Chi-2)	Cox and Snell's R²	Nagelkerke's R²
[Dcal]	244.0	199.7	44.3	2	0.0000	0.2224	0.2965
[Ecal]	244.0	177.5	66.5	5	0.0000	0.3145	0.4193
[Fcal]	244.0	190.6	53.4	4	0.0000	0.2617	0.3490

Table 7.5 Results of -2LL, Model Chi^2 test and R^2-like statistics computed for the regression models calibrated on the learning samples of slope units.

Indipendent variables	Sample [D]			Sample [E]			Sample [F]		
	β coeff.	Wald test	Signif.	β coeff.	Wald test	Signif.	β coeff.	Wald test	Signif.
LTL_clay	/	/	/	/	/	/	6.3129	15.45	0.0001
LTL_cong	/	/	/	/	/	/	/	/	/
LTL_gyps	/	/	/	/	/	/	/	/	/
LTL_sand	/	/	/	/	/	/	5.3579	6.23	0.0126
USE_arab	/	/	/	/	/	/	/	/	/
USE_crop	/	/	/	/	/	/	/	/	/
USE_past	/	/	/	/	/	/	/	/	/
ASP_N	/	/	/	-1.6774	3.77	0.0523	/	/	/
ASP_NE	/	/	/	/	/	/	/	/	/
ASP_E	/	/	/	/	/	/	/	/	/
ASP_SE	/	/	/	/	/	/	/	/	/
ASP_S	/	/	/	/	/	/	/	/	/
ASP_SW	/	/	/	/	/	/	/	/	/
ASP_W	/	/	/	/	/	/	/	/	/
ASP_NW	/	/	/	/	/	/	/	/	/
ELE	-2.5051	7.06	0.0079	-2.6645	7.50	0.0062	/	/	/
ELR	/	/	/	/	/	/	/	/	/
STP	/	/	/	-14.6399	15.73	0.0001	/	/	/
PLC	/	/	/	/	/	/	/	/	/
PRC	/	/	/	/	/	/	-4.2397	6.59	0.0103
SPI	/	/	/	/	/	/	/	/	/
TWI	/	/	/	-15.8756	18.59	0.0000	/	/	/
LSF	/	/	/	/	/	/	/	/	/
TPI	/	/	/	/	/	/	/	/	/
RNL	/	/	/	/	/	/	/	/	/
FDR	5.8784	32.18	0.0000	5.0714	18.22	0.0000	4.8043	19.41	0.0000

Table 7.6 β coefficients, Walt test values and their significance computed for the individual predictors that entered the three regression models trained on slope units.

Sample		Observed cases		Predicted cases					
				Percent correct		Positive		Negative	
[D]	Positive	(88)	70	(73.9)	71.4	(65)	50	(23)	20
	Negative	(88)	107	(71.6)	70.1	(25)	32	(63)	75
	Sum	(176)	177	(72.7)	70.6	(90)	82	(86)	95
[E]	Positive	(88)	70	(76.1)	71.4	(67)	50	(21)	20
	Negative	(88)	107	(72.7)	60.7	(24)	42	(64)	65
	Sum	(176)	177	(74.4)	65.0	(91)	92	(85)	85
[F]	Positive	(88)	70	(75.0)	77.1	(66)	54	(22)	16
	Negative	(88)	107	(72.7)	64.5	(24)	38	(64)	69
	Sum	(176)	177	(73.9)	69.5	(90)	92	(86)	85

Table 7.7 Observed positive and negative slope units, predicted true/false positive and negative cases and percent correct for both calibration and validation datasets.

Predictive performances of the regression models trained on SLUs are evaluated from acceptable to excellent (cf. Hosmer and Lemeshow; 2000), by drawing ROC curves and computing relative AUC values (Fig. 7.3). Small differences of predictive skill are observed between training and test slope units for the samples [D] and [F], while quite diverse AUC values are calculated for the [E] subsets of SLUs; these results, together with the classification matrix of Table 7.7, seem to indicate a problem of overfitting only for the sample [E].

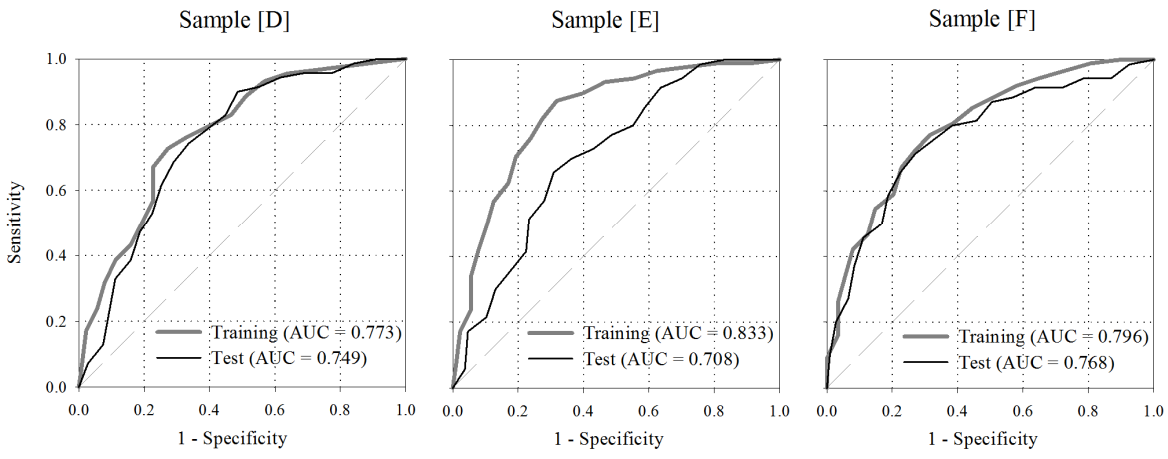

Figure 7.3. ROC curves and AUC values of the SLU-based regression models.

7.3.3 Susceptibility maps

The probability of gully occurrence for all the grid cells and slope units of the study area was computed by performing further logistic regression analyses.

The [A] sample of cells, which was the one providing the highest apparent and validated accuracy, was entirely used as learning dataset to calculate new regression coefficients; these were transferred to ArcGIS for computing the probability (*P*) of gully occurrence for all the cells falling within the study area. By using the whole basin as training area, *P* was calculated also for all the slope units. Hence, the probability values of gully occurrence, assessed for each cell and slope unit, were used to generate two gully erosion susceptibility maps (Fig. 7.4), where probabilities are classified into four susceptibility levels.

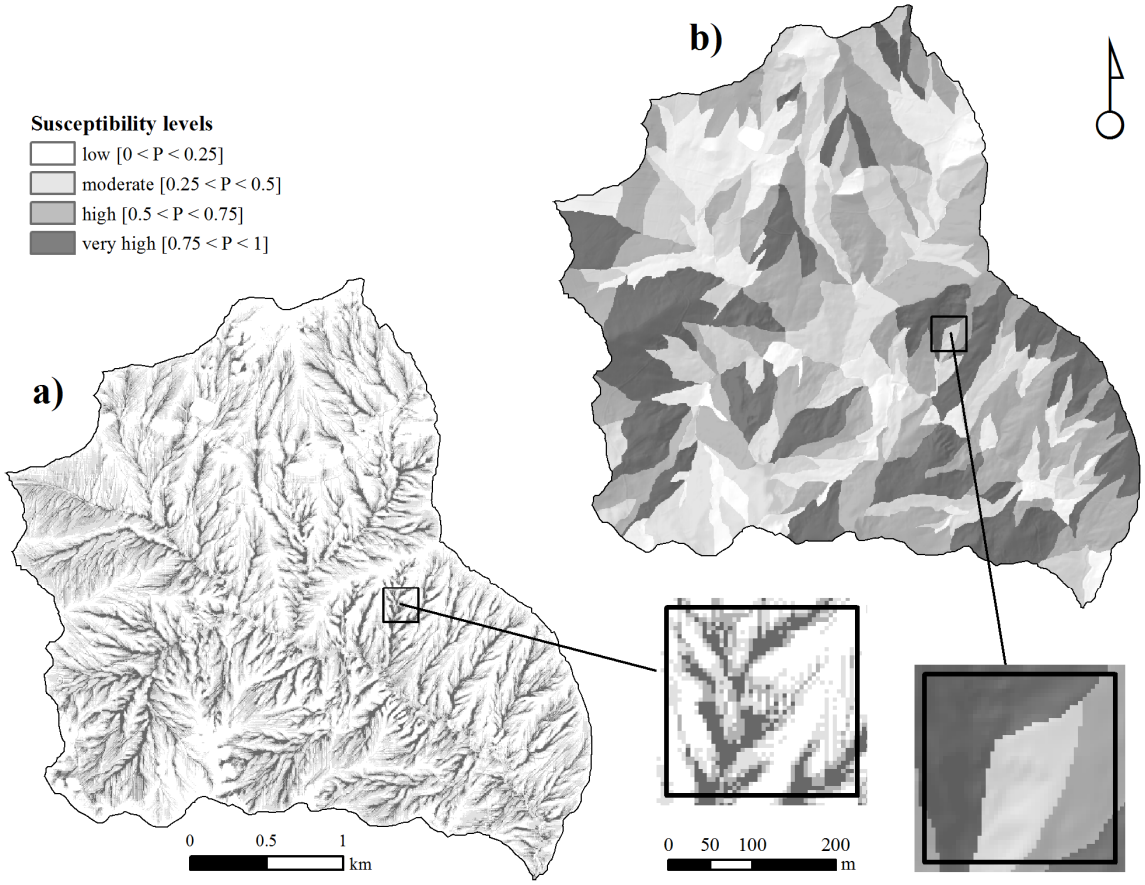

Figure 7.4. CLU-based (a) and SLU-based (b) gully erosion susceptibility maps.

The fit of the susceptibility maps with the gullies spatial distribution was evaluated by calculating ROC curves and AUC values (Fig. 7.5); both the CLU- and SLU-based gully erosion susceptibility maps show an excellent ability (AUC > 0.8) of discriminating between positive and negative grid cells and slope units, respectively.

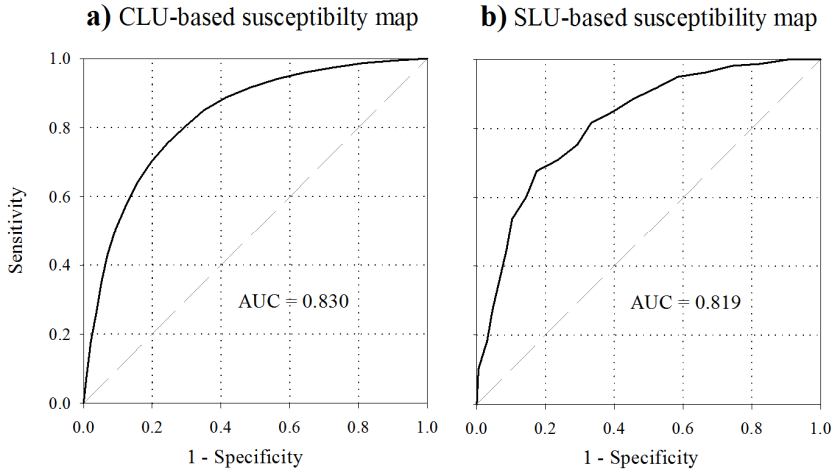

Figure 7.5. ROC curves and AUC values of the CLU-based (a) and SLU-based (b) gully erosion susceptibility maps.

Chapter 8

SIMULATING THE IMPACT OF MAN-INDUCED ELEMENTS ON EROSION PROCESSES IN AGRICULTURAL CATCHMENTS USING EMPIRICAL MODELS

8.1 Modelling approach

To a better understanding of the role of anthropogenic factors in soil erosion phenomenon, a land use scenario analysis is proposed.

The San Giorgio catchment was used to achieve the described goal. In the basin man-induced elements influencing runoff processes are mainly linked to the alteration of original terrain morphology and consequently on the spatial soil redistribution pattern. Farmers play an important role in modifying the natural flow-path both at field and basin scale. Artificial channels, filed boundaries and an intense network of unpaved roads segments are the recognized main cause of important transformation mechanism of the studied agricultural landscape.

In order to simulate the impact of anthropogenic elements on soil loss rate data related to their characteristics and spatial distribution in the basin were collected. These element were included in the RUSLE (Revised Universal Soil Loss Equation) (Renard et al., 1997) model. Annual soil loss rates were predicted under two different environmental situations: The first includes the collected anthropogenic elements (named current scenario), the second environmental condition was constructed by simulating a scenario, where any man-induced landscape modification exists (named hypothetical scenario). Results are described by two maps showing the spatial distribution of annual soil loss rate, due to rill-interrill erosion.

Once constructed the two erosion scenarios, the corresponding maps were compared and differences analyzed. This operation underlined the influence of linear man-induced elements on erosion processes.

Finally the spatial domains hosting any man-induced elements were overlapping to the erosion/deposition map, constructed by the USPED (Unit Stream Prediction Erosion Deposition Process, Mitasova et al., 1996) model application, to better define the distribution of off-site impacts caused by human activities in the basin.

8.2 Models components

8.2.1 Man-induced elements in agriculture catchment

In the San Giorgio River basin the presence of man-induced elements is principally linked to agriculture activities. On field scale, tillage furrows and irrigation channels, as small as 20 cm in depth, were considered to modify the overland flow directions in parcels characterized by a low-moderate slope. Landscape fragmentation in small agricultural parcels characterize the entire study area: The presence of ditches at field boundaries may constitute a preferential flow path for water and consequently be source of sediments. The continuity and the total length of the rural element influences runoff and consequently erosion and deposition processes. The influence of roads regards a larger scale respect to the field parcels. Roads concentrate and change surface runoff, changing the patterns of soil erosion. In the present study the influence of paved roads on soil erosion processes was not considered, being their surface affected by water runoff.

By aerial photographs interpretation (pixel size 0.25 m, 02.09.2007), integrated by filed surveys (during the year 2010) and GIS, 225 linear rural elements (among them artificial channels and field boundaries) were recognized, giving a total length of 45.9 km. Unpaved roads segments are also diffuse in the entire basin; 50 roads elements on a total approximate length of 33.3 km (Fig. 8.1).

The potential topographic surface influencing runoff was defined by assigning a specific buffer to collected man-induced elements. In the study area field boundaries and artificial channels represent depressions in the ground characterized by a cross section width lower than 30 cm. Consequently along these rural elements an equal 30 cm buffer was constructed. To each road segment a specific buffer, ranging from 5 to 10 m, was constructed being runoff direction and intensity influenced both of the upslope and downslope side shapes of a road segment. 12.3% of the San Giorgio catchment is interested by man-induced elements.

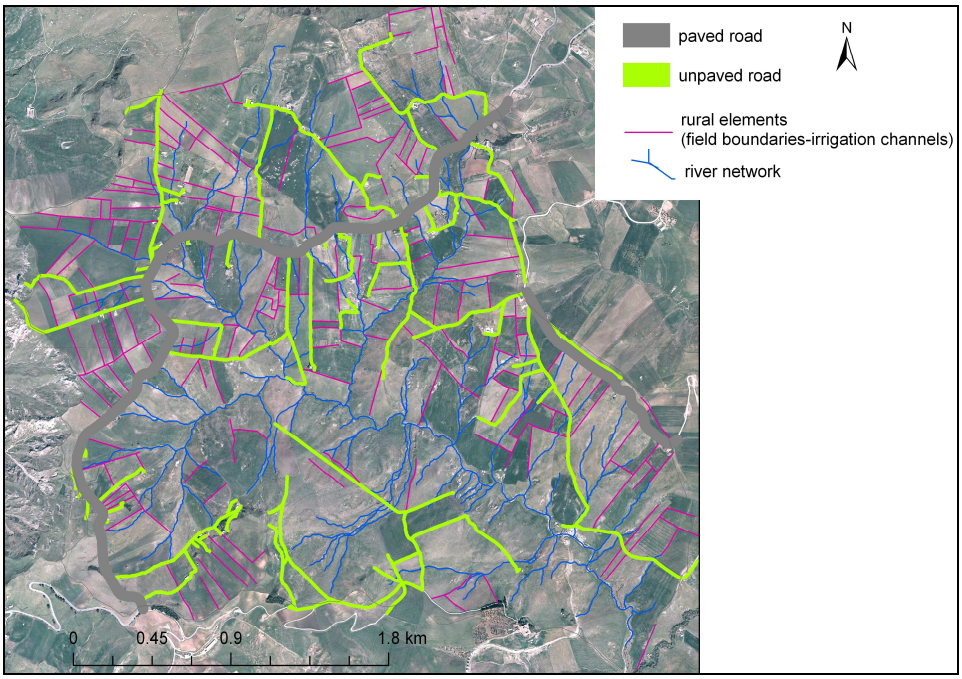

Figure 8.1. Map showing the man-induced elements in the San Giorgio River basin. The recognized categories, mapped from aerial photographs (2007), are paved roads, unpaved roads and rural elements.

8.2.2 Soil erosion scenario construction

The presence of rural elements and roads influences two RUSLE model components: The Topographic factor (LS factor) and the Land cover management factor (C factor).

The rainfall erosivity (R factor) and the soil erodibility (K factor) indices were considered not changing their values in the two simulated situations. The methodologies used to assess these factors and the resulting maps were widely described in Chapter 5.

No erosion control practices (P factor) are used in the watershed. To the P factor, was assigned a value of 1.0 (dimensionless); it has no effect on the erosion calculations in both erosion simulations.

The combined effect of slope, length and steepness on soil loss phenomenon was derived by the 2m-DEM, by calculating the LS factor; it can be considered as a measure of the sediment transport capacity by runoff. Moreover the use of a high defined resolution DEM allowed including the topographic attribute of rural elements in the erosion modelling.

To model erosion using the described hypothetical situation the DEM was modified. The surface containing the man-induced elements was employed as mask to drill the DEM and generate a new elevation model by re-interpolation (TOPOGRID command within ArcInfo). The resulting DEM is not containing preferential artificial paths for the water overland flow due to man-induced topographic modifications (Fig. 8.2).

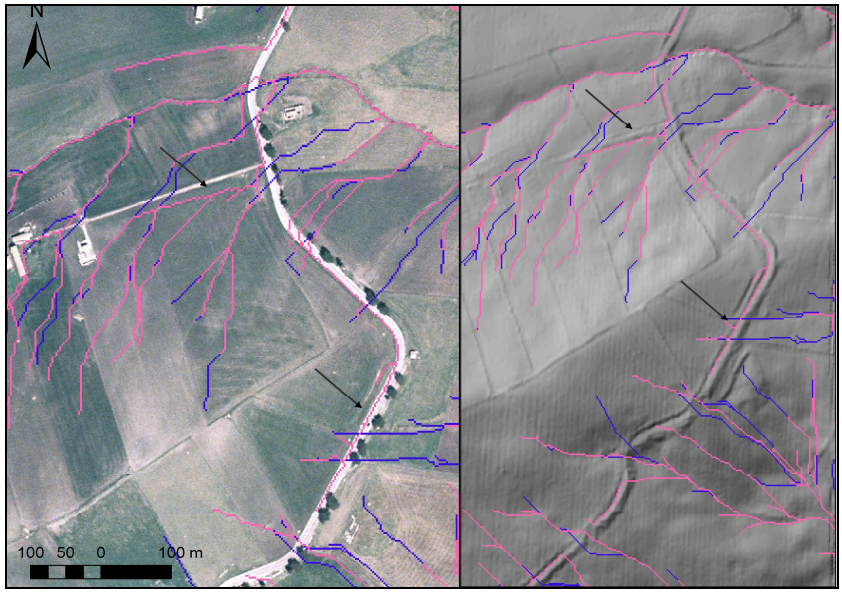

Figure 8.2. Comparing flow accumulation grids in modified (blue lines) and original (pink lines) DEM. Linear features like roads and field boundaries become part of the permanent drainage network.

The erosion scenario simulation also involves changes on the land use factor. Previous works led to use necessary information to assign a value to the C factor for each land use category recognized in the San Giorgio river basin (Table 8.1). Numerical attributes that represent the protective contribute of vegetation cover on soil particles detachment and transport.

In particular, to model erosion in the current environmental situation, a specific land use map, taking anthropogenic landscape features into account, was used (Fig. 8.3a). While in the hypothetical scenario, the land cover associated to roads and rural elements was dissolved to the closest land use category (Fig. 8.3b).

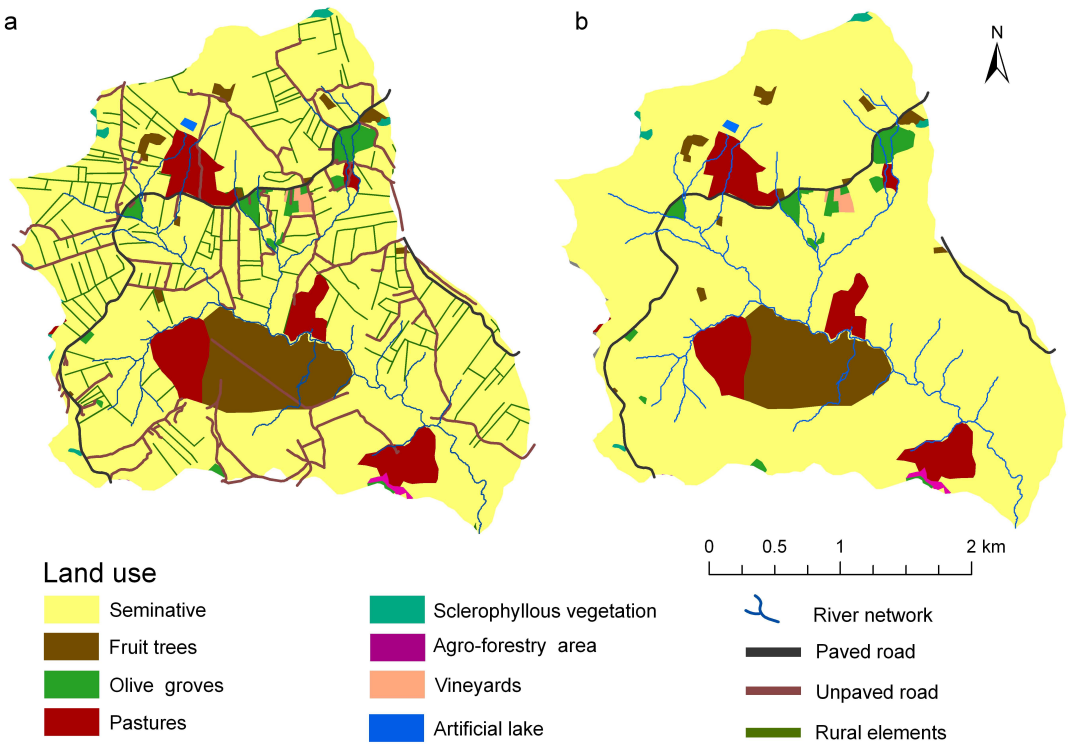

Figure 8.3. San Giorgio River basin current land use (a) and hypothetical land use maps (b).

Land use	C-value
Seminatives	0.12
Pastures	0.15
Sclerophyllous vegetation	0.038
Fruit trees	0.3
Olive groves	0.1
Agro-forestry areas	0.002
Vineyards	0.451
Rural elements; Unpaved road	1
Artificial areas (paved road and urban fabric)	0

Table 8.1 C-values assigned to each land cover category on the basis on previous studies.

8.2.3 Erosion/deposition map

The solution of the USPED model allowed to predict erosion, in areas experiencing an increase in sediment transport capacity, and deposition where a decrease in sediment transport capacity occurs.

Grids containing information related to the transportability coefficient (K_t), were created for each of the factors considered in the USPED model (see Chapter 5): R, K and C factors are the same used in the RUSLE, while the topographic component was calculated by combining the profile and the tangential curvature, upslope contributing area, slope and aspect grid layers.

The erosion/deposition map is shown in Figure 8.4. In the San Giorgio river basin severe soil loss occurs predominantly on convex upper slope landscape positions and soil accumulation occurs on concave lower slope positions.

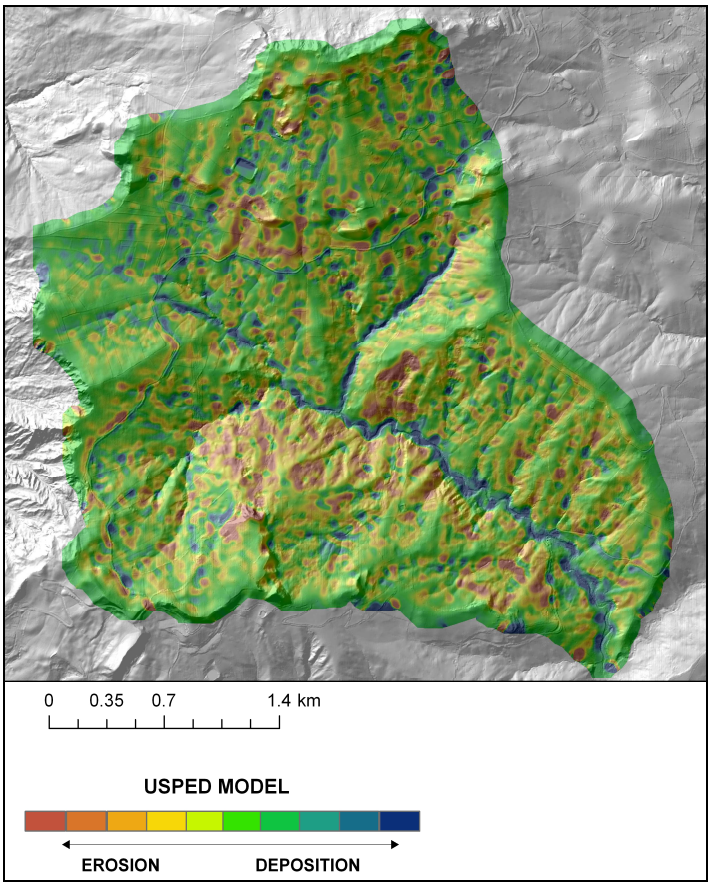

Figure 8.4. Erosion/deposition map for the San Giorgio River basin.

8.3 Results

8.3.1 Soil loss prediction

By applying the RUSLE model, the current and hypothetical soil loss scenarios were constructed (Fig. 8.5). The corresponding maps show the pattern distribution and intensity of rill-interrill erosion. In the San Giorgio river basin the average annual soil loss rate in the current and in the hypothetical scenario was estimated to be 27.7 t/ha year and 22.8 t/ha year respectively. On basin scale, the presence of man-induced elements on erosion processes was measured to increase the soil loss of about 17.4%.

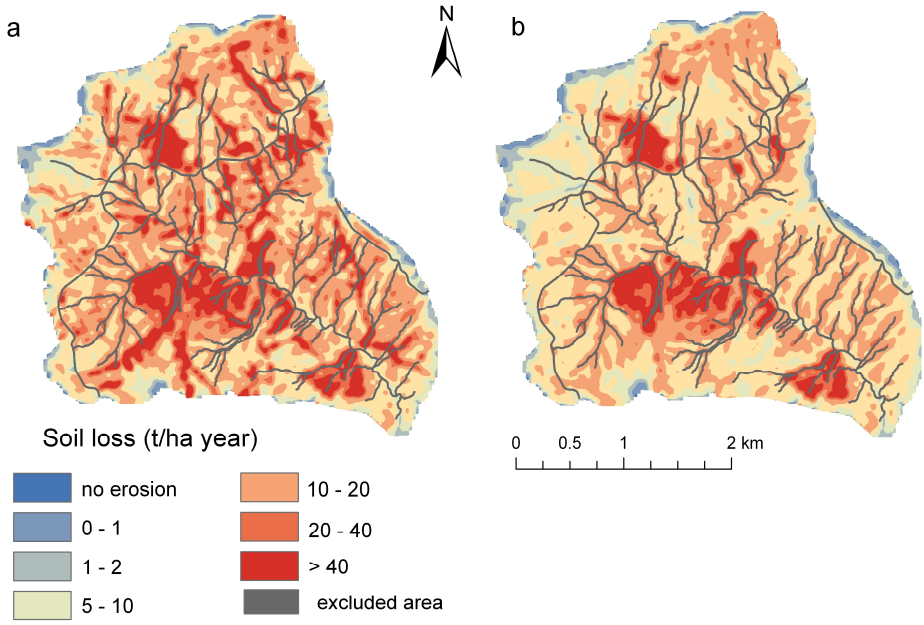

Figure 8.5. Predicted soil loss for current (a) and hypothetical (b) simulated scenarios.

Predicted soil loss rate within the current erosion scenario was compared with the evidence of sheet and rill erosion landforms detected *in situ*. 70% of erosion landforms falls in soil loss rate ranging from 20 up to 40 t/ha year.

In the present thesis the RUSLE model's ability to predict soil erosion potential within the San Giorgio River basin is viewed as sufficient when considering the qualitative and not quantitative purpose of the proposed method.

8.3.2 Man-induced impacts

The simulated erosion scenarios (Fig. 8.5) led to construct a map showing the differences in soil loss amount (Fig. 8.6a). By subtracting to the current erosion scenarios the hypothetical one 6 levels of potential changes were identified (Fig. 8.5b). They describe a potential increase (classes 1, 2, 3) or decrease (classes 5, 6, 7) in the predicted soil loss rate. The surface interested by any changes (class 4) is the most diffuse and covers a surface of 44.7% (Fig. 8.5c).

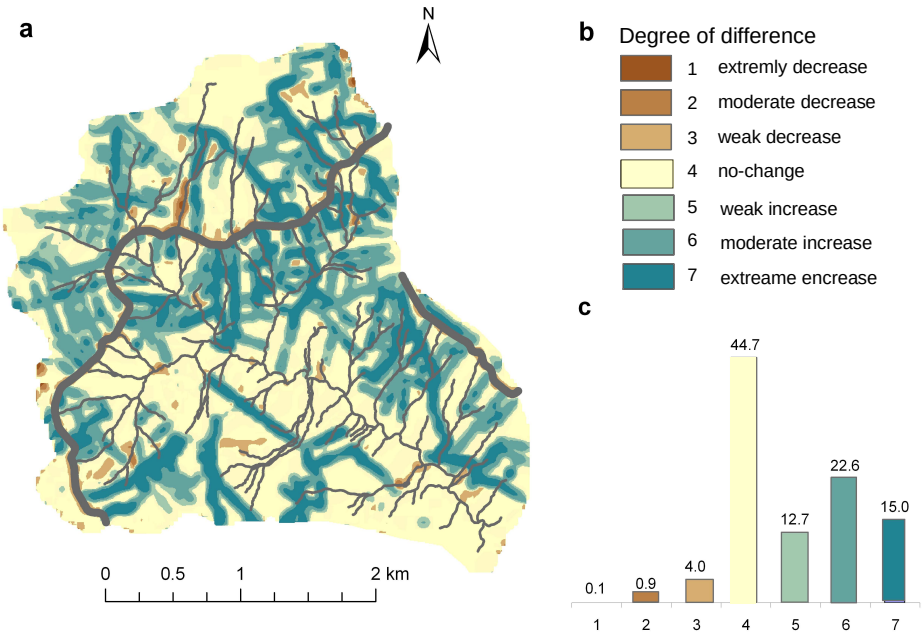

Figure 8.6. Map of predicted changes in soil loss modelling, constructed subtracting the current and hypothetical erosion scenarios (a). 7 classes, indicating the levels of change, were created (b). The percentage of surface interested by different degree of soil loss changes is indicated (c).

Moreover, in order to identify which man-induced elements causing high changes in soil loss rates, the changed erosion scenario was investigated along the area occupied by: artificial channels, field boundaries and unpaved road segments (Fig. 8.7).

As expected, along unpaved roads the major changes in the amount of eroded soil resulted; the topographic and land use management factors have undergone substantial changes along these surfaces. Unpaved roads impact showed the important role played by this artificial structure. Their surface is interested by weak (22.5%), moderate (41.3%) and extreme (60.2%) soil loss rate increase. Generally in the study area, unpaved roads run across topographic gradients, inducing runoff concentration and accelerating soil erosion.

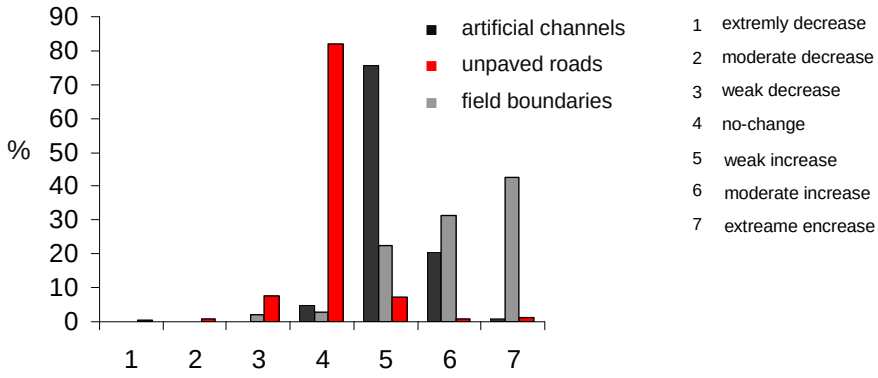

Figure 8.7. Levels of difference occurring along artificial channels, field boundaries and unpaved roads segments.

74.4% of the surface occupied by artificial channels falls in class 5 and only 22 % in class 6, indicating that along their surface soil loss generally weakly increases in a moving window between the current and the hypothetical erosion scenario. These results are justified by the consideration that sediments translocated by artificial channels and field boundaries, are deposited not so far from the source area. Consequently soil loss predicted by the two scenarios is not changing so far.

The simulation results showed that field boundaries do not play a relevant role in determining the spatial patterns of soil redistribution at border zones. 81% of the surface occupied by this element fall along the no-change class, and 8% contribute to decrease soil loss rate on the basin. Since field boundaries represent real physical barriers, which interrupt tillage and consequently soil transport flux, sources of uncertainty arise when modelling tillage translocation near the field boundary.

Artificial channels are constructed along two preferential topographic constrains: along the line of steepest slope, alternating flow path directions, and perpendicular to these line, constituting an obstacle for water flow. In the first case by masking the presence of these rural elements soil loss is reduced, in the second one rural element contribute to impending the water flow and so their obliteration is a potential cause of soil loss increase. In both cases superficial overland flow is only locally modified.

Moreover to better understand the occurrence of off-site impacts, defined as the effects of man-induced elements in cells not hosting any man-induced elements in the study area, the erosion/deposition map was used (Fig. 8.8a).

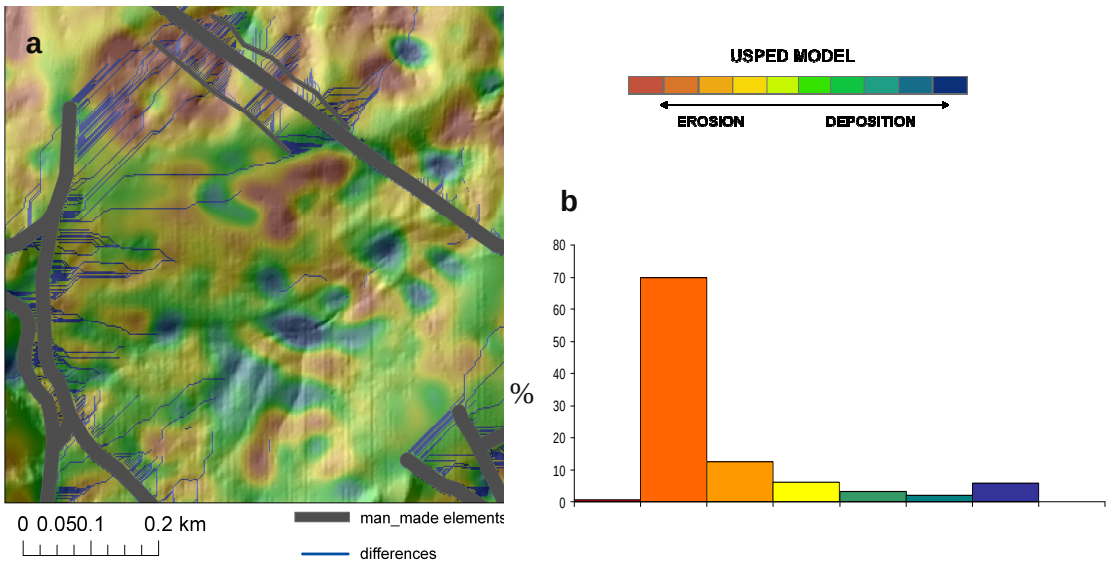

Figure 8.8. Detail of the of man-induced elements off-site impacts spatial distribution (blue lines) in the erosion/deposition map (a). The percentage of surface predicted to change and their predisposition to erosion or deposition processes is shown (b).

The RUSLE and the USPED modelling results were combined and off-site impacts defined depending on the topographic conditions.

Results showed how 70% of the surface interested by off-site impacts mainly fall in areas experiencing an increase in sediment transport capacity (net erosion) (Fig. 8.8 b), and only the 8% is located in depositional zones. The predicted locations of major hillslope erosion-prone areas in terms of sediment production correspond to surface characterized by high topographic connectivity.

Chapter 9

CONCLUDING REMARKS

9.1 Discussion and conclusions

The present thesis is the results of three years of investigation carried out to develop erosion susceptibility models in the Mediterranean and contribute significantly to a better understanding of the factors affecting runoff and soil erosion.

The research contributed to explore the methodological advantages as well as limitations in applying different modelling approaches, both statistical and empirical, to predict soil erosion in Sicily (south of Italy), considering this region as representative of the main Mediterranean environmental conditions. In this region soil degradation problems, due to water erosion, become always more serious; consequently, the definition of models able to predict erosion susceptibility and discriminate the environmental factors mainly controlling erosion is an important step to preserve soil resource.

In natural hazard studies, the application of statistic techniques enables the screening of large data and the generation of erosion susceptibility maps that well reflect the spatial distribution of the processes. Results showed that the use of a boosting regression trees method, allows an investigator to define functional relationships between a set of several environmental attributes and different erosion and mass wasting processes.
The TreeNet can be considered able to decipher the importance of certain variables for specific erosion and mass wasting processes. Stream power index, catchment area, elevation, altitude above the channel network and convergence index resulted to be the environmental attributes that play a predominant role in soil erosion and mass wasting susceptibility assessment; the ranking of variables importance contributed to better understand which are the factors mainly governing erosion process in a typical Mediterranean watershed.

Among the analyzed processes, bank and gully erosion were the more accurately predicted, with an outstanding and an excellent overall performance, while mass wasting and sheet-rill erosion showed an acceptable performance. The no-erosion class was the only one predicted with low accuracy. This misclassification attests for the difficulty in natural hazard phenomenon prediction to model areas saved from erosion processes, because of their present environmental conditions might bear the potential for a specific erosion process in future, e.g. when land use will change or rain erosivity will increase.

Moreover, being gully erosion the most representative process affecting soil loss in the Mediterranean, environmental aspects related to their prediction were most accurately investigated by means of logistic regression analysis. The functional relationships between erosion processes and a set of environmental attributes have been assessed, on grid cell (CLU) and slope unit scale (SLU). The adopted method generated gully erosion susceptibility maps that well reflect the spatial distribution of gullies within the study area. Both CLU- and SLU-based maps provide excellent predictive performances, confirming that logistic regression analysis constitute an effective tool also for erosion susceptibility analysis. Moreover, the results of the accuracy tests attest for the goodness of susceptibility maps that were generated by following objective and reproducible procedures, based on input data available or easily acquirable at regional and watershed scale.

Comparing the results obtained by applying the two statistical approaches, the TreeNet and the logistic regression analysis, the significance of the independent variables clearly indicate that continuous topographic attributes are the variables more frequently contributing to the accuracy of the predictive models. This is true particularly for models based on grid cells where all continuous topographic variables are always characterized by high significance values.

This research underlines also that gully erosion susceptibility analysis can be carried out at the scale of slope units; the adoption of this type of mapping units allows for avoiding the intrinsic limits of the application of a pure statistical approach to a geomorphological issue. A cell unit approach, which is the most adopted for susceptibility analysis, does not take into account the influence of each cell to the surroundings one; in this approach, grid cells are considered as individual case not related to the others, while geomorphological processes do not recognize the limits of a square cell. Hence, a slope unit approach could be better, even if some problems arise when variables defined at cell scale (e.g. topographic attributes) have to be associated to slope units; moreover, in order to produce more stable models and a finer resolution of the susceptibility maps, the number of SLUs has to be large enough. In this research, this could have been obtained only by reducing the size of slope units, but this operation would have produced landforms crossing the boundaries of the SLUs and depriving them of their significance of hydrological barriers.

The experiments carried out in the basin of San Giorgio River and the results obtained encourage further application of logistic regression analysis to gully erosion susceptibility analysis; the adopted method, in fact, demonstrated to be suitable for the preparation of reliable gully erosion susceptibility maps that could constitute a useful instrument for planning erosion control practices and reducing socio-economic impact of soil loss produced by gullies.

Moreover in the gully erosion susceptibility model the potential effect of roads was investigated by calculating the distance from the closest road segment and the total length of roads. Results showed that both parameters do not influence significantly the model prediction. Consequently to better characterize the impact of these linear features on the drainage patterns and consequently soil erosion dynamics, a new procedure to investigate the impact of anthropogenic elements in cultivated Mediterranean landscape was proposed.

By applying the RUSLE and USPED models the impact of man-induced elements on erosion processes was evaluated. The scenario analysis results underlined the predominant influence of unpaved roads compared to artificial channels and field boundaries to cause changes in soil erosion dynamics. The erosion scenario simulation demonstrated how the hydrological connectivity is strongly affected by the changing in land use patterns and in topographic surface.
The proposed method uses simple empirical models for predicting the impact of anthropogenic elements on soil erosion processes and has the advantage of being easy to understand and data are readily available. The applied procedure may find practical use in land management and planning, where it can supplement to small-scale field experiments.

9.2 Final remarks

The experimental applications carried out in the Sicilian Region and the obtained results encourage further applications to continue investigating soil erosion by using statistical and empirical models.
Results clearly indicate that the statistical analysis is a good instrument to predict erosion susceptibility in Mediterranean. The adopted methods demonstrated to be suitable for the

preparation of reliable susceptibility maps, which constitute a useful instrument for planning erosion control practices and reducing socio-economic impact of soil loss produced by erosion. At the same time the results also highlighted some new questions:

- When the areas modeled as no susceptible to erosion and mass wasting processes can be considered “saved areas”?
- How stochastic analysis can be used to better classify surfaces no-prone to erosion and mass wasting processes?
- How to measure the intrinsic predisposition to develop erosion processes in future of those mapping units classified as “no-erosion” cases?

The use of empirical method to predict soil erosion stressed the necessity to the need for detailed field data over large areas, in order to test the proposed approach and to export it in similar environmental conditions. Anyway, considering different scenarios of land use in erosion modeling assisted in interpreting the enormous complexity of catchment responses to man-induced impacts and can be very valuable for the development of sustainable land management systems.

Concluding, future researches and experimental applications are desirable, to better understanding the involved mechanisms and the interaction of environmental factors controlling the development of erosion response.

REFERENCES

Abate, B., Catalano, R., Renda, P., 1982. I monti di Palermo. In: Catalano R. & D'Argenio B. (Eds.), Guida alla Geologia della Sicilia Occidentale. Guide Geologiche Regionali. Mem. Soc. Geol. It. 24 (Suppl. A), 43-48.

Abate, B., Renda, P., Tramutoli, M., 1988. Carta Geologica dei Monti di Termini Imerese e delle Madonie occidentali (Sicilia Centro-settentrionale), scala 1: 50000. Dipartimento di Scienze della Terra e del Mare (DiSTeM) dell'Università di Palermo. Stab. Tip. Salomone, Roma.

Abate, B., Renda, P., Tramutoli, M., 1992. Note illustrative della Carta Geologica dei Monti di Termini Imerese e delle Madonie Occidentali (Sicilia centro-settentrionale). Mem. Soc. Geol. It., 41, 1988,: 475-505, 20 figg., 1 carta geol., Roma.

Agnesi, V., Di Maggio, C., Macaluso, T., Madonia, G., Messana, V., 2000. Morphotectonic setting of the Madonie area (central Northern Sicily). Mem. Soc. Geo. It. 55, 373-379.

Agnesi, V., 2004. Sicily in the last one million years. Bocconea. 17, 23-32.

Agnesi, V., Conoscenti, C., Di Maggio, C., Madonia, G., Rotigliano, E., 2006. Geomorphological setting of Madonie Geopark (Italy). On the development of Geoparks. Anogia, Crete Island, Greece. 2-5 October 2003. Irakleion, Typokreta. Proceeding volume 25-33. ISBN: 960-89138-0-2.

Agnesi, V., Cappadonia, C., Conoscenti C., 2007. Carta Geomorfologica del bacino idrografico del Rio Spinasanta e note illustrative (Sicilia centro-settentrionale). Naturalista siciliano. S. IV, 31 (3-4), 127-145.

Agnesi, V., Angileri, S., Cappadonia, C., Conoscenti, C., Rotigliano, E., 2011. Multi-parametric GIS analysis to assess gully erosion susceptibility: a test in southern Sicily, Italy. In: Zglobicki, W. (Ed.), Landform Analysis, Proceedings of International Symposium on Gully Erosion. Lublin, 19-24 April 2010, pp. 15-20.

Akgün, A., Türk, N., 2011. Mapping erosion susceptibility by a multivariate statistical method: A case study from the Ayvalik region, NW Turkey. Computers & Geosciences 37, 1515-1524. doi:10.1016/j.cageo.2010.09.006.

Amore, E., Modica, C., Nearing, M.A., Santoro, V.C., 2004. Scale effect in USLE and WEPP application for soil erosion computation from three Sicilian basins. Journal of Hydrology. 293, 100–114.

Arnoldus, H.M.J., 1980. An approximation of the rainfall factor in the Universal Soil Loss Equation. In: De Boodt, M., Gabriels, D., (Eds.), Assessment of erosion. Wiley, UK. pp 127–132.

Bagarello, V., D'Asaro, F., 1994. Estimating single storm erosion index. Trans ASAE. 3, 785–791.

Bagarello, V., Di Stefano, C., Ferro, V., Kinnell, P.I.A., Pampalone, V., Porto, P., Todisco F., 2011. Predicting soil loss on moderate slopes using an empirical model for sediment concentration. Journal of Hydrology. 400, 267–273.

Bai, S.B., Wang, J., Lü, G.N., Zhou, P.G., Hou, S.S., Xu, S.N., 2010. GIS-based logistic regression for landslide susceptibility mapping of the Zhongxian segment in the Three Gorges area, China. Geomorphology. 115, 23-31.

Bajracharya, R.M., Lal, R., 1998. Crusting effects on erosion processes under simulated rainfall on a tropical Alfisol. Hydrol. Processes. 12, 1927–1938.

Bakker, M.M., Govers, G., Van Doorn, A., Quetier, F., Chouvardas, D., Rounsevel, M., 2008. The response of soil erosion and sediment export to land-use change in four areas of Europe: The importance of landscape pattern. Geomorphology. 98, 213–226.

Barrow, C.J., 1994. Land degradation development and breakdown of terrestrial environments. Cambridge University Press. pp 295.

Bates, R.L., Jackson, J.A., 1987. Glossary of Geology. 2nd Ed., American Geological Institute, Alexandria, Virginia.

Beck, M.B., Jakeman, A.J., McAleer, M.J., 1995. Construction and evaluation of models of environmental systems. In: Beck, M.B., McAleer, M.J., (Eds.), Modelling Change in environmental Systems. John Wiley and Sons. 3–35.

Beguería, S., 2006. Validation and Evaluation of Predictive Models in Hazard Assessment and Risk Management. Natural Hazards. 37, 315-329.

Beven, K.J., Kirkby, M.J., 1993. Channel network hydrology. (Eds.) John Wiley and Sons.

Borselli, L., Cassi, P., Torri, D., 2008. Prolegomena to sediment and flow connectivity in the landscape: A GIS and field numerical assessment. Catena. 75, 268–277.

Bou Kheir, R., Wilson, J., Deng, Y., 2007. Use of terrain variables for mapping gully erosion susceptibility in Lebanon. Earth Surface Processes and Landforms. 32, 1770-1782.

Brice, J.C., 1966. Erosion and deposition in the loess-mantled Great Plains, Medicine Creek drainage basin, Nebraska. USGS Prof. Pap. 352-H, 255-339.

Brown, L.R., 1984. The global loss of topsoil. J. Soil Water Conserv. 39 (3), 162–165.

Buccolini, M., Coco, L., 2010. The role of the hillside in determining the morphometric characteristics of “calanchi”: The example of Adriatic central Italy. Geomorphology. 123, 200-210.

Butzer Karl, W., 2005. Environmental history in the Mediterranean world: Cross-disciplinary investigation of cause-and-effect for degradation and soil erosion. Journal of Archaeological Science. 32, 1773-1800.

Campbell, J.B., 2002. Introduction to Remote Sensing. The Guilford Press, New York, 3rd Ed. pp. 621.

Cappadonia, C., Conoscenti, C., Rotigliano, E., 2011. Monitoring of erosion on two calanchi fronts – Northern Sicily (Italy). In: Zglobicki, W. (Ed.), Landform Analysis, Proceedings of International Symposium on Gully Erosion. Lublin, 19-24 April 2010, pp. 21-25.

Capra, A., Scicolone, B., 2002. Ephemeral gully erosion in a wheat-cultivated area in Sicily (Italy). Biosystems Engineering. 83 (1), 119–126.

Capra, A., Mazzara, L.M., Scicolone, B., 2005. Application of the EGEM model to predict ephemeral gully erosion in Sicily, Italy. Catena. 59, 133-146.

Casali, J., Loizu, J., Campo, M., Desantisteban, L., Alvarezmozos, J., 2006. Accuracy of methods for field assessment of rill and ephemeral gully erosion. Catena. 67, 128-138.

Catalano, R., D'Argenio, B., Lo Cicero, G., Di Stefano, P., Montanari, L., Abate, B., Monteleone, S., Macaluso, T., Pipitone, G., Di Stefano, E., 1978. Contributi alla conoscenza della Geologia della Sicilia occidentale. Mem. Soc. Geol. It.. 19, 485-493.

Catalano, R., Di Stefano, P., Sulli, A., Vitale, F.P., 1996. Paleogeography and structure of the central Mediterranean: Sicily and its offshore area. Tectonophysics. 260, 291-323.

Claessens, L., Heuvelink, G.B.M., Schoorl, J.M., Veldkamp, A., 2005. DEM resolution effects on shallow landslide hazard and soil redistribution modelling. Earth Surface Processes and Landforms. 30, 461–477.

Conforti, M., Aucelli, P.P.C., Robustelli, G., Scarciglia, F., 2011. Geomorphology and GIS analysis for mapping gully erosion susceptibility in the Turbolo stream catchment (Northern Calabria, Italy). Natural Hazards. 56, 881-898.

Conoscenti, C., 2006. Valutazione dell'erosione prodotta dai processi di dilavamento nel bacino del Fiume Mendola (Sicilia, Italia). Naturalista siciliano. S. IV, 30 (1), 107-124.

Conoscenti, C., Di Maggio, C., Rotigliano, E., 2008a. Soil erosion susceptibility assessment and validation using a geostatistical multivariate approach: a test in Southern Sicily. Natural Hazards. 46, 287-305.

Conoscenti, C., Di Maggio, C., Rotigliano, E., 2008b. GIS analysis to assess landslide susceptibility in a fluvial basin of NW Sicily (Italy). Geomorphology. doi: 10.1016/j.geomorph. 2006.10.039.

Conoscenti, C., Agnesi, V., Angileri, S., Cappadonia, C., Rotigliano, E, Märker, M., 2011. A GIS-based approach for gully erosion susceptibility modelling: a test in Sicily, Italy. Environmental Earth Sciences (submitted).

Conrad, O., 2007. SAGA - Entwurf, Funktionsumfang und Anwendung eines Systems für Automatisierte Geowissenschaftliche Analysen. Electronic Doctoral Dissertation, University of Göttingen.

Costa, F.M., Bacellar, L.de. Almeida Prado, 2007. Analysis of the influence of gully erosion in the flow pattern of catchment streams, Southeastern Brazil. Catena. 69, 230–238.

D'Asaro, F., Santoro, M., 1983. Aggressività della pioggia nello studio dell'erosione idrica del territorio siciliano. Quaderni dell'Istituto di Idraulica dell'Università di Palermo. 164.

Davis, J.C., Ohlmacher, G.C., 2002. Landslide hazard prediction using generalized logistic regression. In: Proceedings of IAMG 2002. September 15–20, 2002, Berlin, 501-506.

De Jong, S.M., Paracchini, M.L., Bertolo, F., Folving, S., Megier, J., De Roo, A.P.J., 1999. Regional assessment of soil erosion using the distributed model SEMMED and remotely sensed data. Catena. 37, 291–308.

De'ath, G., 2007. Boosted trees for ecological modeling and prediction. Ecology. 88, 243–251.

Della Seta, M., Del Monte, M., Fredi, P., Lupia Palmieri, E., 2007. Direct and indirect evaluation of denudation rates in Central Italy. Catena. 71, 21-30.

Della Seta, M., Del Monte, M., Fredi, P., Lupia Palmieri, E., 2009. Space–time variability of denudation rates at the catchment and hillslope scales on the Tyrrhenian side of Central Italy. Geomorphology. 107, 161-177.

Desmet, P.J.J., Govers, G., 1996. A GIS procedure for automatically calculating the USLE LS factor on topographically complex landscape units. J. Soil Water Cons. 51, 427-433.

Desmet, P.J.J., Poesen, J., Govers, G., Vandaele, K., 1999. Importance of slope gradient and contributing area for optimal prediction of the initiation and trajectory of ephemeral gullies. Catena. 37, 377–392

Di Stefano, C., Ferro, V., 2011. Measurements of rill and gully erosion. Sicily Hydrol. Process.

Dikau, R., 1989. The application of a digital relief model to landform analysis in geomorphology. In: Raper, J. (Eds.), Three dimensional applications in geographic information systems. London: Taylor and Francis. 51-77. DOI 10.1007/s11069-011-9846-0.

Diodato, N., 2004. Estimating Rusle's rainfall factor in the part of Italy with a Mediterranean rainfall regime. Hydrol. Earth Syst. Sci. 8, 103–107.

Drago, A., Cartabellotta, D., Lo Bianco, B., Lombardo, M., 2000. Atlante Climatologico della Regione Siciliana (Climatological atlas of the Sicilian Administrative Region). Assessorato Regionale Agricoltura e Foreste, U. O. di Agrometeorologia, Regione Siciliana, Palermo.

Dunne, T., Black, R.D., 1970. Partial area contributions to storm runoff in a small New England watershed. Water Resour. Res. 6 (5), 1296-1311.

Dunne, T., 1983. Relation of field studies and modelling in the prediction of storm runoff. Journal of Hydrology. 65, 25-48.

Elith, J., Leathwick, J.R., Hastie, T., 2008. A working guide to boosted regression trees. J. Anim. Ecol. 77, 802 – 813.

Ellison, W.D., 1947. Soil erosion studies-part I. Agric. Eng. 28, 145–146.

Eswaran, H., Lal, R., Reich, P.F., 2001. Land degradation: An overview. In: Bridges E.M., Hannam I.D., Oldeman L.R., Response to Land Degradation.

Fairbridge, R.W., 1968. Denudation. In: Fairbridge, R.W. (Eds.), The Encylopedia of Geomorphology. Reinhold Book Corporation. pp. 261-271.

Fawcett, T., 2006. An introduction to ROC analysis. Pattern Recognition Letters. 27, 861-874.

Ferro, V., Giordano, G., Iovino, M., 1991. Isoerosivity and erosion risk map for Sicily. Hydrological Sciences Journal. 12.

Fielding, A.H., Bell, J.F., 1997. A review of methods for the assessment of prediction errors in conservation presence/ absence models. Environmental Conservation. 24, 38–49.

Fierotti, G., 1988. Carta dei Suoli della Sicilia. Istituto di Agronomia, Università di Palermo e Regione Sicilia, Assessorato Territorio ed Ambiente, Palermo.

Flanagan, D.C., Nearing, M.A., 1995. USDA-Water Erosion Prediction Project: hillslope profile and watershed model documentation. NSERL Report No 10. USDA-ARS National Soil Erosion Research Laboratory, West Lafayette, Indiana.

Flügel, W.A., Märker, M., Moretti, S., Rodolfi, G., 2003. Integrating GIS, Remote Sensing, Ground Truthing and Modeling Approaches for Regional Erosion Classification of semi-arid catchments in South Africa and Swaziland. Hydrological Processes. 17, 929-942.

Food and Agriculture Organization of the United Nations. 1961–2002. World Grain Production. Rome: FAO, Quarterly Bulletin of Statistics.

Foster, I.D.L., Dearing, J.A., Appleby, P.G., 1986. Historical trends in catchment sediment yields: a case study in reconstruction from lake-sediment records in Warwickshire, UK. Hydrol. Sci. J. 31(3), 427-443.

Fournier, F., 1960. Climate and Erosion. Presses Universitaires de France, París.

Frattini, P., Crosta, G., Carrara, A., 2010. Techniques for evaluating the performance of landslide susceptibility models. Engineering Geology 111, 62-72.

Friedman, J.H., 1999. Stochastic gradient boosting. Technical Report. Department of Statistics, Stanford University, USA.

Friedman, J.H.,2002. Stochastic gradient boosting. Computational Statistics & Data Analysis. 38, 367-378.

Foster, G.R. and L.D. Meyer. 1972. Transport of soil particles by shallow flow. Transactions of the ASAE. 15 (1), 99-102.

Geissen, V., Kampichler, C., López-de Llergo-Juárez, J.J., Galindo-Acántara, A., 2007. Superficial and subterranean soil erosion in Tabasco, tropical Mexico: Development of a decision tree modeling approach. Geoderma. 139, 277-287.

Goodenough, D.J., Rossmann, K., Lusted, L.B., 1974. Radiographic applications of receiver operating characteristic (ROC) curves. Radiology. 110, 89-95.

Grasso, M., Lentini, F., Vezzani, L., 1978. Lineamenti stratigrafico-strutturali delle Madonie (Sicilia centrosettentrionale). Geologica Romana. 17, 45-69.

Grauso, S., Diodato, N., Verrubbi, V., 2010. Calibrating a rainfall erosivity assessment model at regional scale in Mediterranean area. Environ. Earth Sci. 60, 1597–1606.

Grimm, M., Jones, R.J.A., Rusco, E., Montanarella, L., 2003. Soil erosion risk in Italy: a revised USLE approach. European Soil Bureau Research Report No. 11, EUR 20677 EN, 24pp. Office for Official Publications of the European Communities, Luxembourg.

Gutiérrez, Á.G., Schnabel, S., Felicísimo, Á.M., 2009a. Modelling the occurrence of gullies in rangelands of southwest Spain. Earth Surface Processes and Landforms. 34, 1894-1902.

Gutiérrez, Á.G., Schnabel, S., Lavado Contador, J.F., 2009b. Using and comparing two nonparametric methods (CART and MARS) to model the potential distribution of gullies. Ecological Modelling. 220, 3630-3637.

Guzzetti, F., Carrara, A., Cardinali, M., Reichenbach, P., 1999. Landslide hazard evaluation: a review of current techniques and their application in a multi-scale study, Central Italy. Geomorphology. 31, 181-216.

Hanley, J.A., McNeil, B.J., 1982. The meaning and use of the area under a receiver operating characteristic (ROC) curve. Radiology. 143, 29-36.

Hauge, C., 1977. Soil erosion definitions. California Geol. 30, 202-203.

Hochschild, V., 1999. Parameterization of Hydrological Models: The Contribution of Remote Sensing to Water Resources Management. Proceedings of the MODSIM'99, International Congress on Modelling and Simulation, 06.-09.12.99, Hamilton, NZ.

Hochschild, V., Märker, M., Rodolfi, G., Staudenrausch, H., 2003. Delineation of erosion classes in semi-arid southern African grasslands using vegetation indices from optical remote sensing data. Hydrol. Process. 17, 917–928.

Horton, R.E., 1933. The role of infiltration in the hydrologic cycle. Trans. Amer. Geophys. Union. 14, 446-460.

Hosmer, D.W., Lemeshow, S., 2000. Applied Logistic Regression. Wiley, New York.

Hudson, N., 1995. Soil Conservation. Iowa State University Press, Ames, Iowa.

Hudson, N.W., 1971. Soil Conservation. Batsford: London, 320.

Imeson, A.C., Kwaad, F.J.P.M., 1980. Gully types and gully prediction. K.N.A.G. Geogr. Tjds. XVI 5, 430-441.

ISSS Working Group RB, 1998. World Reference Base for Soil Resources. In: Batjes, N.H., Bridges, M., Nachtergaele, F.O. (Eds.), Atlas. Acco: Leuven, Belgium.

Jenness, J., 2006. Topographic Position Index. Extension for ArcView 3.x, v. 1.2. Jenness Enterprises. http://www.jennessent.com/arcview/tpi.htm.

Jenson, S.K., Domingue, J.0., 1988. Extracting topographic structure from digital elevation data for geographic information system analysis. Photoyrammetric Engineering and Remote Sensing. 54 (11), 1593-1600.

Jones, J.A., Swanson F.J., Wemple B.C., Snyder K.U., 2000. Effects of Roads on Hydrology, Geomorphology, and Disturbance Patches in Stream Networks. Conservation Biology. 14 (1), 76-85.

Kakembo, V., Xanga, W.W., Rowntree, K., 2009. Topographic thresholds in gully development on the hillslopes of communal areas in Ngqushwa Local Municipality, Eastern Cape, South Africa. Geomorphology 110, 188-194.

Knisel, W.G., 1980. CREAMS: A field scale model for chemicals, runoff and erosion from agricultural management systems. US Department of Agriculture. Conservation Research Report 26, 474-485.

Kosmas, C., Danalatos, N.G., Gerontidis, S., 2000. The effect of land parameters on vegetation performance and degree of erosion under Mediterranean conditions. Catena. 40, 3–17.

Köthe, R., Lehmeier, F., 1993. SARA - Ein Programmsystem zur Automatischen Relief-Analyse. Standort - Z. f. Angewandte Geographie.

Kuhnert, P., Kinsey-Henderson, A., Herr, A., 2007. Incorporating uncertainty in gully erosion mapping using the random forests modelling approach. CSIRO Mathematical and Information Sciences. No Report 07/79 CSIRO.

Lal, R., 2001. Soil degradation by erosion. Land Degradation & Development. 12 (6),1311 519 – 539.

Lal, R., 2004. Soil carbon sequestration impacts on global climate change and food security. Science. 304, 1623–1627.

Lamb, M.P, 2008. Formation of Amphitheater-Headed Canyons. Doctor of Philosofphy Dissertation Thesis. Earth & Planetary Science in the Graduate division of the University of California, Berkeley.

Lasko, T.A., Bhagwat, J.G., Zou, K.H., Ohno-Machado, L., 2005. The use of receiver operating characteristic curves in biomedical informatics. Journal of Biomedical Informatics 38, 404-415.

Lavee, H., Imeson, A.C., Sarah, P., 1998. The impact of climate change on geomorphology land desertification along a Mediterranean-arid transect. Land Degrad. Develop.. 9, 407-422.

Lei, T., Nearing M.A., Haghigi, K., Bralts, V.F., 1998. Rill erosion and morphological evolution: A simulation model. Water Resour. Res.. 34 (11), 3157–3168.

Lopez-Bermudez, F., Romero-Diaz, A., Martinez-Fernandez, J., Martinez-Fernandez, J., 1998. Vegetation and soil erosion under a semi-arid Mediterranean climate: a case study from Murcia (Spain). Geomorphology. 24, 51–58.

Louise, J., Bull, L., Kirkby, M., 2002. Dryland Rivers, Hydrology and Geomorphology of Semi-Arid Channels. (Ed.) John Wiley, New York.

Lucà, F., Conforti, M., Robustelli, G., 2011. Comparison of GIS-based gullying susceptibility mapping using bivariate and multivariate statistics: Northern Calabria, South Italy. Geomorphology 134, 297-308.

Märker, M., Moretti, S., Rodolfi, G., Zanchi, C., 1999. Delineation of erosion reference units (six classes erosion map). INQUA, Durban/South Africa.

Märker, M., 2002. Regionale Erosionsmodellierung unter Verwendung des Konzepts der Erosion Response Units (ERU) am Beispiel zweier Flusseinzugsgebiete im südlichen Afrika. PhD-Thesis, Friedrich-Schiller-University of Jena, Chemistry and Geoscience Faculty.

Märker, M., Sidorchuk, A., 2003. Assessment of gully erosion process dynamics for water resources management in a semiarid catchment of Swaziland, Southern Africa. In: de Boer, D.H., Froehlich, W., Mizuyama, T., Pietroniro, A. (Eds.), Erosion Prediction in Ungauged Basins (PUBs): Integrating Methods and Techniques: IAHS Publication. 279, 188-198.

Märker, M., Angeli, L., Bottai, L., Costantini, R., Ferrari, L., Innocenti, L., Siciliano, G., 2008. Assessment of land degradation susceptibility by scenario analysis. A case study in Southern Tuscany, Italy. Geomorphology. 3 (1-2), 120-129.

Märker, M., Pelacani, S., Schröder, B., 2011. A functional entity approach to predict soil erosion processes in a small Plio-Pleistocene Mediterranean catchment in Northern Chianti, Italy. Geomorphology. 125, 530-540.

Martínez-Casasnovas, J.A., 2003. A spatial information technology approach for the mapping and quantification of gully erosion. Catena. 50, 293-308.

Mathew, J., Jha, V.K., Rawat, G.S., 2009. Landslide susceptibility zonation mapping and its validation in part of Garhwal Lesser Himalaya, India, using binary logistic regression analysis and receiver operating characteristic curve method. Landslides. 6, 17-26.

Menard, S., 1995. Applied Logistic Regression Analysis, Online. Sage Publications.

Merkel, W.H., Woodward, D.E., Clarke, C.D., 1988. Ephemeral gully erosion model (EGEM). Agricultural, Forest, and Rangeland Hydrology. American Society of Agricultural Engineers Publication. 07-88, 315-323.

Meyer, A., Martínez-Casasnovas, J.A., 1999. Prediction of existing gully erosion in vineyard parcels of the NE Spain: a logistic modelling approach. Soil and Tillage Research. 50, 319-331.

Mitasova, H., Hofierka, J., Zlocha, M., Iverson, L.R., 1996. Modeling topographic potential for erosion and deposition using GIS. International Journal of GIS. 10, 629–641.

Mitra, B., Scott, H.D., Dixon, J.C., McKimmey, J.M., 1998. Application of fuzzy logic to the prediction of soils erosion in a large watershed. Geoderma. 86, 183–209.

Montana, G., Polito, A.M., Caruso, A., Azzaro, E., 2011. Le “Argille ceramiche” della Sicilia occidentale e centrale. In: IlionBooks (Eds). ISBN 978-88-903626-2-0.

Montgomery, D.R., Dietrich, W.E., 1992. Channel initiation and the problem of landscape scale. Science. 255, 826-830.

Montgomery, D.R., Foufoula-Georgiou E., 1993. Channel network source representation using digital elevation models. Water Resour. Res. 29, 3925–3934.

Moore, I.D., Burch, G.J., 1986. Sediment transport capacity of sheet and rill flow: application of unit stream power theory. Water Resources Research. 22 (8),1350-1360.

Moore, I.D., Wilson J.P., 1992. Length-slope factors for the Revised Universal Soil Loss Equation: Simplified method of estimation. Journal of Soil and Water Conservation. 47, 423-428.

Moretti, S., Rodolfi, G., 2000. A typical calanchi'' landscape on the Eastern Apennine margin (Atri, Central Italy): geomorphological features and evolution. Catena 40, 217 - 228.

Morgan, R.P.C., Nearing, M., 2010. Handbook of Erosion Modelling. In: Morgan, R.P.C, Nearing, M. (Eds.), John Wiley & Sons. pp 416.

Morgan, R.P.C., Nearing, M.A., 2011. Handbook of Erosion Modelling. Wiley-Blackwell Publishing Ltd (Eds.),. West Sussex, UK. pp. 398.

Motha, J.A., Wallbrink, P.J., Hairsine, P.B., Grayson, R.B., 2004. Unsealed roads as suspended sediment sources in an agricultural catchment in south-eastern Australia. Journal of Hydrology. 286, 1-18.

Mueller, T.G., Cetin, H., Fleming, R.A., Dillon, C.R., Karathanasis, A.D., Shearer, S.A., 2005. Erosion probability maps: Calibrating precision agriculture data with soil surveys using logistic regression. Journal of Soil and Water Conservation. 60, 462-468.

Nandi, A., Shakoor, A., 2009. A GIS-based landslide susceptibility evaluation using bivariate and multivariate statistical analyses. Engineering Geology. 110, 11-20.

Nearing, M.A., 2001. Potential changes in rainfall erosivity in the U.S. with climate change during the 21st century. Journal of Soil and Water Conservation. 56 (3), 229–232.

Nefeslioglu, H., Gokceoglu, C., Sonmez, H., 2008. An assessment on the use of logistic regression and artificial neural networks with different sampling strategies for the preparation of landslide susceptibility maps. Engineering Geology. 97, 171-191.

Neuhäuser, B., Terhorst, B., 2007. Landslide susceptibility assessment using ‘‘weights-of-evidence’’ applied to a study area at the Hurassic escarpment (SW-Germany). Geomorphology. 86, 12-24.

Ohlmacher, G.C., Davis, J.C., 2003. Using multiple logistic regression and GIS technology to predict landslide hazard in northeast Kansas, USA. Engineering Geology. 69, 331-343.

Olaya, V., 2004. A gentle introduction to SAGA GIS. Göettingen, Germany.

Olaya, V., Conrad, O., 2008. Geomorphometry in SAGA. In: Hengl, T., Reuter, H.I. (Eds.), Geomorphometry: Concepts, Software, Applications. Elsevier, Amsterdam. 293-308.

Oldeman, L. R., 1994. The global extent of soil degradation. In: Greenland, D.J., Szablocs, T. (Eds.), Soil Resilience and Sustainable Land Use. Commonwealth Agricultural Bureau International, Wallingford, UK. 99–118.

Pacini, C.A., Wossink, A., Giesen, G., Vazzanna, C.,Huine, R., 2003. Evaluation of sustainability of organic, integrated and conventional farming systems: A farm and field-scale analysis. Agriculture, Ecosystems and Environment. 95, 273–288.

Pagliai M., 1988. Soil porosity aspects. International Agrophysics. 4, 215-232.

Penning de Vries, F.W.T., Scherr, S.J., Sombatpanit S. (Eds). Science Publishers, Inc: Enfield, New Hampshire, USA. 20–35.

Phillips, C., 1998. The badlands of Italy: a vanishing landscape? Applied Geography 18, 243-257.

Pimentel, D., Terhune, E.C., Dyson-Hudson, R., Rochereau, S., Samis, R., Smith, E.A., Denman, D., Reifschneider, D.R., Shepard, M., 1976. Land degradation: Effects on food and energy resources. Science. 194, 149-155.

Pimentel, D., Harvey, C., Resosudarmo, P., Sinclair, K., Kurz, D., McNair, M., Crist, S., Shpritz, L., Fitton, L., Saffouri, R., Blair, R., 1995. Environmental and economic costs of soil erosion and conservation benefits. Science. 267, 1117– 23.

Pimentel, D., 2006. Soil erosion: a food and environmental threat. Environment, Development and Sustainability. 8, 119-137.

Planchon, O., Darboux, F., 2001. A fast, simple and versatile algorithm to fill the depressions of digital elevation models. Catena. 46, 159–176.

Poesen, J.W., Ingelmo-Sanchez, F., 1992. Runoff and sediment yield from topsoils with different porosity as affected by rock fragment cover and position. Catena. 19, 451–474.

Poesen, J., 1993. Gully typology and gully control measures in the European loess belt. In: Wicherek, S. (Eds.), Farmhand Erosion in Temperate Plains Environment and Hills. Elsevier, Amsterdam. 221-239.

Poesen, J., Nachtergaele, J., Verstraeten, G., Valentin, C., 2003. Gully erosion and environmental change: importance and research needs. Catena. 50, 91-133.

Raimondo, F.M., Surano, N., Schicchi, R., 2004. Carta del paesaggio e della biodiversità vegetale del Parco delle Madonie (Sicilia settentrionale). Naturalista siciliano. S 4, 28 (1-2), 71-137.

Rakotomalala, R., 2005. Tanagra: un logiciel gratuit pour l’enseignement et la recherche. In: Actes De EGC. 697–702.

Reineking, B., Der, B., 2006. Constrain to perform: Regularization of habitat models. Ecological Modelling. 193, 675-690.

Reineking, B., Schröder, B., 2006. Constrain to perform: regularization of habitat models. Ecological Modelling. 193 (3-4), 675-690.

Renard, K.G., Freimund, J.R., 1994. Using monthly precipitation data to estimate the R-factor in the revised USLE. J Hydrol. 157:287–306.

Renard, K.G., Foster, G.R., Weesies, G.A., McCool, D.K., Yoder, D.C., 1997. Predicting Soil Erosion by Water: A Guide to Conservation Planning with the Revised Universal Soil Loss Equation (RUSLE). Agriculture Handbook No. 703. Washington, DC: US Department of Agriculture.

Ripley, B.D., 1996. Pattern Recognition and Neural Networks, Analysis. Cambridge University Press, Cambridge.

Ritchie, J.C., 2000. Combining 137-Cesium and topographic surveys for measuring soil erosion/deposition patterns in a rapidly accreting area. Acta Geol.Hisp. 35, 207–212.

Robichaud, P.R., Elliot, W.J., Pierson, F.B., Hall, D.E., Moffet, C.A., 2007. Predicting postfire erosion and mitigation effectiveness with a web-based probabilistic erosion model. Catena. 71, 229–241.

Roering, J.J., Kirchner, J. W., Dietrich, W. E., 1999. Evidence for nonlinear, diffusive sediment transport on hillslopes and implications for landscape morphology. Water Resources Research. 35, 853–870.

Rotigliano, E., Cappadonia, C., Conoscenti, C., Costanzo, D., Agnesi, V., 2011. Slope units-based flow susceptibility model: using validation tests to select controlling factors. Natural Hazards, DOI 10.1007/s11069-011-9846-0, 2011b.

Rouet, I., Gay, D., Allenbach, M., Selmaoui, N., Ausseil, A.G., Mangeas, M., Maura, J., Dumas, P., Lille, D., 2009. Tools for soil erosion mapping and hazard assessment: application to New Caledonia, SW Pacific. In: 18th World IMACS / MODSIM Congress. Cairns, Australia 13-17 July 2009, pp. 1986-1992.

Selby, M.J., 1993. Hillslope Materials and Processes. Oxford University Press, 2nd Edition.

Sidorchuk, A., 1999. Dynamic and static models of gully erosion. Catena. 37, 401-414.

Sidorchuk, A., Märker, M., Moretti, S., Rodolfi, G., 2003. Gully erosion modelling and landscape response in the Mbuluzi River catchment of Swaziland. Catena. 50, 507-525.

Süzen, M.L., Doyuran, V., 2004. A comparison of the GIS based landslide susceptibility assessment methods: multivariate versus bivariate. Environmental Geology. 45, 665-679.

Tayfur, G., Ozdemir, S., Singh, V.P., 2003. Fuzzy logic algorithm for runoff-induced sediment transport from bare soil surfaces. Adv. Water Resour. 26, 1249–1256.

Thorne, C.R., 1990. Effects of vegetation on riverbank erosion and stability. In: Thornes, J.B. (Eds.), Vegetation and Erosion: Processes and Environments. (Eds.) John Wiley & Sons. 125–144.

Valentin, C.H., 1994. Surface sealing as affected by various rock fragment cover in West Africa. Catena. 23, (1-2), 87-98.

Van Den Eeckhaut, M., Reichenbach, P., Guzzetti, F., Rossi, M., Poesen, J., 2009. Combined landslide inventory and susceptibility assessment based on different mapping units: an example from the Flemish Ardennes, Belgium. Natural Hazards and Earth System Science. 9, 507-521.

Van Rompaeya, A., Krasab, J., Dostal, T. 2007. Modelling the impact of land cover changes in the Czech Republic on sediment delivery Land Use Policy. 24, 576–583.

Vandaele, K., Poesen, J., 1995. Spatial and temporal patterns of soil erosion rates in an agricultural catchment, central Belgium. Catena. 25, 213-226.

Wainwright, J., Thornes, J.,B., 2003. Environmental Issues in the Mediterranean: Processes and Perspectives from the Past and Present. In: Taylor & Francis (Eds).

Wemple, B.C., Swanson, F.J., Jones, J.A., 2001. Forest roads and geomorphic process interactions, Cascade Range, Oregon, Earth Surface Processes Landforms. 26, 191–204.

Wilson, J.P., Gallant, J.C., 2000. Digital terrain analysis. In: Wilson, J.P., Gallant, J.C, (Eds.), Terrain Analysis: Principles and Applications. John Wiley: New York. 1–27.

Wischmeier, W.H., Smith, D.D., 1959. A Rainfall Erosion Index for a Universal Soil Loss Equation. Soil. Sci. Soc. Amer. Proc. 23, 246-249.

Wischmeier, W.H., Smith, D.D., 1965. Predicting rainfall erosion losses from cropland east of the Rocky Mountains: Guided for selection of practices for soil and water conservation. U.S. Dep. Agric. Handb. N°282.

Wischmeier, W.H., Smith, D.D., 1978. Predicting rainfall erosion losses–A guide to conservation planning. Agriculture Handbook No. 537. Washington, DC: US Department of Agriculture.

Yalcin, a., Reis, S., Aydinoglu, A.C., Yomralioglu, T., 2011. A GIS-based comparative study of frequency ratio, analytical hierarchy process, bivariate statistics and logistics regression methods for landslide susceptibility mapping in Trabzon, NE Turkey. Catena. 85, 274-287.

Zevenbergen, L.W., Thorne, C.R., 1987. Quantitative analysis of the land surface topography. Earth Surface Process And Landform. 12, 47-56.

Zhang, W., Montgomery, D.R., 1994. Digital Elevation Model Grid Size, Landscape Representation, and Hydrologic Simulations. Water Resources Research. 30(4), 1019-1028.

Zhang, D.W., Shao, J., Lin, J., Zhang, N., Lu, B.J., Lin, S.C., Dong, M.Q., Han, J., 2009. Science. DOI 10.1126/science.1172308.

Ziegler, A.D., Giambelluca, T.W., 1997. Importance of rural roads as source areas for runoff in mountainous areas of northern Thailand. J. Hydrol. 196, 204–229.

List of Figures

List of Tables